Electron Energy Loss Spectrometry

Cécile Hébert
Centre Interdisciplinaire de Microscopie Electronique
Laboratoire de Spectrométrie et Microscopie Electronique
Ecole Polytechnique Fédérale de Lausanne

Abstract

EELS (electron energy loss spectrometry) is a technique used in TEM. It analyses the energy *lost* by the incoming fast electrons when they travel through the sample. While diffraction effects in the TEM are driven by the interaction of the fast electrons with the nucleus, in EELS, one deals with electro-electron interactions. This is the interaction between the electron of the beam and the electrons in the sample. Therefore EELS is able to provide information about the electronic structure of the sample. EELS can also be used for chemical analysis, and can provide quantitative information about the composition of the specimen. Since the energy lost is relatively small compared to the energy of the incoming electron (at most 2 to 3000 eV compared to 120 -300 keV in conventional microscopes), the electrons which have lost energy can still be “used” for imaging the specimen. Imaging the specimen with electrons which have lost energy characteristic for a certain atom will provide a cartographic picture of the repartition of this kind of atom in the sample. This is called chemical mapping.

Looking at the fine structure in the EELS spectrum will give information about the electronic state in the samples, and these results can be compared to theoretical calculations.

Outline

- Introduction: EELS in the TEM
- Instrumentation
- Core Loss EELS
  - Theory
  - Applications
- Low losses
- Imaging (EFTEM)
- ELNES

Outline

- Introduction: EELS in the TEM
- Instrumentation
- Core Loss EELS
  - Theory
  - Applications
- Low losses
- Imaging (EFTEM)
- ELNES

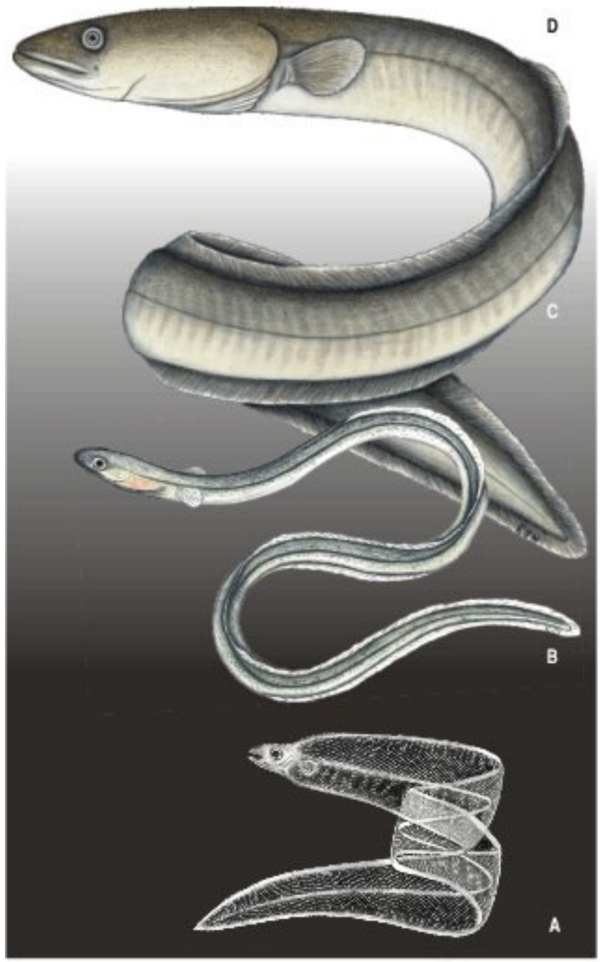

Introduction

EELS in the TEM

Probe = electrons
100-300 kV
Velocity: 0.55-0.77 c

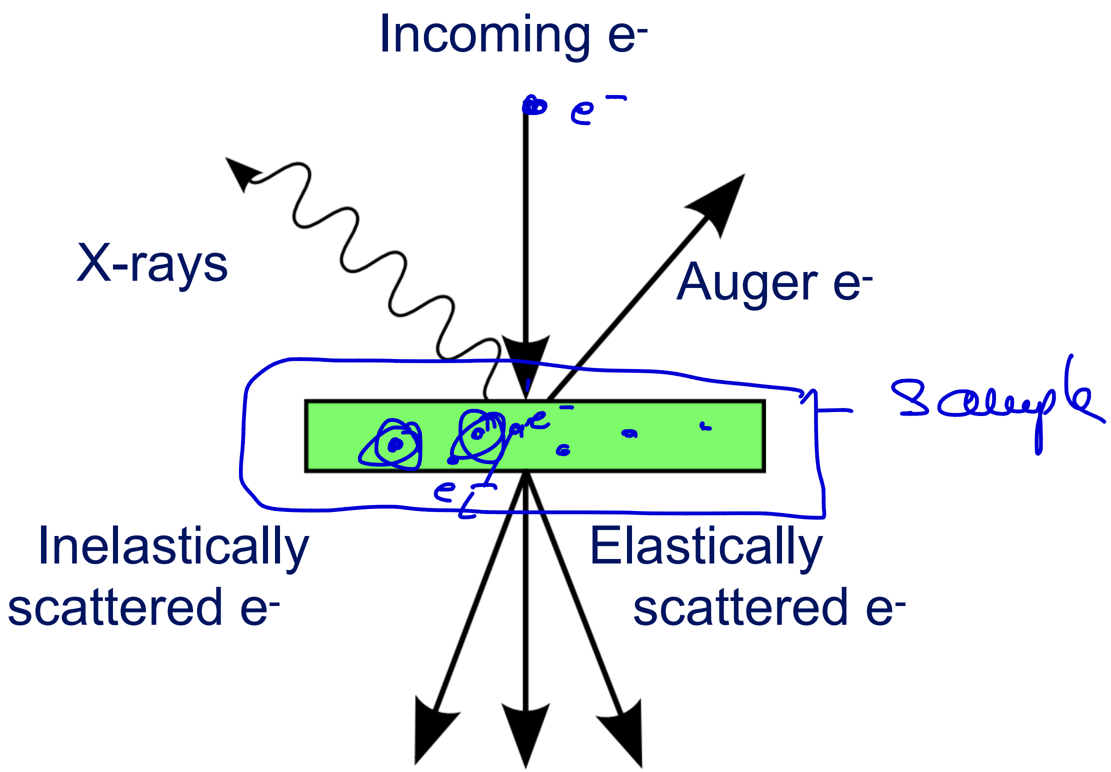

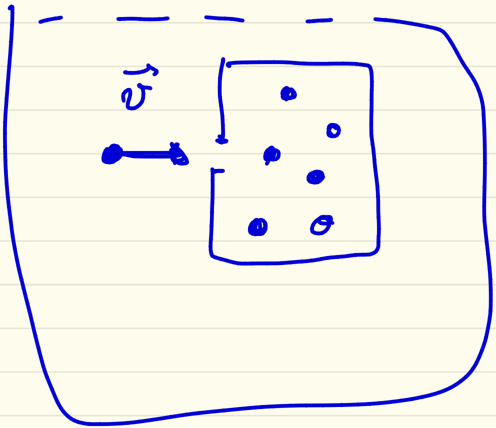
$\vec{v}$

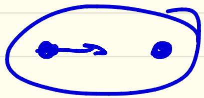

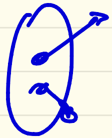

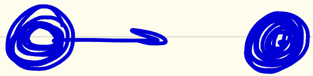

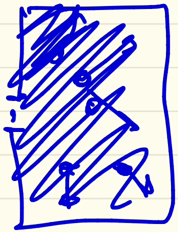

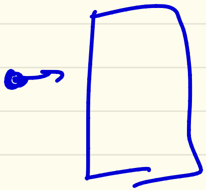

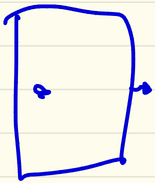

Introduction

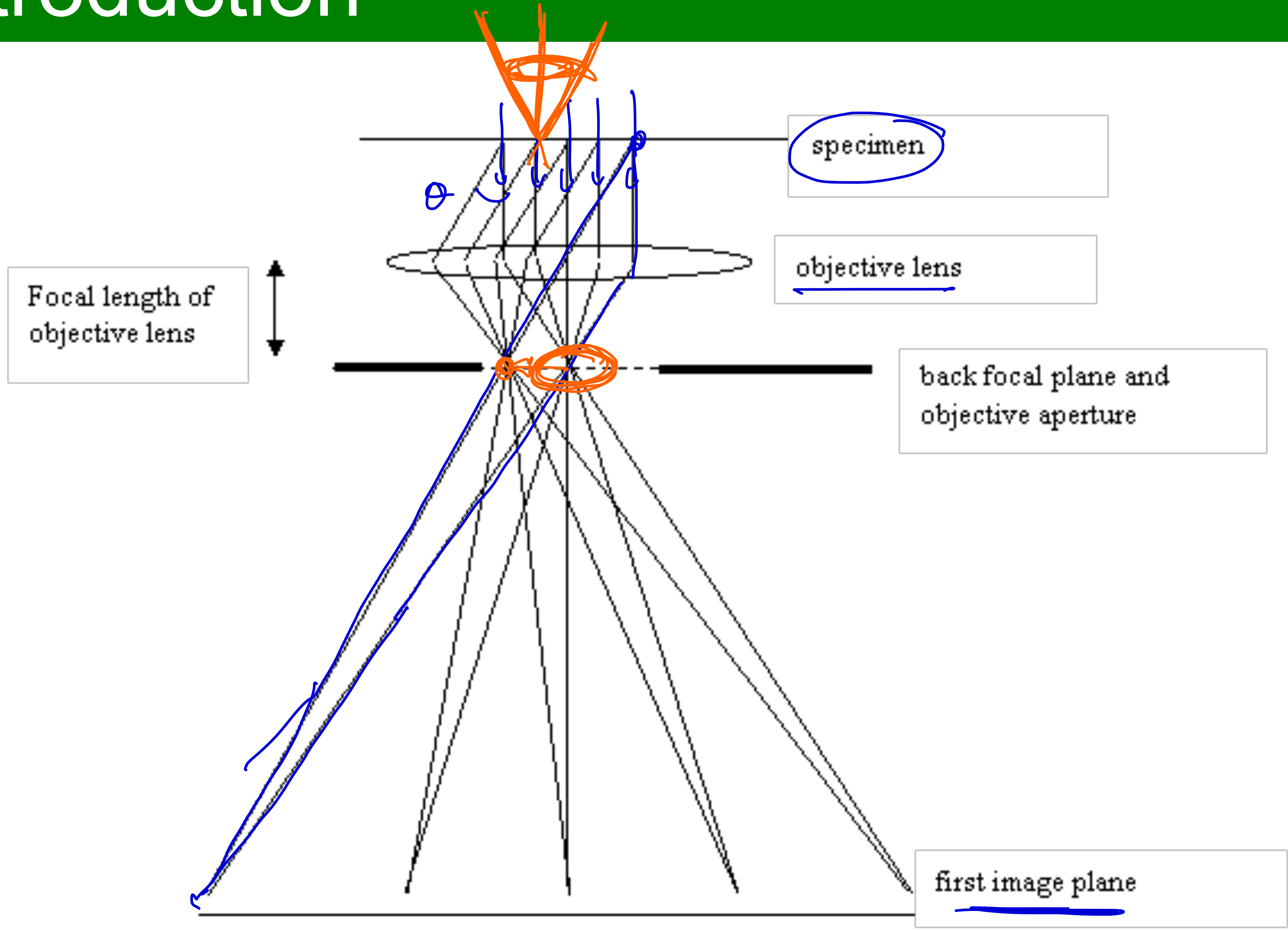

Introduction

Scattering geometry

$$q^2 = k^2 + (k')^2 - 2kk'\cos\theta$$

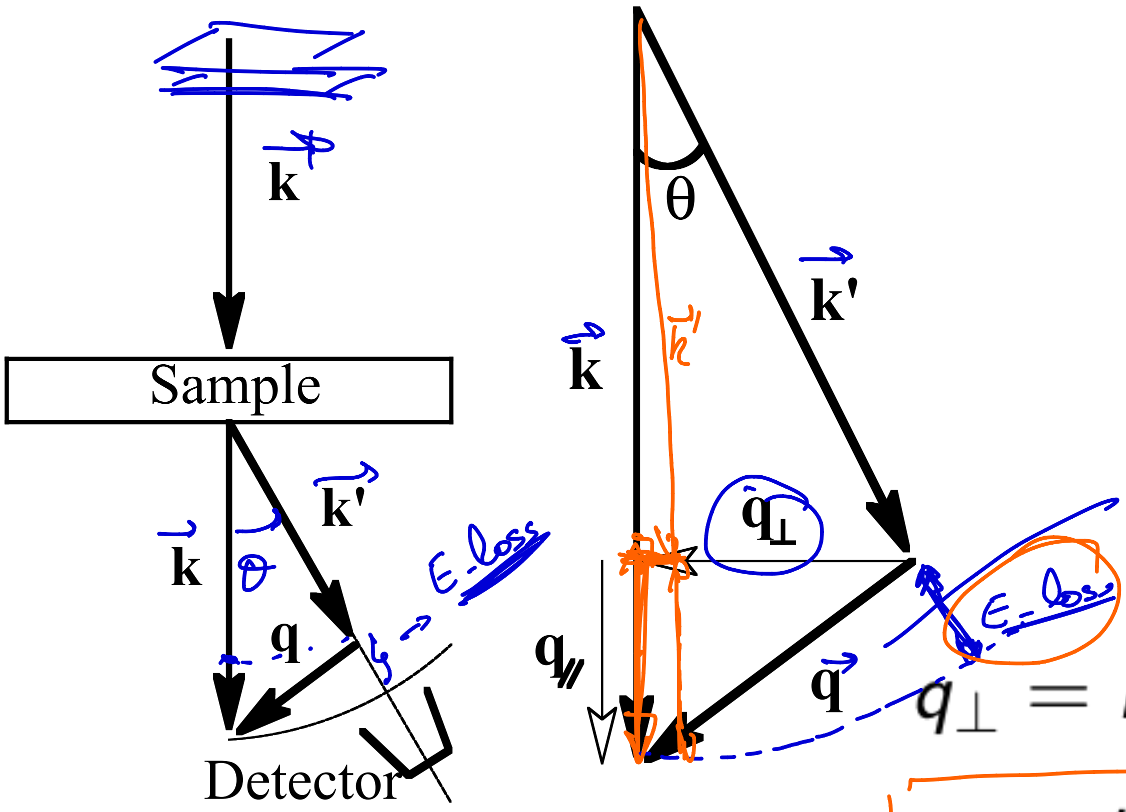

0 < θ < 100 mrad ~0,1 rad ≪ 1

To avoid aberrations
0 < θ < 25 mrad

@200 kV [111] spot
in fcc Cu: 11 mrad

"momentum transfer" $\vec{p} = \hbar\vec{q}$

$|\vec{k}'| \simeq |\vec{k}|$ → E-loss small compared to E_0

$q_\perp = k\vartheta$ (geometry)

$q_\parallel = k\vartheta_E$ (definition of ϑ_E)

$q^2 = q_\perp^2 + q_\parallel^2 = k^2\theta^2 + \theta_E^2 k$

$\vartheta \ll 1$ therefore $q^2 = k^2(\vartheta_E^2 + \vartheta^2)$

$$\theta_E = \Delta E m\gamma/\hbar^2 k^2$$

(E-loss)

$\gamma = \frac{1}{\sqrt{1 - v^2/c^2}}$ "relativistic factor"

Excitation process

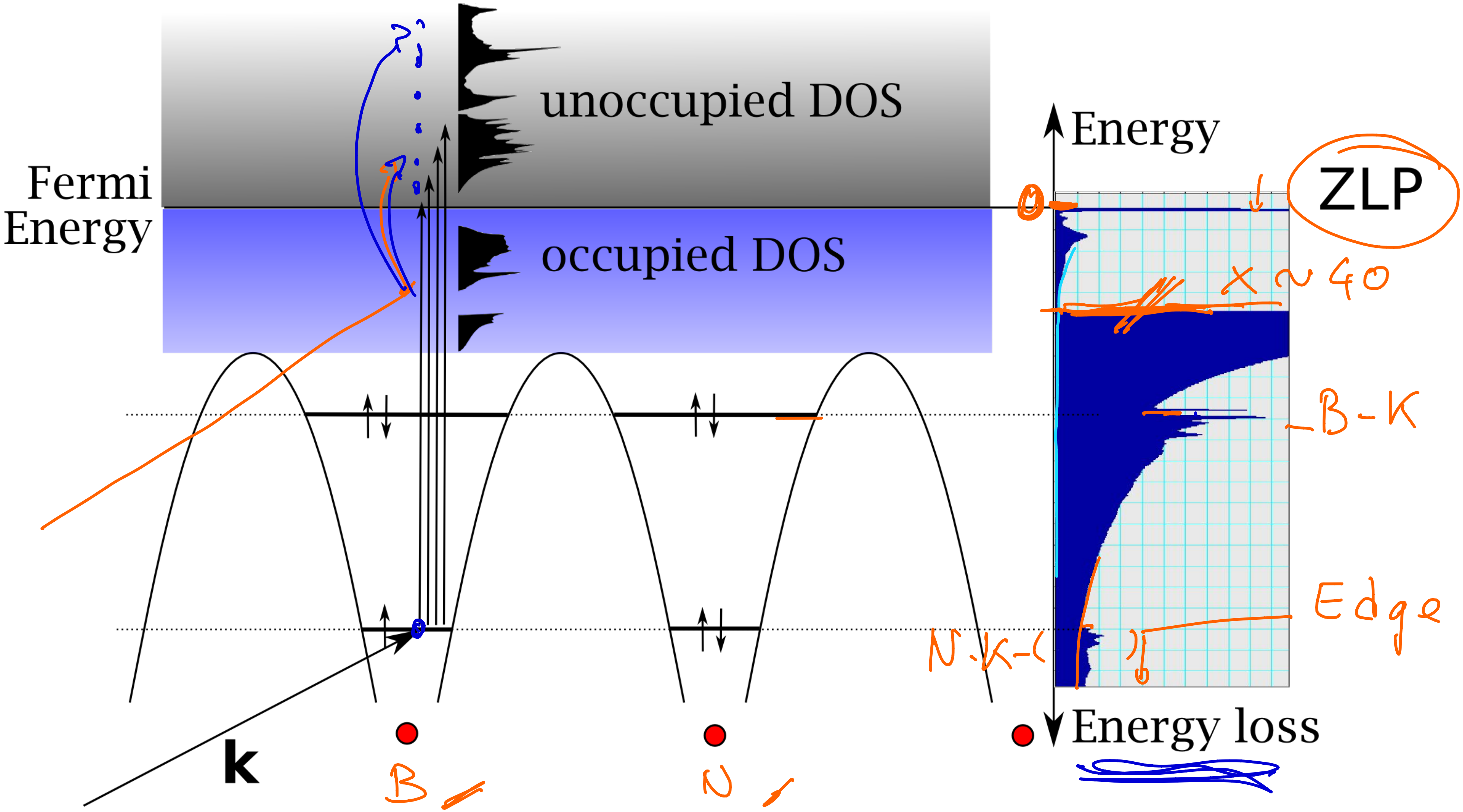

Introduction

E_0=100-300kV

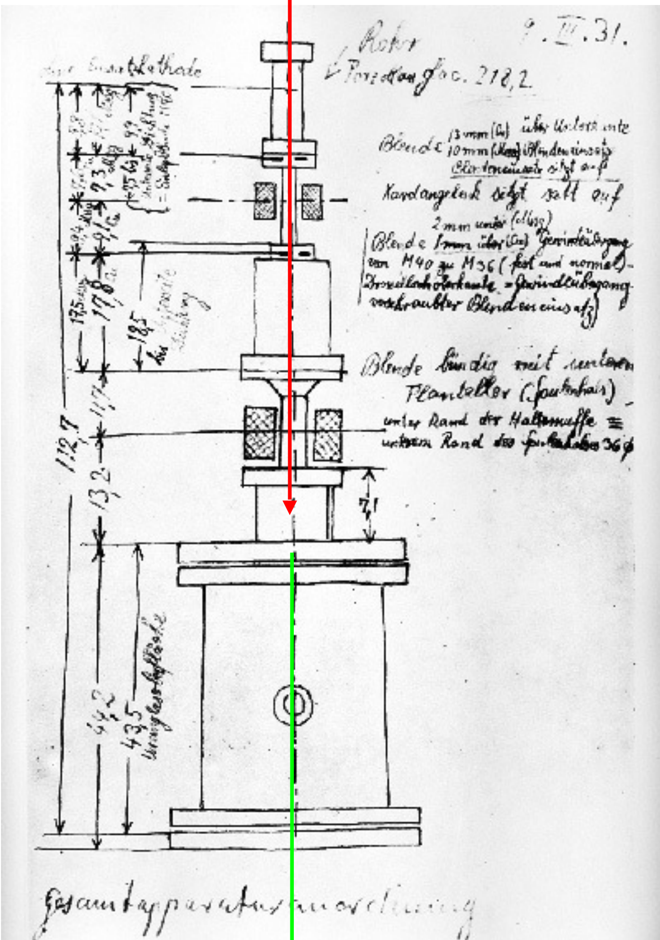

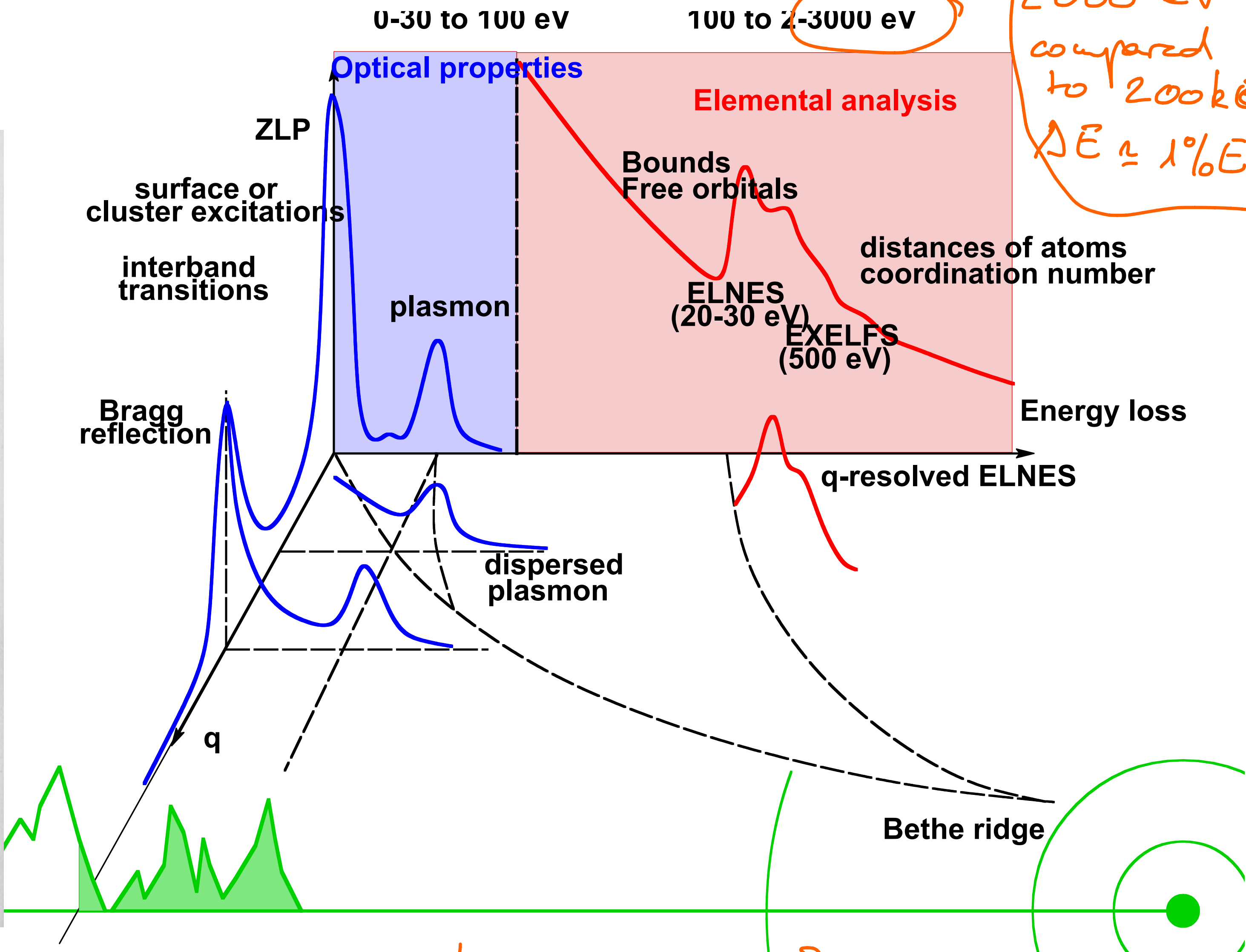

ΔE=0-3kV

2000 eV compared to 200keV $\Delta E \approx 1\% E_0$

E-spread of e-beam in TEM?

W-filament ~ 3.2 eV ; LaB_6 ~ 1,6 FEG 0,8 eV Monochromator

Introduction

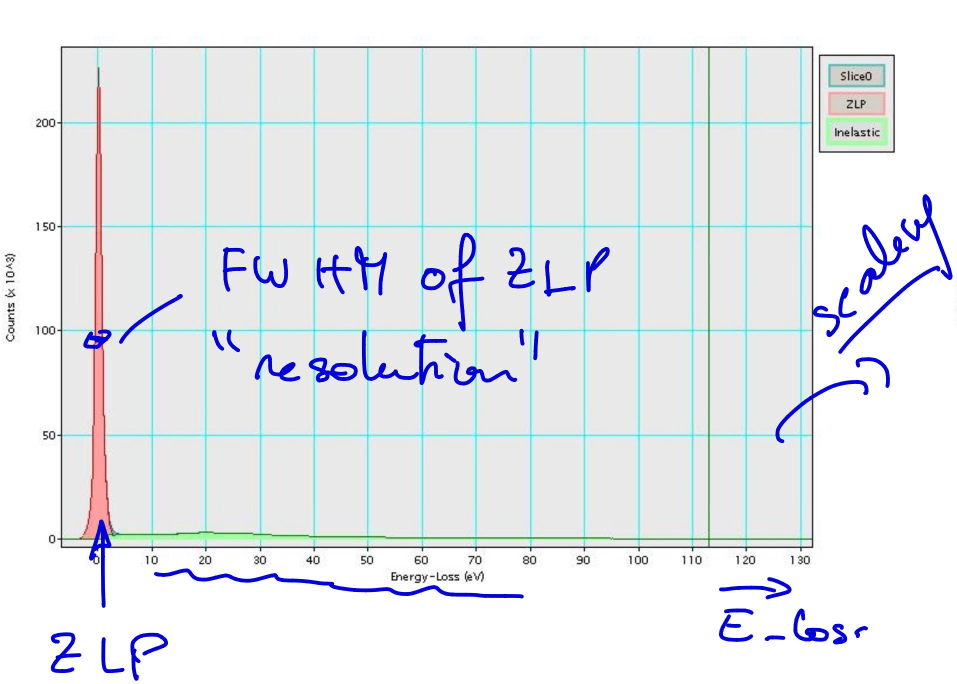

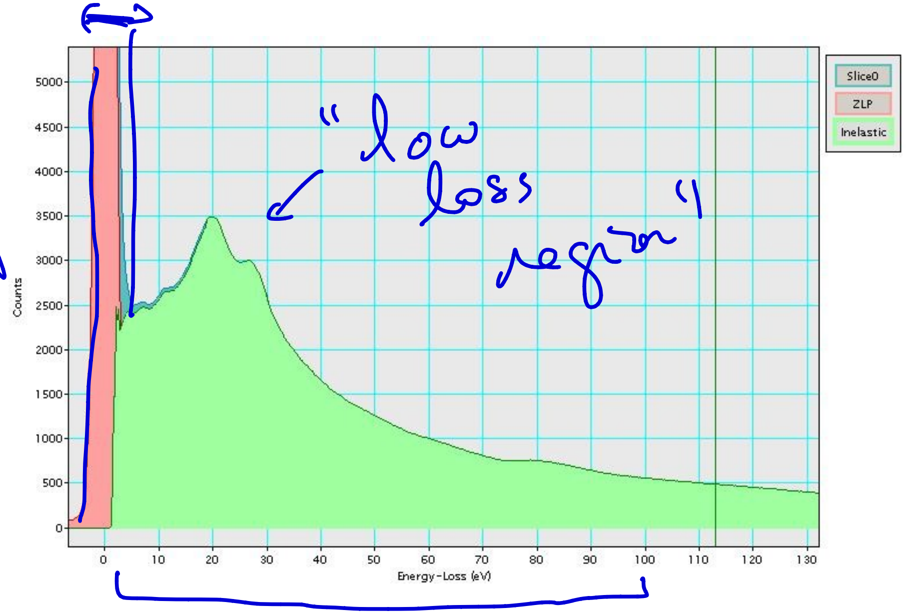

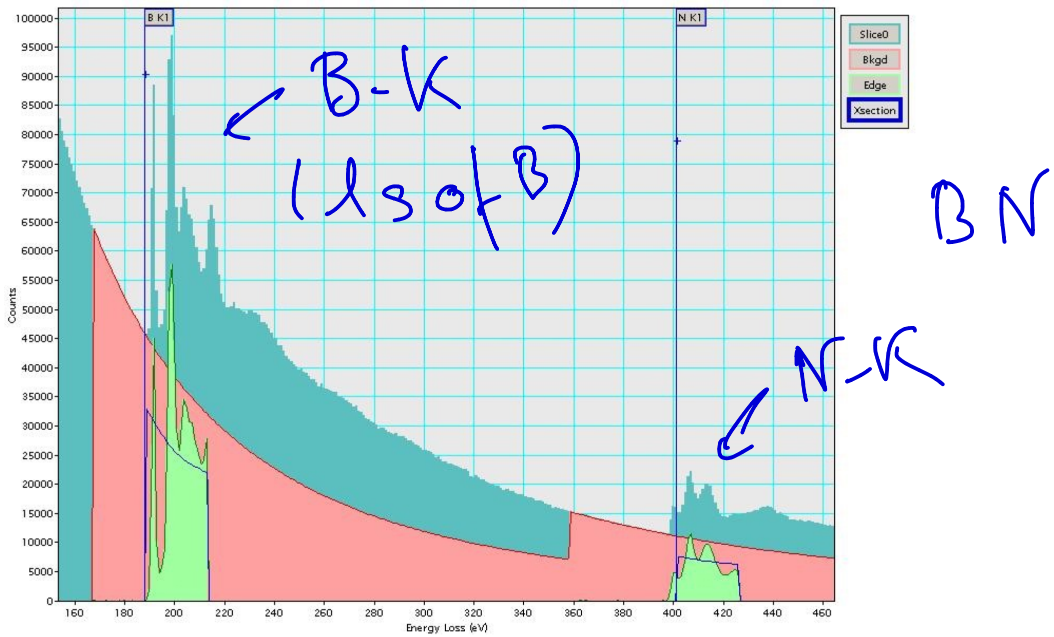

Introduction

Edge nomenclature

EELS

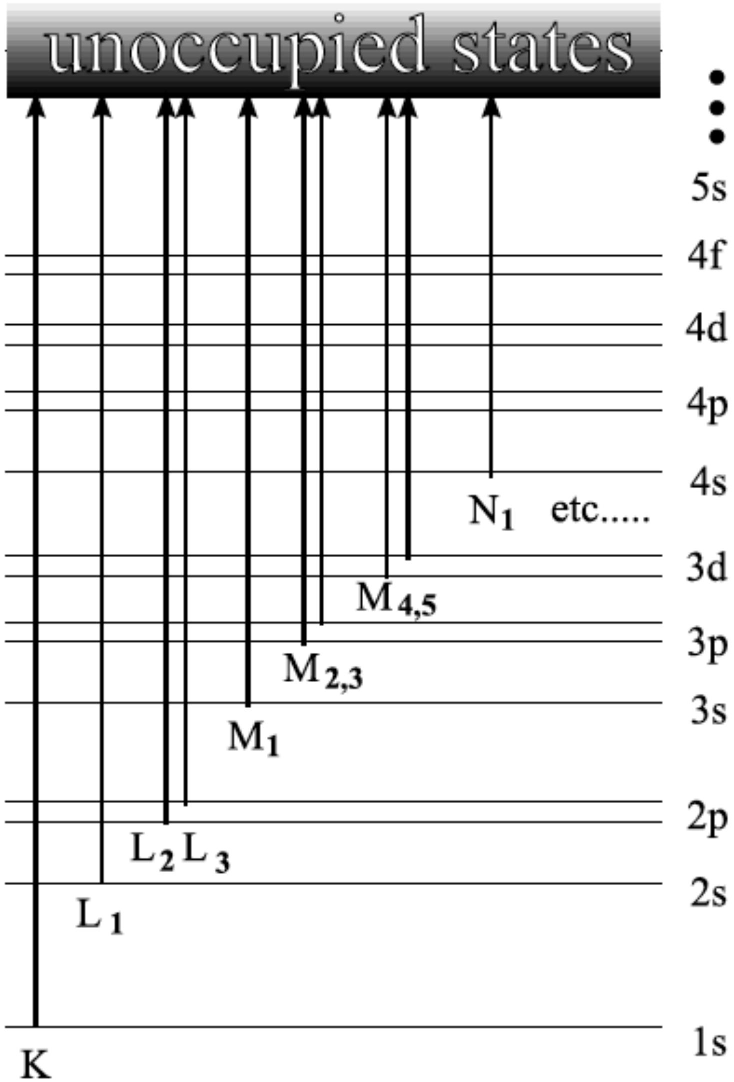

EDX

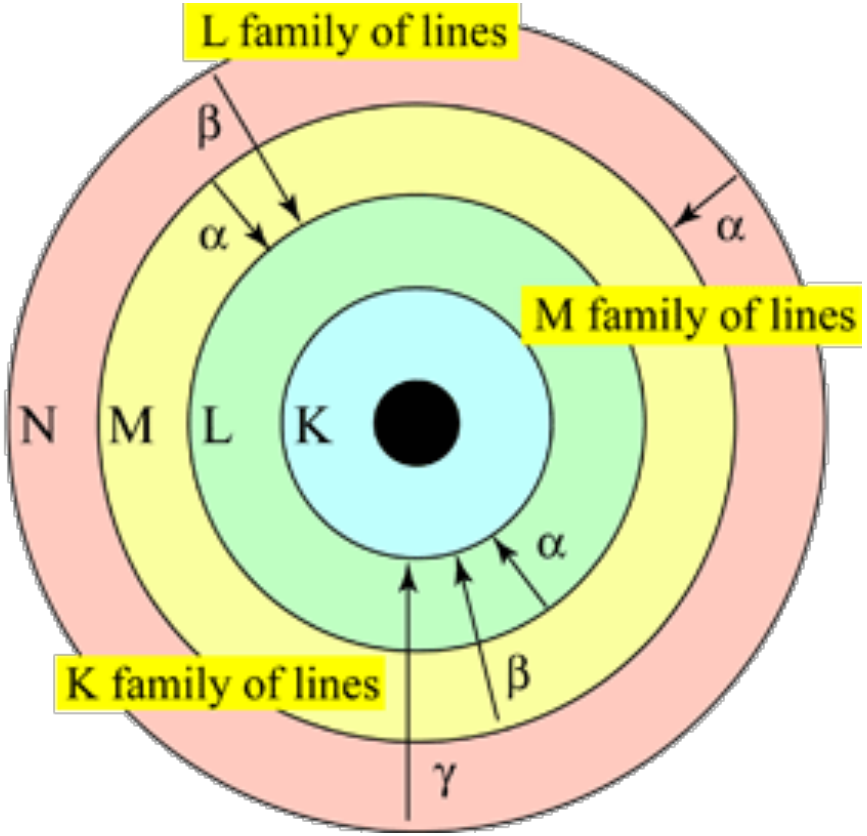

Plural scattering; mean free path

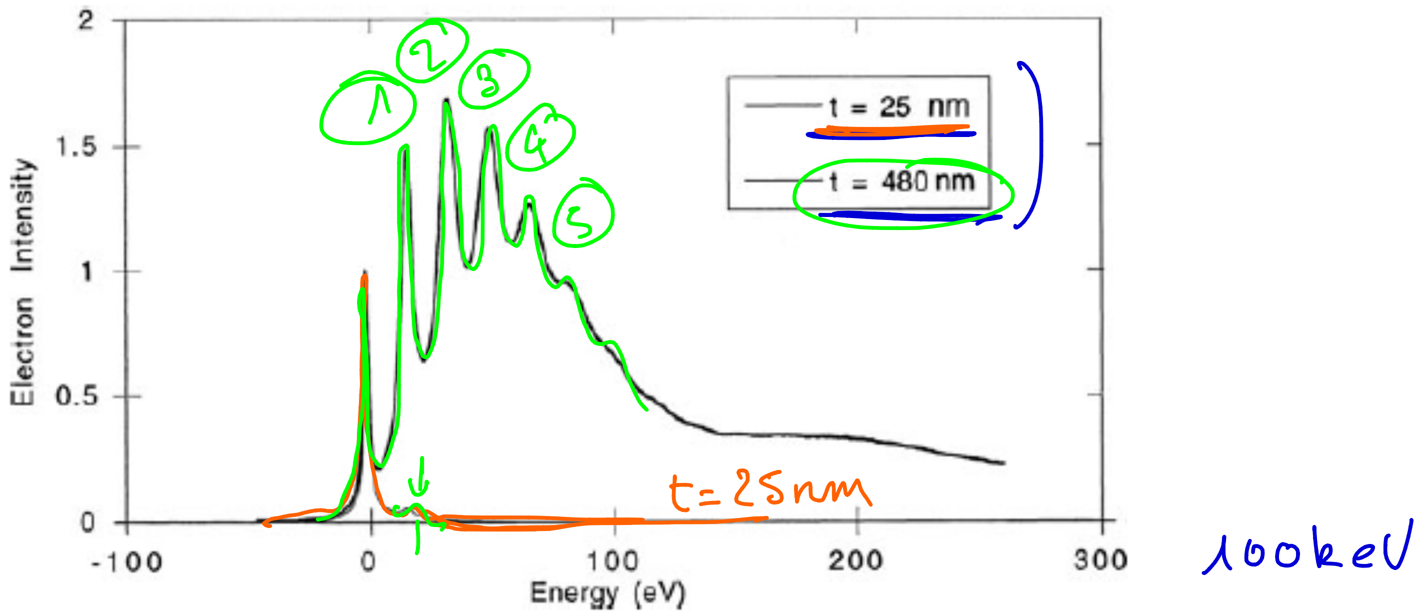

Fig. 1.5 Energy-loss spectra recorded from silicon specimens of two different thicknesses. The thin sample gives a strong zero-loss peak and a weak first-plasmon peak; the thicker sample provides plural scattering peaks at multiples of the plasmon energy

An incident electron can interact many times with the specimen: plural scattering is likely to occur

The inelastic mean free path gives the average distance between 2 inelastic scattering events. It is typically 50-150 nm

Plural scattering; mean free path

inelastic mean free path depends.

Z $Z \nearrow$ $\lambda \searrow$

E_0 $E_0 \nearrow$ $\lambda \nearrow$

$\beta \nearrow$ "collection angle" $\lambda \searrow$

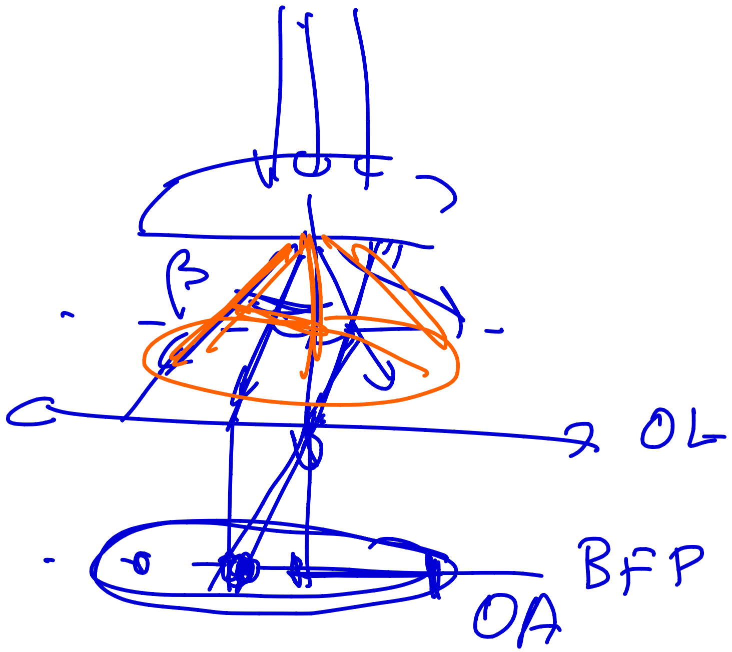

Thickness measurements

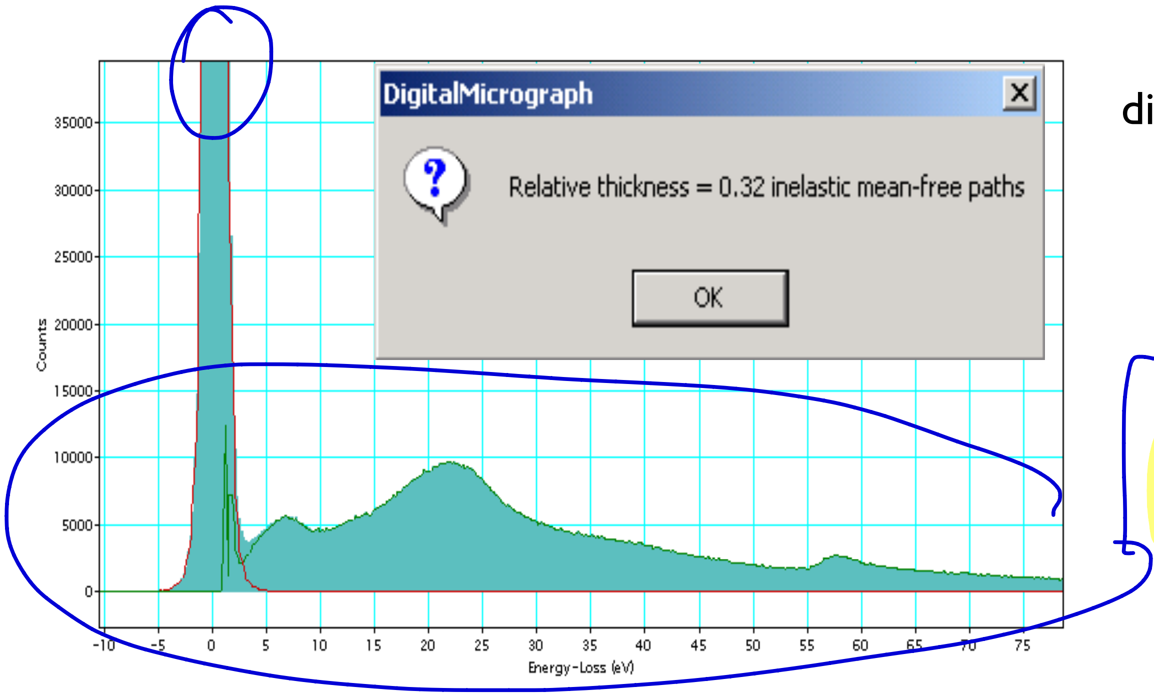

direct link between :

- specimen thickness
- inelastic mean free path
- relative intensity in the ZLP/ total intensity

$$\frac{t}{\lambda} = \ln \frac{I_t}{I_0}$$

Be careful, λ depends on the acquisition conditions !

$$\lambda \approx \frac{106F(E_0/E_m)}{\ln(2\beta E_0/E_m)}$$

$$F = \frac{T}{E_0} = \frac{m_0 v^2}{2E_0} = \frac{1 + E_0/1022\text{ keV}}{(1 + E_0/511\text{ keV})^2}$$

$$E_m \approx 7.6 Z^{0.36}$$

⇒ λ is known with ~ 20% accuracy

Outline

- Introduction: EELS in the TEM
- Instrumentation
- Core Loss EELS
  - Theory
  - Applications
- Low losses
- Imaging (EFTEM)
- ELNES

Instrumentation

Spectrometer

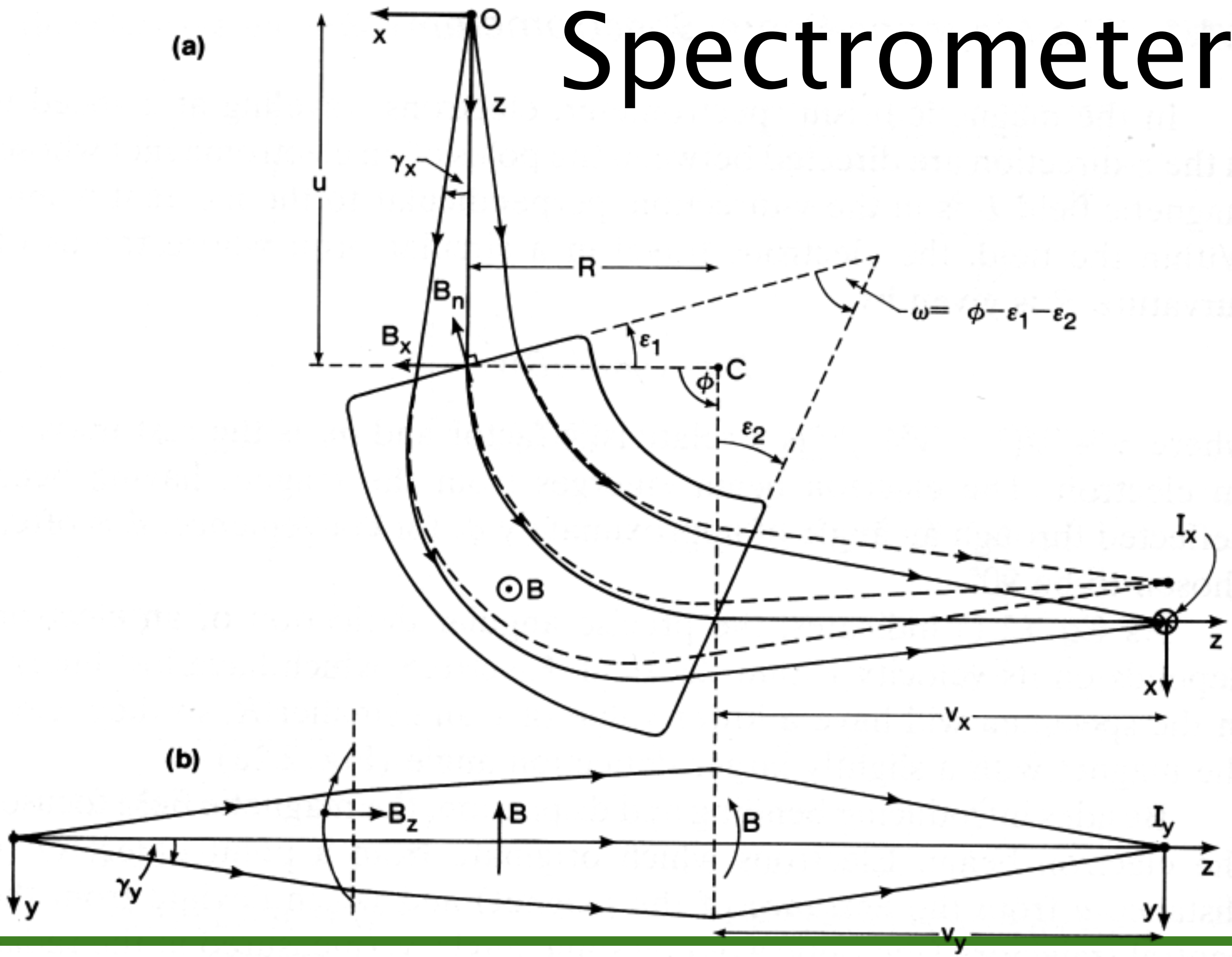

Instrumentation

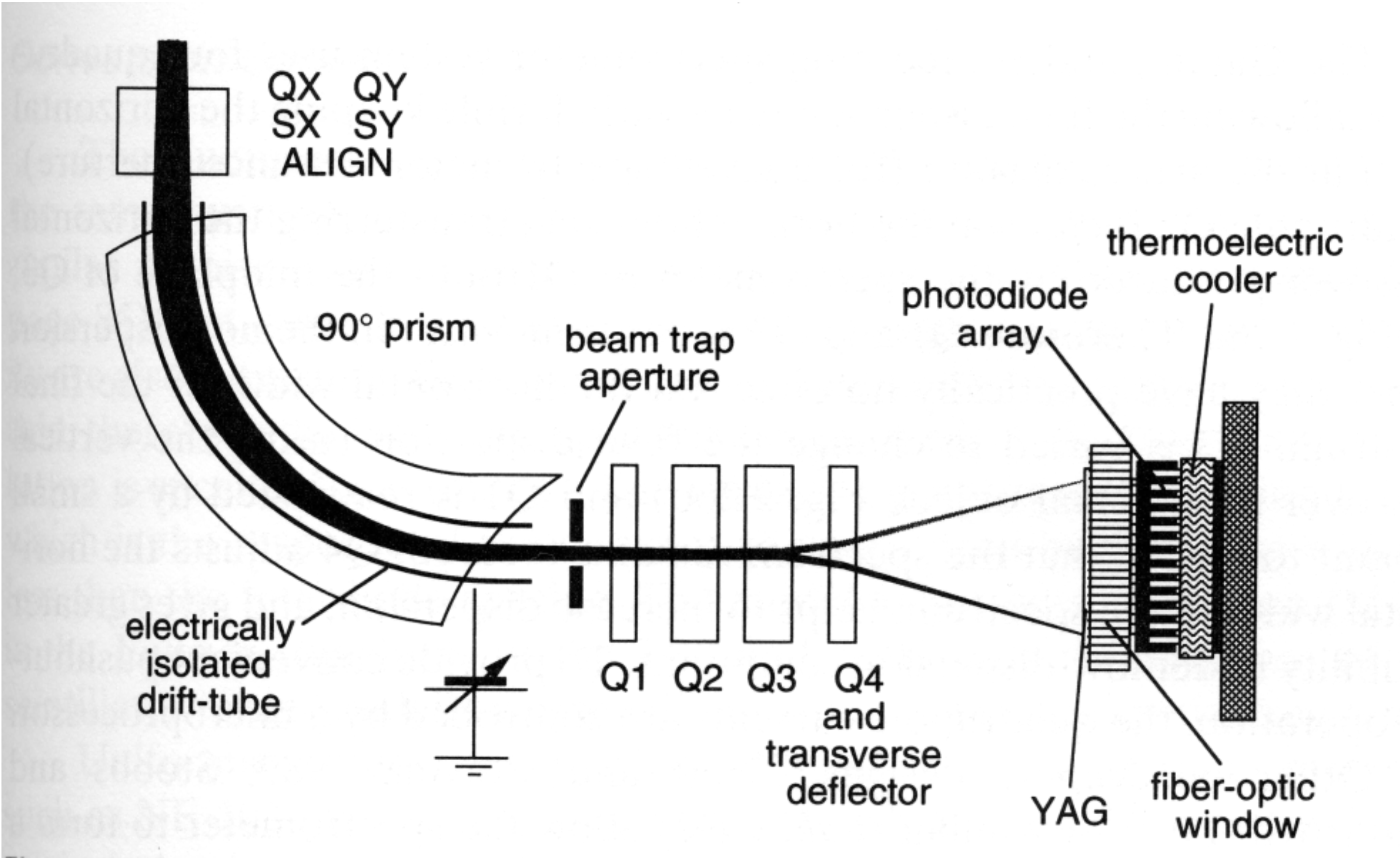

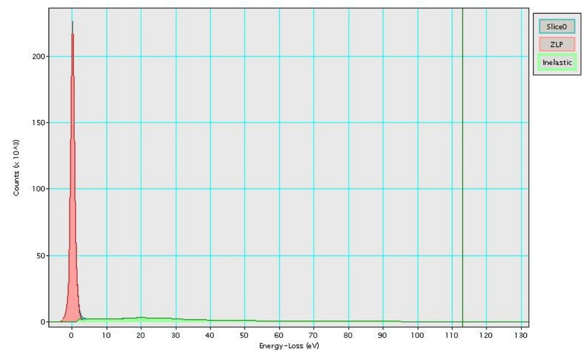

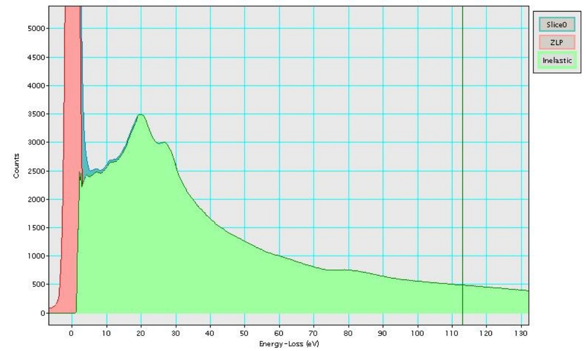

Gatan PEELS 666
Gatan digi-PEELS 766
Gatan Enfina

Instrumentation: energy filter

Operated as energy filter

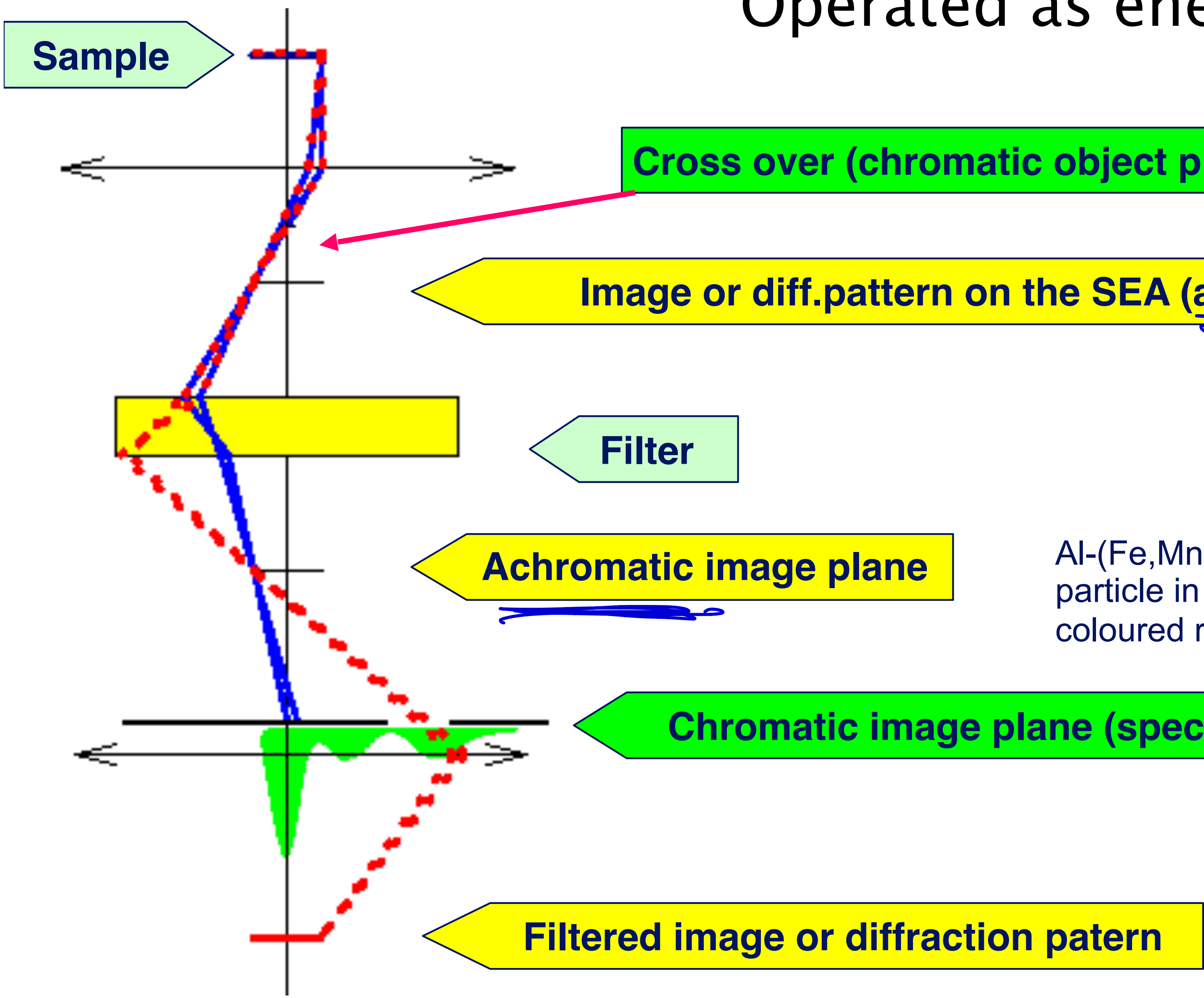

Al-(Fe,Mn)-Si phase intermetallic particle in aluminium alloy. Al is coloured red, Fe blue, and Mn green.

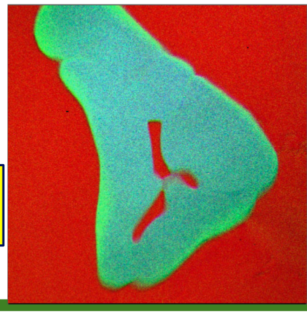

Instrumentation: energy filter

Operated as spectrometer

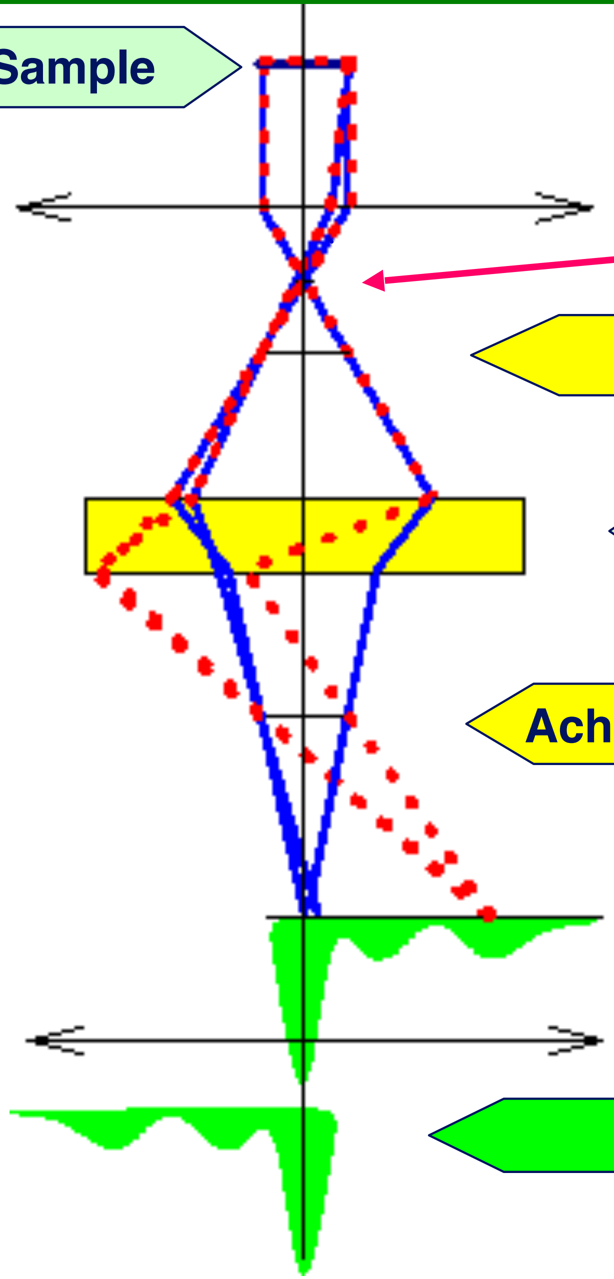

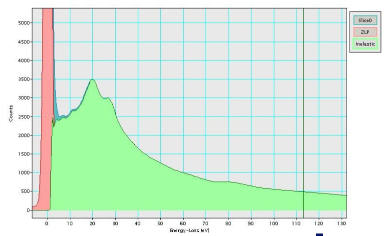

Two possibilites: in- or post-column

Instrumentation energy filter

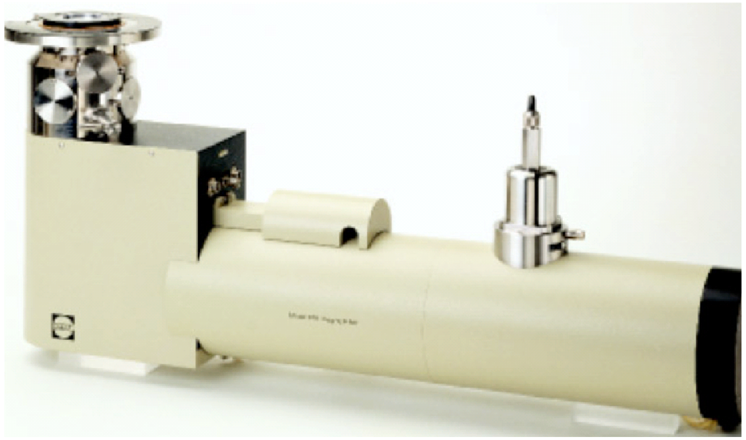

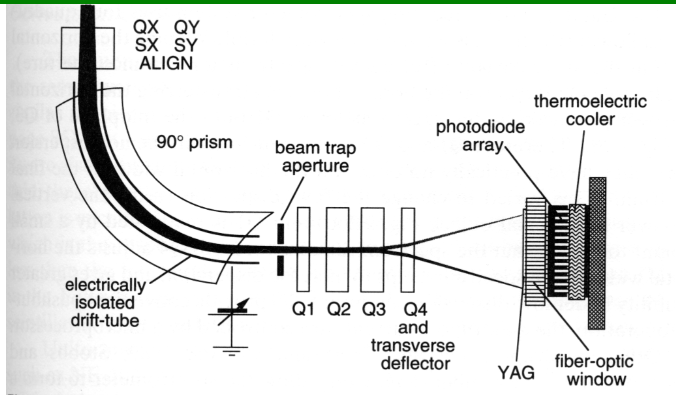

Gatan Imaging Filter

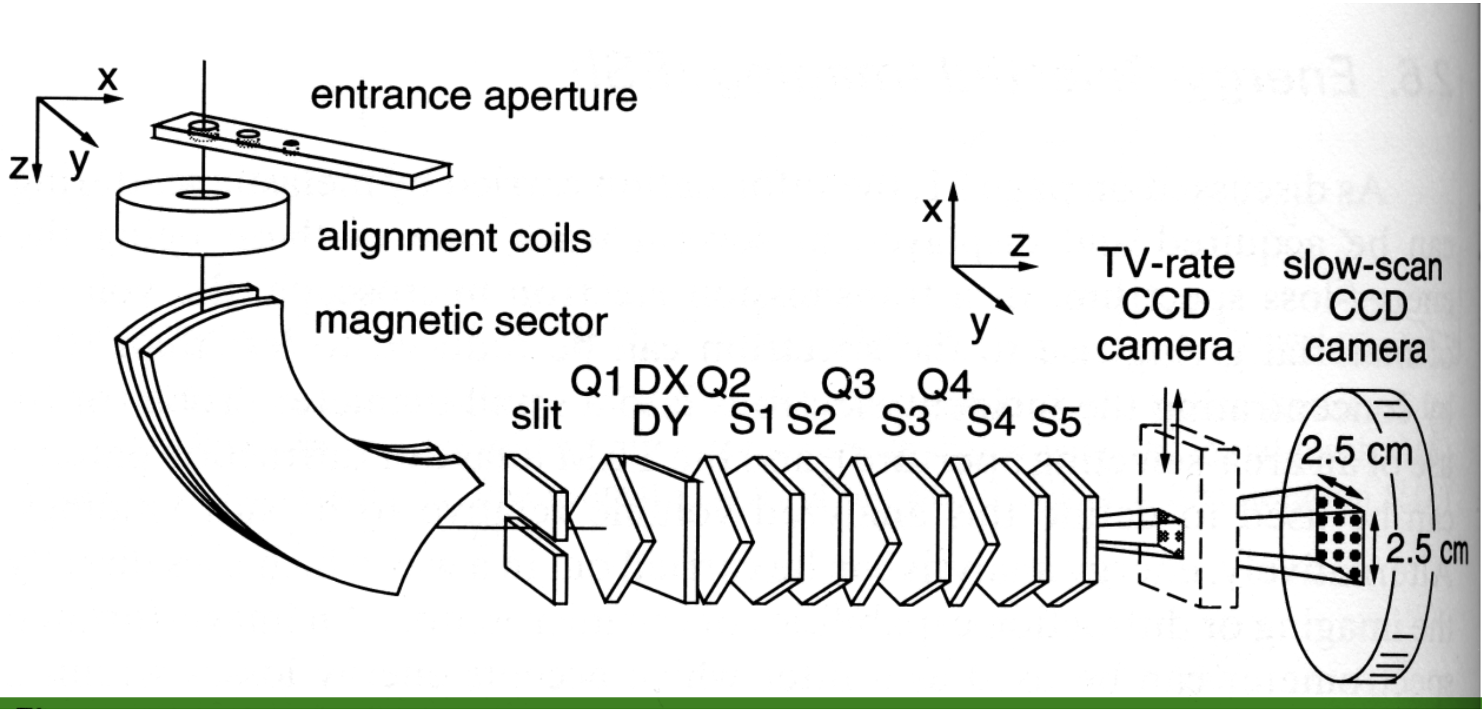

Instrumentation: energy filter

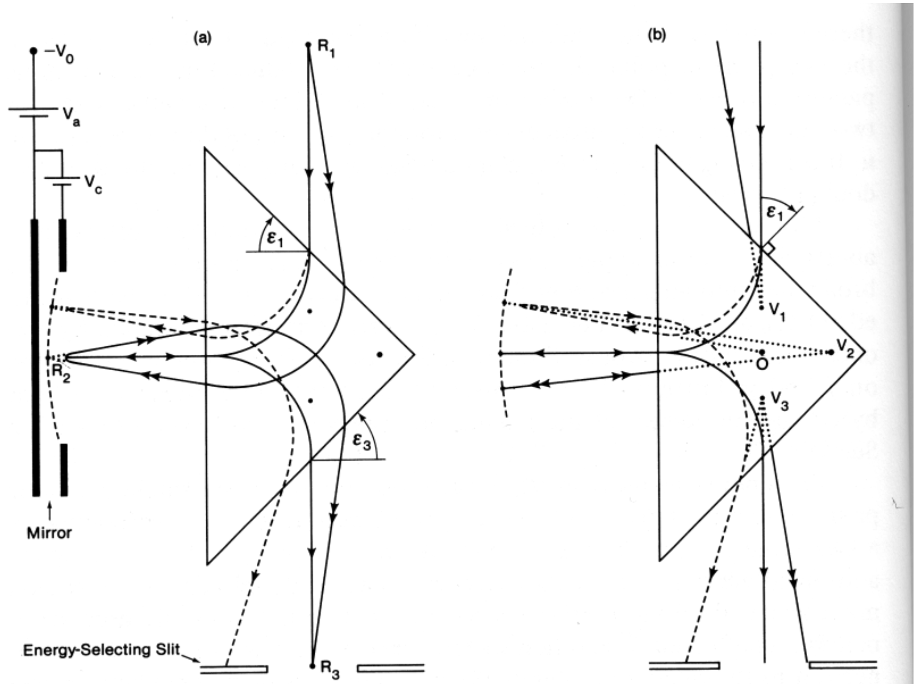

1962: Castaing-Henry filter

1984: Zeiss 902

Instrumentation: energy filter

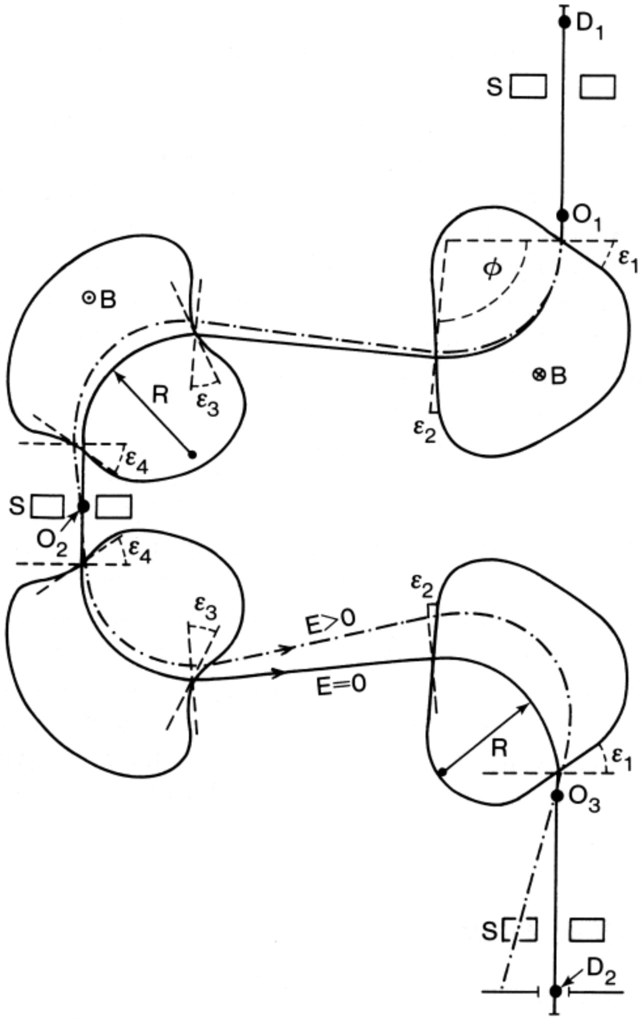

Zanchi; Krahl: Omega filter

1992: Zeiss 912

Instrumentation: energy filter

Jeol: omega

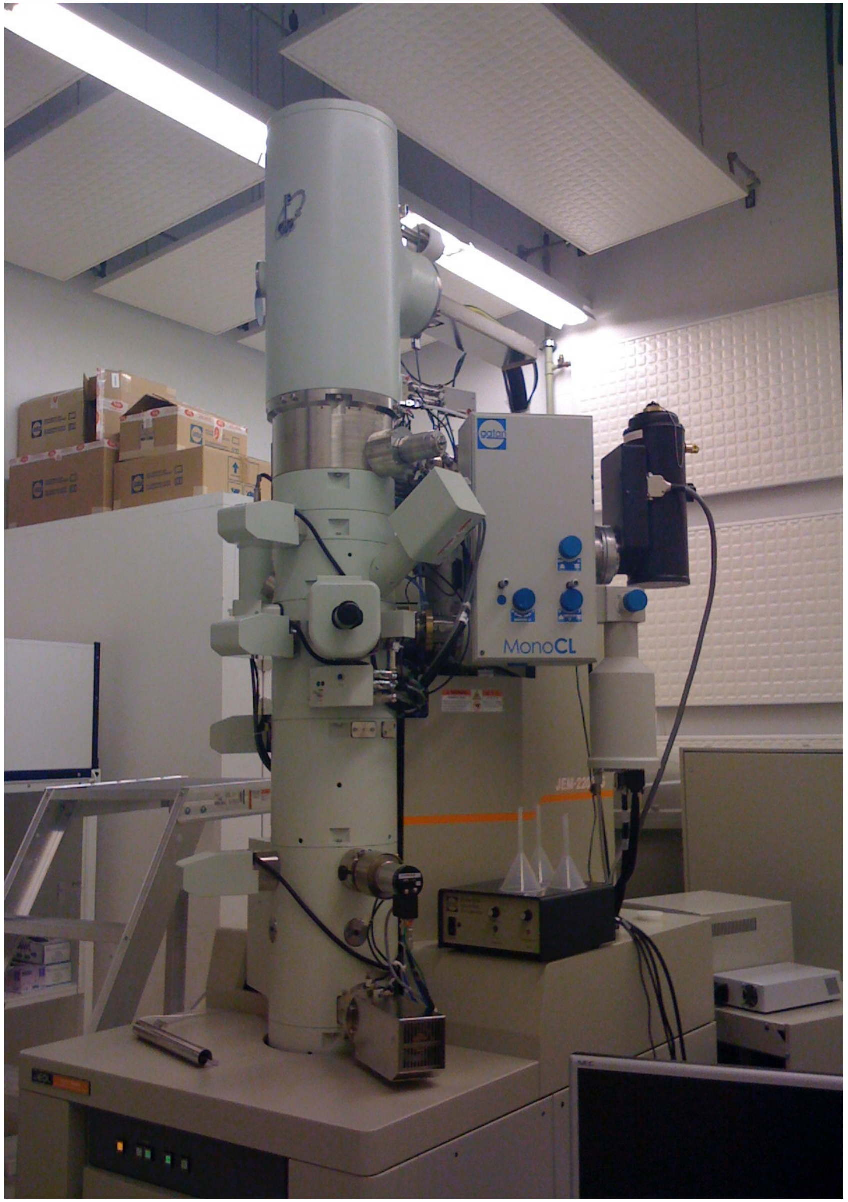

Zeiss libra: corrected omega

Instrumentation: energy filter

Mandoline:

SESAM project (Zeiss)

Installed and working in Stuttgart

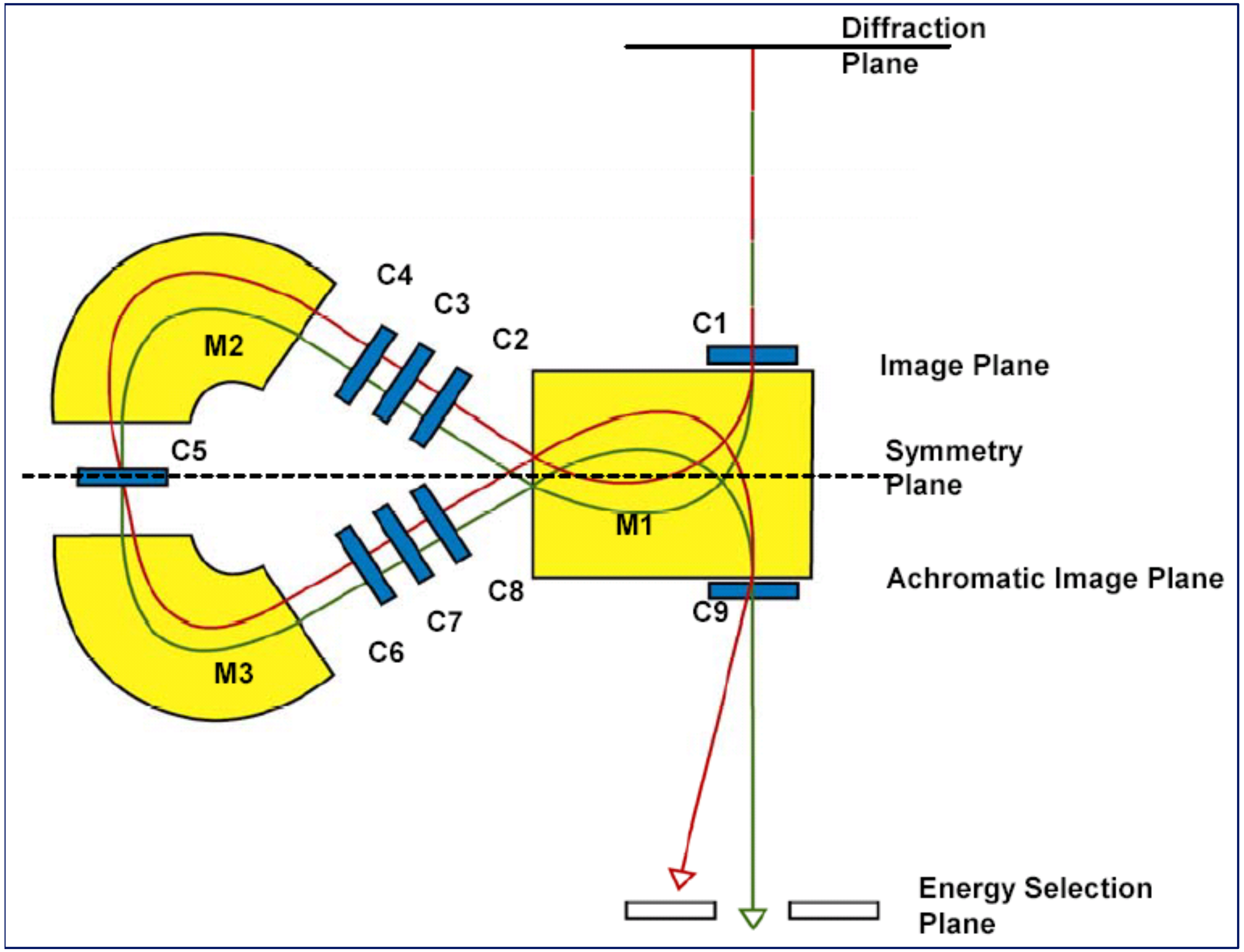

Instrumentation: data acquisition

3D Data cubes: EFTEM vs. (STEM)-EELS

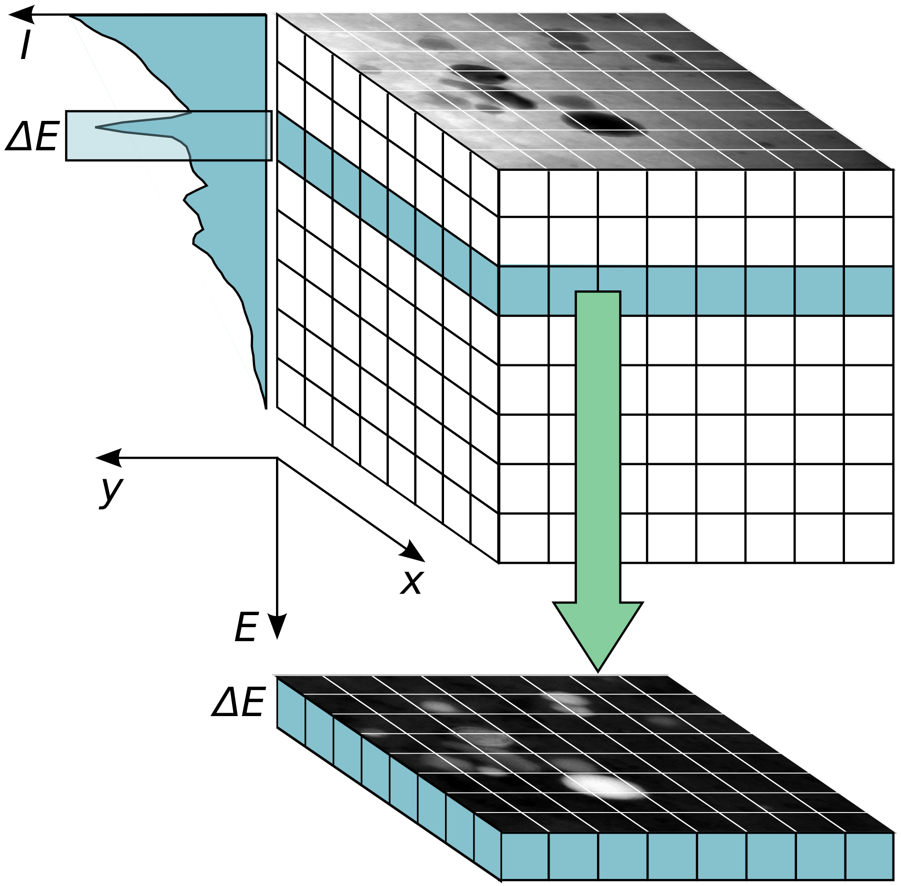

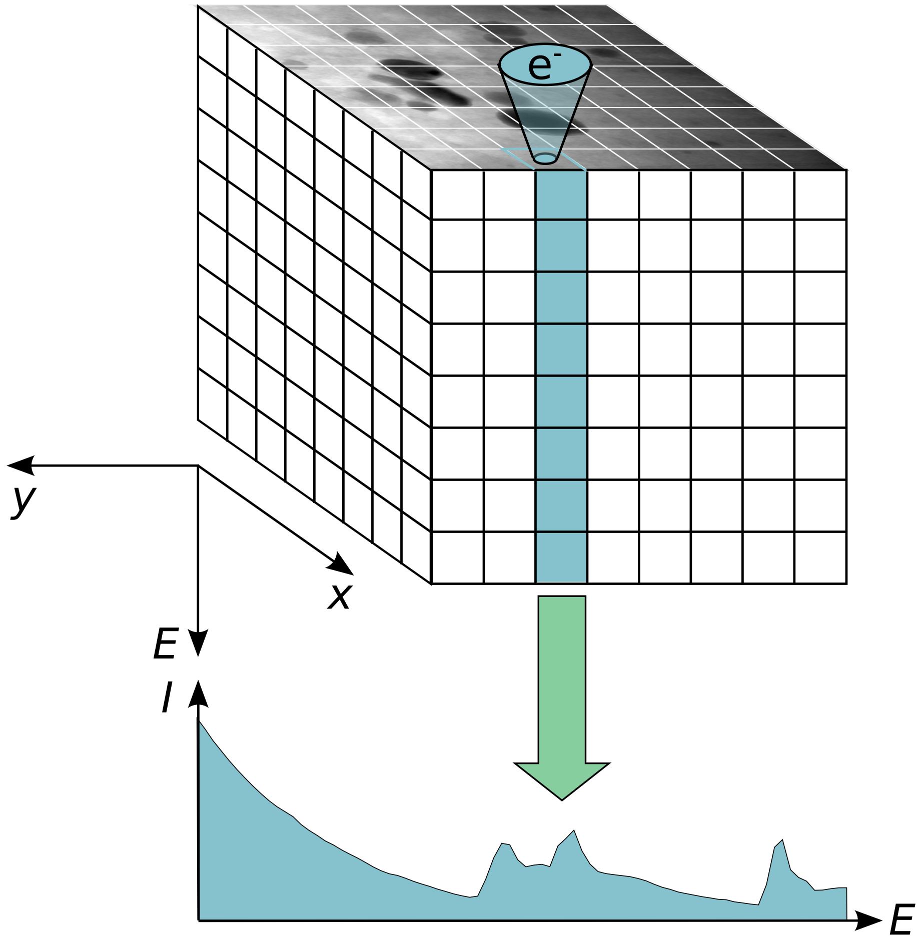

An energy filtered image is a slice from the 3D data cube.

Each recorded spectrum corresponds to a column in the 3D data cube.

Outline

- Introduction: EELS in the TEM
- Instrumentation
- Core Loss EELS
  - Theory
  - Applications
- Low losses
- Imaging (EFTEM)
- ELNES

Theory of core losses

transition from core (occupied) to unoccupied state
We need quantum mechanics!
System = fast incoming electron + target electron
first order perturbation theory
First Born approximation
perturbation potential is Coulomb potential

H.A.Bethe: 1930:

Zur Theorie des Durchgangs schneller Korpuskularstrahlen durch Materie

Annalen der Physik, vol. 397, Issue 3, pp.325-400

Core loss EELS: theory

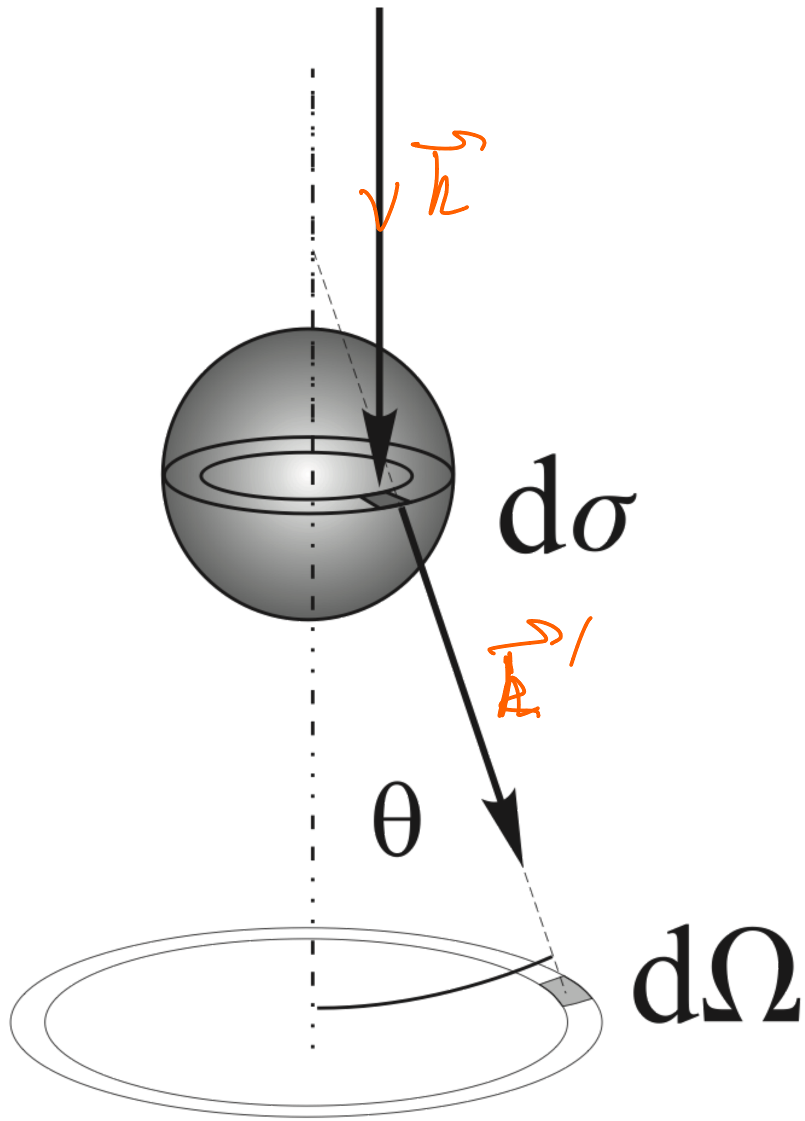

Relevant quantity: scattering cross-section as a function of angle θ and energy loss E.

It is given for one atom.

We consider a transition from initial state | I > to final state | F > for the core electron of the atom

$$q^2 = k^2(\theta^2 + \theta_E^2)$$

q: momentum transfer

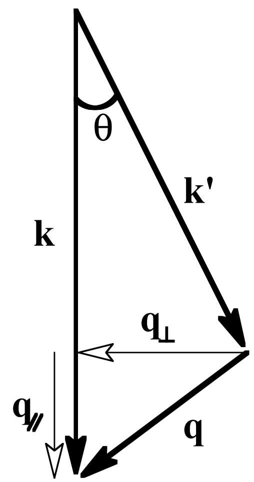

Theory of core loss

Transition probability per unit time dP_{if} from an initial state $|i\rangle$ to a final state $|f\rangle$ situated between ν_f and $\nu_f + d\nu_f$.

→ system core electron + fast electron

$$dP_{if} = \frac{2\pi}{\hbar} |\langle f | V | i \rangle|^2 d\nu_f \, \delta(E_i - E_f)$$

→ V = perturbation potential (Coulomb)

Initial and final state of the system :

$$|i\rangle \;=\; |\vec{k}\rangle \otimes |I\rangle$$

→ e.g. |1s⟩ state (K)

$$\textit{and}$$

$$|f\rangle \;=\; |\vec{k}'\rangle \otimes |F\rangle$$

→ final state in unoccupied DOS

$|I\rangle$ and $|F\rangle$ Initial and final states of the target electron.

Theory of core loss

$\vec{k}$ before the interaction $\vec{k}'$ after.

$\vec{q} = \vec{k} - \vec{k}'$

$$dP_{if} = \frac{2\pi}{\hbar} \left| \langle F| \otimes \langle \vec{k}'|V|\vec{k}\rangle \otimes |I\rangle \right|^2 d\nu_f \delta(E_I - E_F + E)$$

$\langle \vec{k}'|V|\vec{k}\rangle$?? $\longrightarrow$ V Coulomb potential

$$\langle \vec{k}'|V|\vec{k}\rangle = \frac{1}{4\pi\epsilon_0} \int (2\pi)^{-3} d^3r \frac{e^2}{|\vec{r} - \vec{R}|} e^{i\underbrace{(\vec{k}-\vec{k}')}_{\vec{q}}\vec{R}}$$

$\vec{r}$ position vector of the fast electron $\vec{R}$ of the target electron

Theory of core loss

$$\langle \vec{k}' | V | \vec{k} \rangle = \frac{e^2}{(2\pi)^3 \epsilon_0 q^2} e^{i\vec{q}.\vec{R}}$$

$$dP_{if} = \frac{e^4}{(2\pi)^5 \hbar \epsilon_0^2 q^4} |\langle F | e^{i\vec{q}.\vec{R}} | I \rangle|^2 d\nu_f \, \delta(E_I - E_F + E)$$

depends on E-loss & θ

Theory of core loss

$$d\sigma = \sum_{i,f} \frac{dP_{if}}{j_0}$$

j_0 current density of the plane wave

$\psi_{\vec{k}}(\vec{R}) = (2\pi)^{-3/2} e^{i\vec{k}.\vec{R}}$ $\qquad j_0 = (\hbar k)/((2\pi)^3 m)$

$$d\sigma = \sum_{I,F} \frac{me^4}{(\hbar 2\pi\varepsilon_0)^2 q^4 k} |\langle F| e^{i\vec{q}.\vec{R}} |I\rangle|^2 d\nu_f \delta(E_I - E_F + E)$$

$d\nu_f = d\nu_t \, d\nu_e$ ($d\nu_t$: target electron, $d\nu_e$: fast electron)

$d\nu_e = (k' m)/\hbar^2 dE d\Omega$

Theory of core loss

If the final state is expressed in an orthogonal basis set :
$d\nu_t = 1$

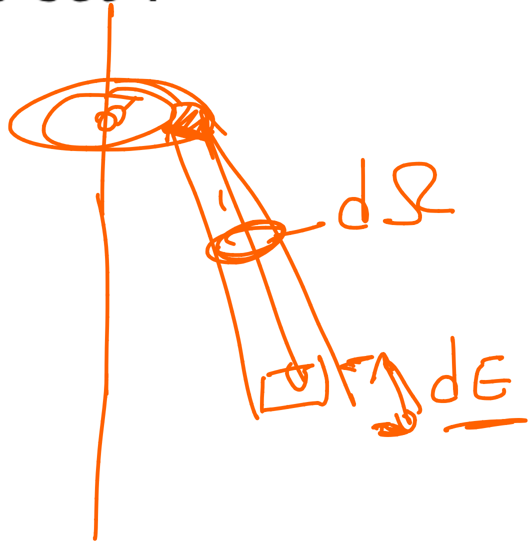

$$d\nu_f = k' \frac{m}{\hbar^2} dE d\Omega$$

$$\frac{\partial^2 \sigma}{\partial E \partial \Omega} = \sum_{I,F} 4 \frac{m^2 e^4}{\hbar^4 (4\pi)^2 \varepsilon_0^2 q^4} \frac{k}{k'} |\langle F| e^{i\vec{q}.\vec{R}} |I\rangle|^2 \delta(E_I - E_F + E)$$

Relativistic effects : $m \rightarrow \gamma m$

$$\gamma = \frac{1}{\sqrt{1 - \frac{v^2}{c^2}}}$$

Core loss EELS: theory

$$\frac{\partial^2\sigma}{\partial E \partial \Omega} = \sum_{I,F} \frac{4\gamma^2}{a_0^2 q^4} \frac{k'}{k} |\langle F| e^{i\vec{q}.\vec{R}} |I\rangle|^2 \delta(E_I - E_F + E) = \frac{4\gamma^2}{a_0^2 q^4} \frac{k'}{k} S(\vec{q}, E)$$

$$S(\vec{q}, E) = \sum_{F} |\langle F| e^{i\vec{q}.\vec{R}} |I\rangle|^2 \delta(E_I - E_F + E)$$

S: Dynamic form factor

a_0 : Bohr radius

$$a_0 = \frac{4\pi\varepsilon_0 \hbar^2}{me^2}$$

$$\vec{q} = \vec{k} - \vec{k}'$$

$$\gamma = (1 - v^2/c^2)^{-1/2}$$

R F Egerton, *Electron energy-loss spectroscopy in the TEM*, Rep. Prog. Phys. 72 (2009) 016502 (25pp); Egerton R F 1996 *Electron Energy-Loss Spectroscopy in the Electron Microscope* 2nd edn (New York: Plenum/Springer)

Introduction

Dipole approximation

$$S(\vec{q},E)=\sum_F |\langle F|e^{i\vec{q}.\vec{R}}|I\rangle|^2\delta(E_I-E_F+E)$$

If $\vec{q}.\vec{R} \ll 1$ we can write $e^{i\vec{q}.\vec{R}} \simeq 1+i\vec{q}.\vec{R}$

$$S(\vec{q},E)=\sum_F |\langle F|i\vec{q}.\vec{R}|I\rangle|^2\delta(E_I-E_F+E)$$

$$S(\vec{q},E)\propto q^2 \quad ; \quad \frac{\partial^2\sigma}{\partial E\partial\Omega}\propto\frac{1}{q^4}S(\vec{q},E)$$

with the scattering geometry, $q^2=k^2(\vartheta_E^2+\vartheta^2)$

$$\frac{\partial^2\sigma}{\partial E\partial E}\propto\frac{1}{q^2}=\frac{1}{k^2(\theta^2+\theta_E^2)}$$

Lorenzian distribution

$$\frac{\partial^2\sigma}{\partial E\partial\Omega}\propto\frac{1}{\vartheta^2+\vartheta_e^2}$$

Angular distribution of the ionisation

$$f(x) = \frac{1}{a^2 + x^2}$$

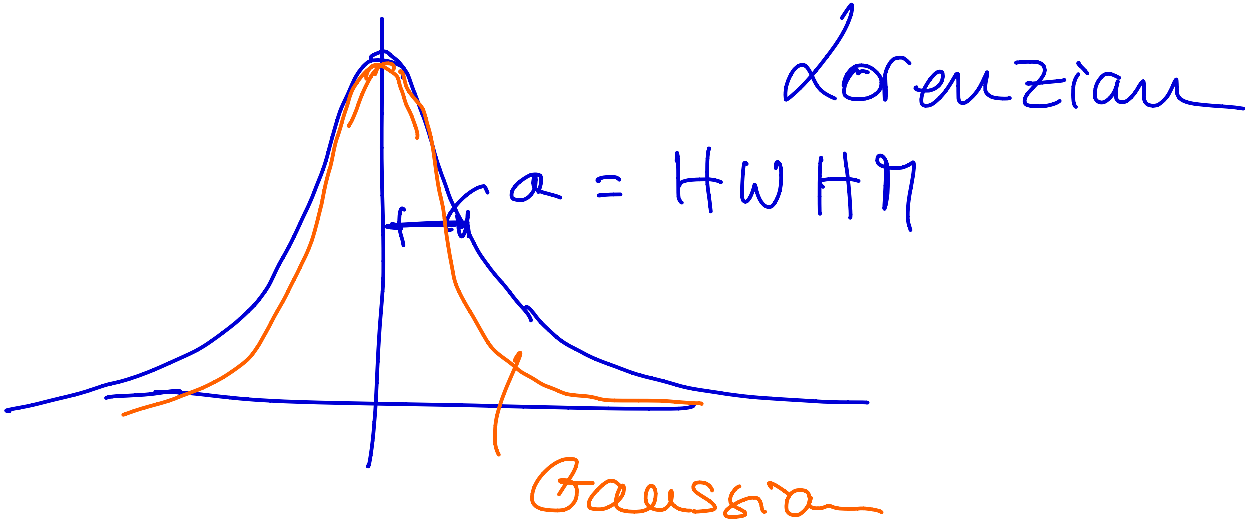

$$f(\theta) = \frac{1}{\theta_E^2 + \theta^2}$$

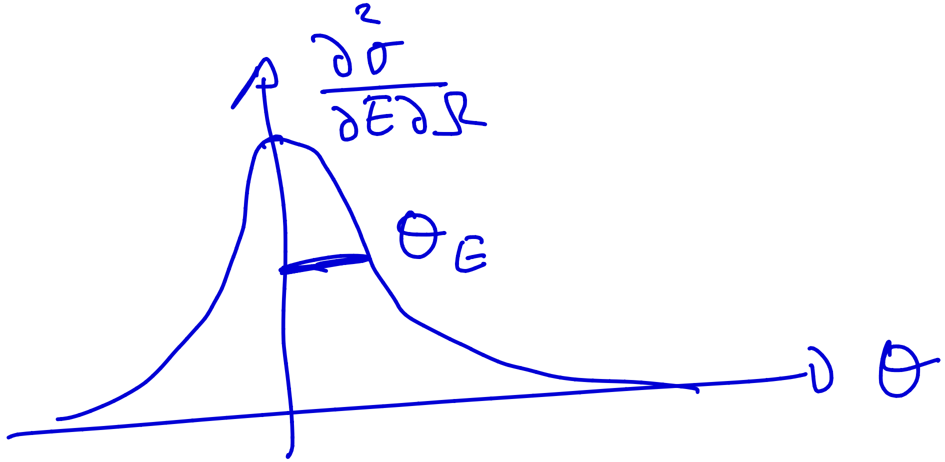

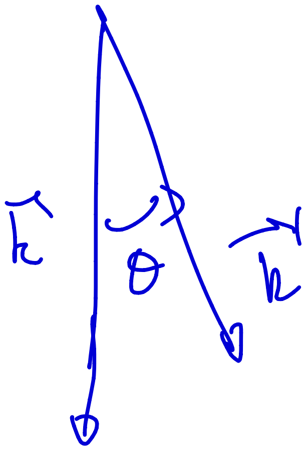

DEMOS 13:30 @ CIME

MXC 012

Core loss EELS: theory

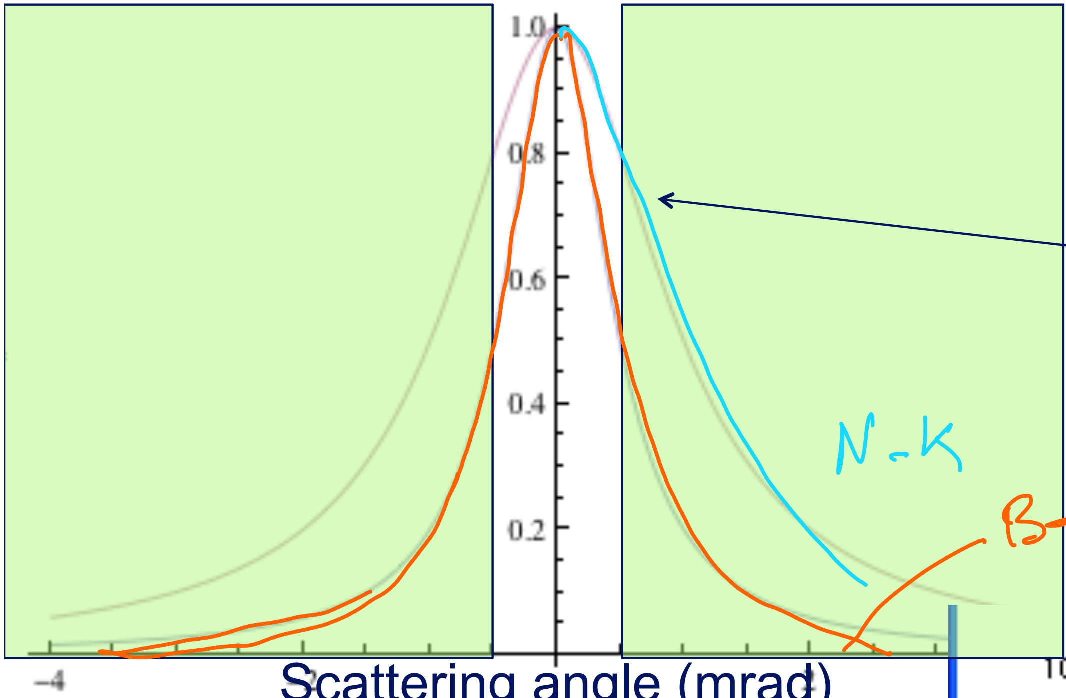

Scattering angle (mrad)

Cutoff (obj. aperture)

Example BN
B-K @200 eV
N-K @400 eV

$$\theta_E = \Delta E m \gamma / \hbar^2 k^2$$

$\theta_E \sim \Delta E / 2E_0$; @200kV:

$\theta_{E\ B\text{-}K}$=0.5 mrad
$\theta_{E\ N\text{-}K}$=1 mrad

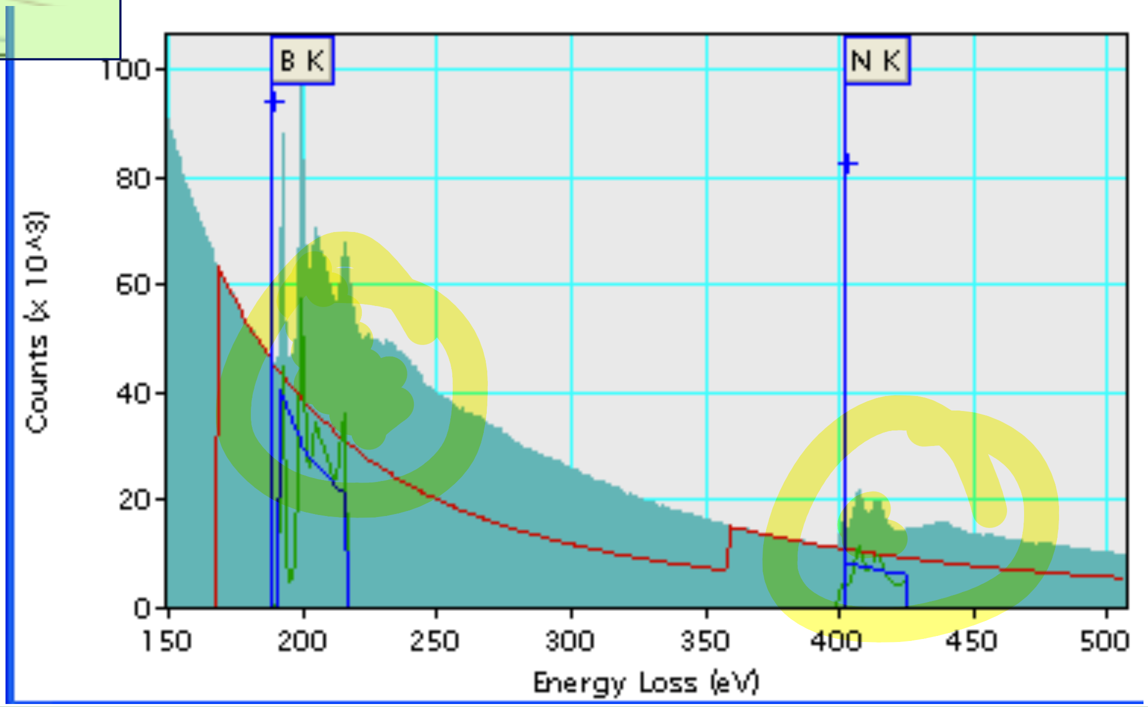

Introduction

$$S(\vec{q},E) = \sum_F |\langle F|e^{i\vec{q}.\vec{R}}|I\rangle|^2 \delta(E_I - E_F + E)$$

Final state: ??

Unoccupied DOS

Initial state:
Core state

e.g. B-K

B |1s⟩

Easiest approximation: forget about crystal: atomic model
(Hydrogenic, Hartree –Slater, …)

Used for quantification
Can already explain some features

E_F

Next step: take crystal into account for |F> → DFT

Further : consider real electron wave in the crystal (instead of plane wave)
Work in progress P. Schattschneider (TU Vienna), Oxley & Pantelides (Oak Ridge)

Core loss EELS: quantification

☞ Intensity in the EELS spectrum will be used for quantification

The *partial* ionisation cross section is given by :

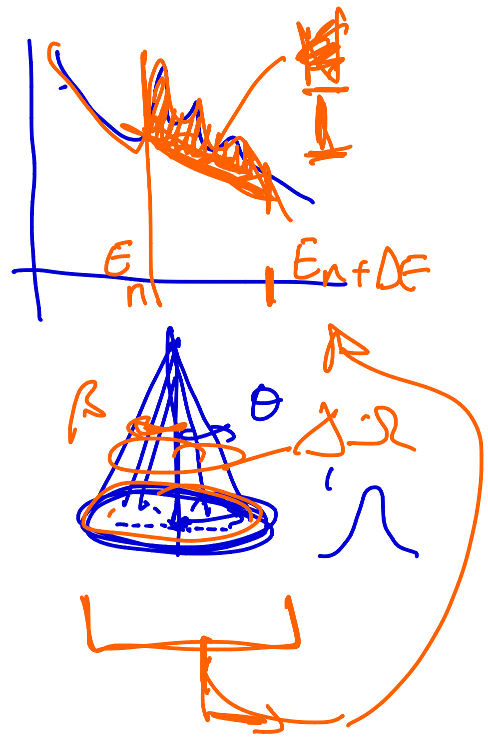

$$\Delta\sigma = \int_{E_n}^{E_n+\Delta E} \int_{\Delta\Omega} dE d\Omega \frac{\partial^2 \sigma}{\partial E \partial \Omega}.$$

$\Delta\sigma$ has the dimension : m^2/atom.

An incident beam of *curent density* j_0 will generate a detected current I (within the interval $\Delta E \Delta \Omega$) if it crosses a sample with N atoms

$$I = N \Delta\sigma j_0.$$

$$N = \frac{I}{\Delta\sigma \cdot j_0}$$

Core loss EELS: quantification

Multiple scattering:
Fourier-ratio deconvolution

High energy tail of lower energy losses:
Background removal

$\propto AE^{-r}$

Dark signal correction

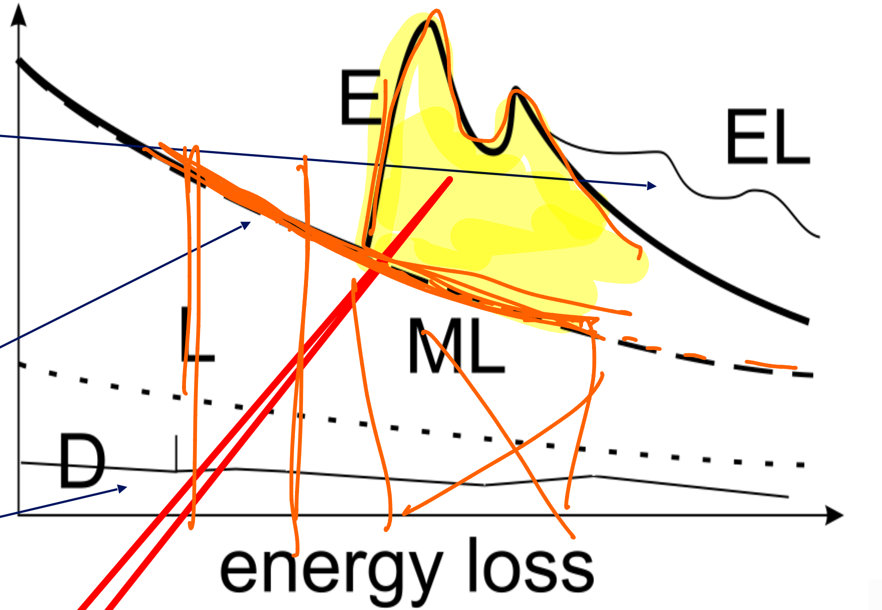

$$N = \frac{I}{j_0 \Delta\sigma}$$

Theoretical model
Egerton's programm
(Digital micrograph)

~ 10 to 20% accuracy.

$$\frac{N_a}{N_b} = \frac{I_a}{I_b} \underbrace{\frac{\Delta\sigma_b}{\Delta\sigma_a}}_{\text{k-factor}}$$

Relative quantification: No need of j_0

Core loss EELS: theory

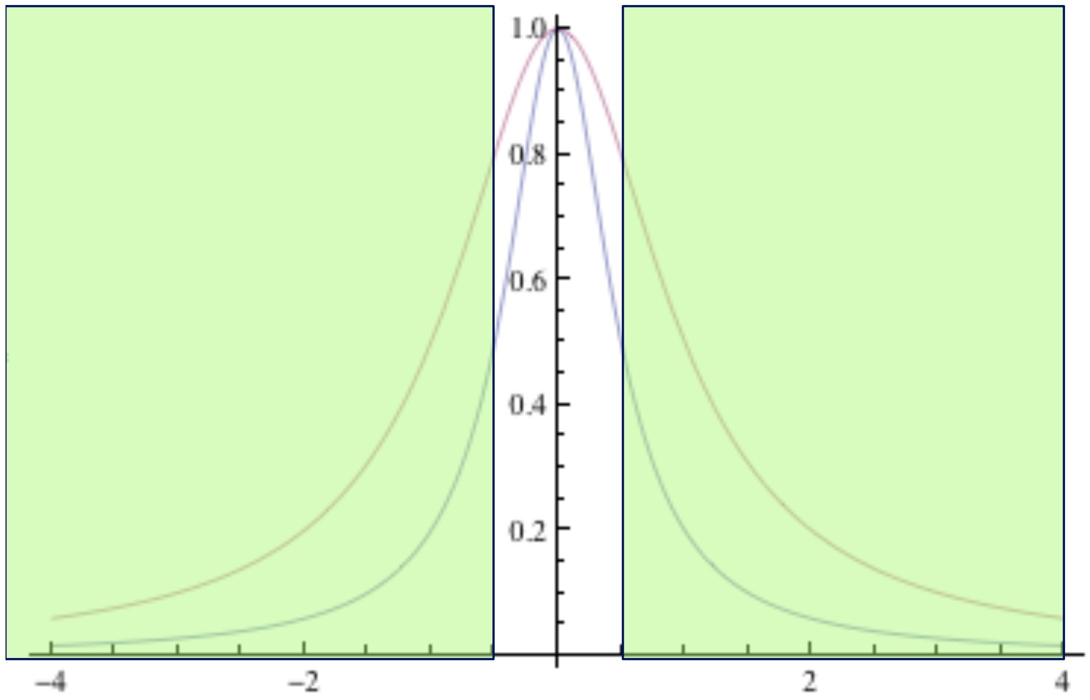

Beam Energy: 200 keV
Convergence Semi-Angle: 0 mrad
Collection Semi-Angle: **100 mrad**

Relative quantification:

Elem.	Atomic ratio (/N)	% content
B	0.89 ± 0.126	~~47.08~~ ± 4,708
N	1.00 ± 0.000	~~52.92~~

→ 47 ± 5 %

Beam Energy: 200 keV
Convergence Semi-Angle: 0 mrad
Collection Semi-Angle: **0.5 mrad**

$\theta_E \sim \Delta E / 2E_0$

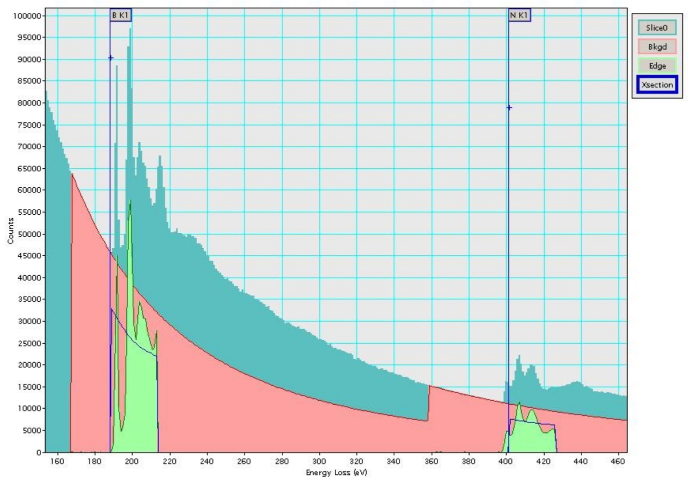

Relative quantification:

Elem.	Atomic ratio (/N)	% content
B	0.30 ± 0.042	22.89
N	1.00 ± 0.000	77.11

Outline

- Introduction: EELS in the TEM
- Instrumentation
- Core Loss EELS
  - Theory
  - Applications
- Low losses
- Imaging (EFTEM)
- ELNES

Core loss EELS: applications

L. Samet & al. Eur. Phys. J. B 34, 179-192 (2003)

EELS study of interfaces in magnetoresistive LSMO/STO/LSMO tunnel junctions

$La_{0.66}Sr_{0.33}MnO_3$,/$SrTiO_3$ /$La_{0.66}Sr_{0.33}MnO_3$

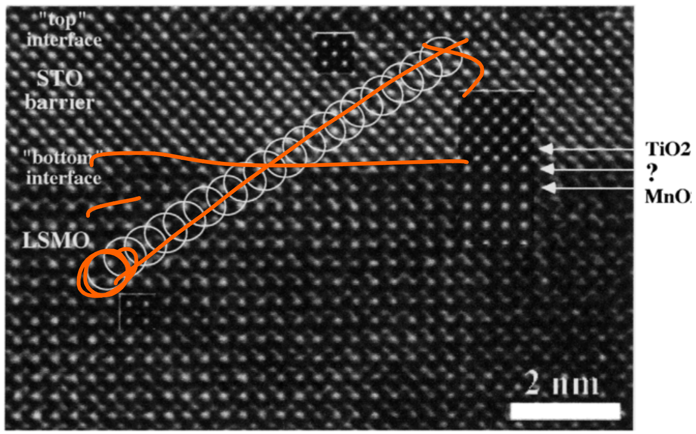

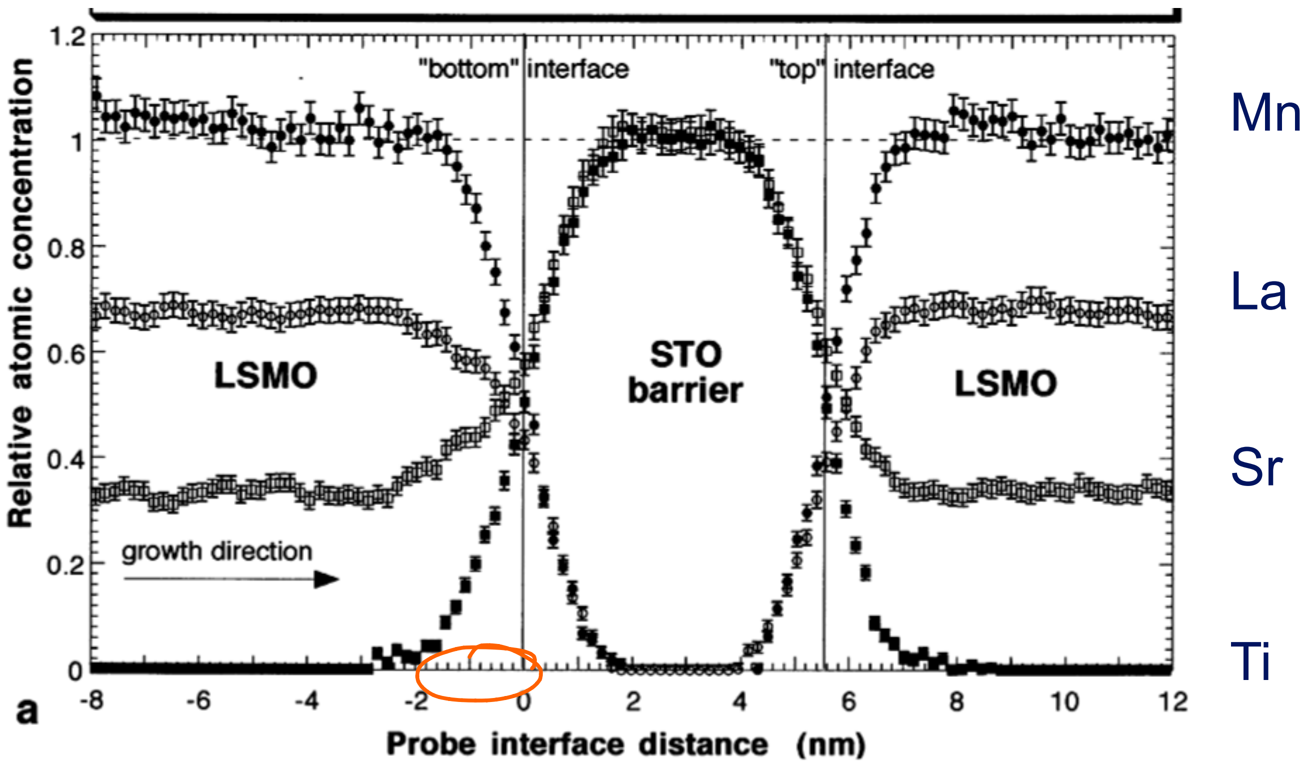

Core loss EELS: applications

Atomic-Scale Chemical Imaging of Composition and Bonding by Aberration-Corrected Microscopy
D. A. Muller, *et al.*
Science **319**, 1073 (2008);
DOI: 10.1126/science.1148820

Fig. 1. Spectroscopic imaging of a $La_{0.7}Sr_{0.3}MnO_3$/$SrTiO_3$ multilayer, showing the different chemical sublattices in a 64 × 64 pixel spectrum image extracted from 650 eV–wide electron energy-loss spectra recorded at each pixel. (**A**) La M edge; (**B**) Ti L edge; (**C**) Mn L edge; (**D**) red-green-blue false-color image obtained by combining the rescaled Mn, La, and Ti images. Each of the primary color maps is rescaled to include all data points within two standard deviations of the image mean. Note the lines of purple at the interface in (D), which indicate Mn-Ti intermixing on the B-site sublattice. The white circles indicate the position of the La columns, showing that the Mn lattice is offset. Live acquisition time for the 64 × 64 spectrum image was ~30 s; field of view, 3.1 nm.

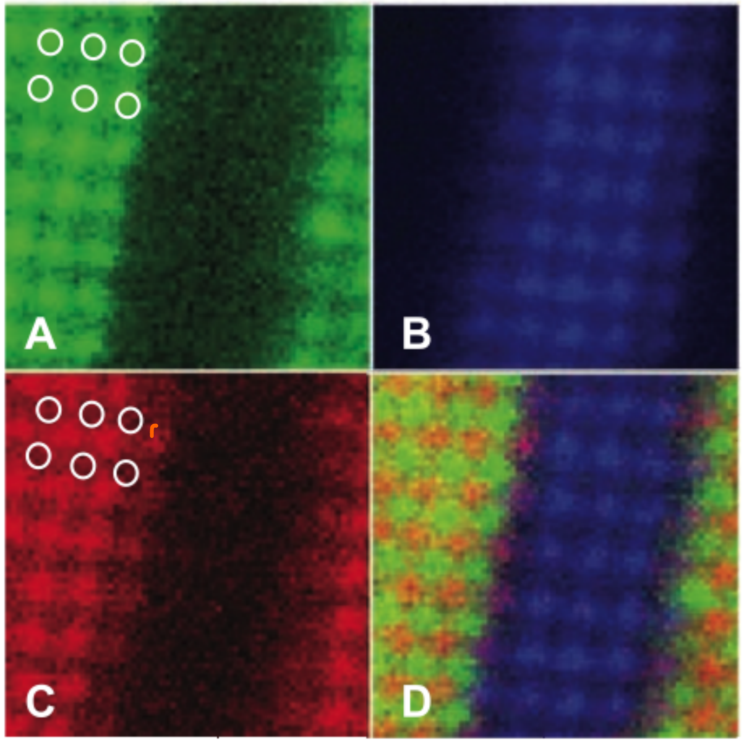

Core loss EELS: applications

ELSEVIER

Journal of Structural Biology 150 (2005) 144–153

www.elsevier.com/locate/yjsbi

Electron tomography of
with abnormal regu

Peijun Zhang [a], William Land [b], Stantc
Sophia R. Smith [b], David Germai
Tracey A. Rouault

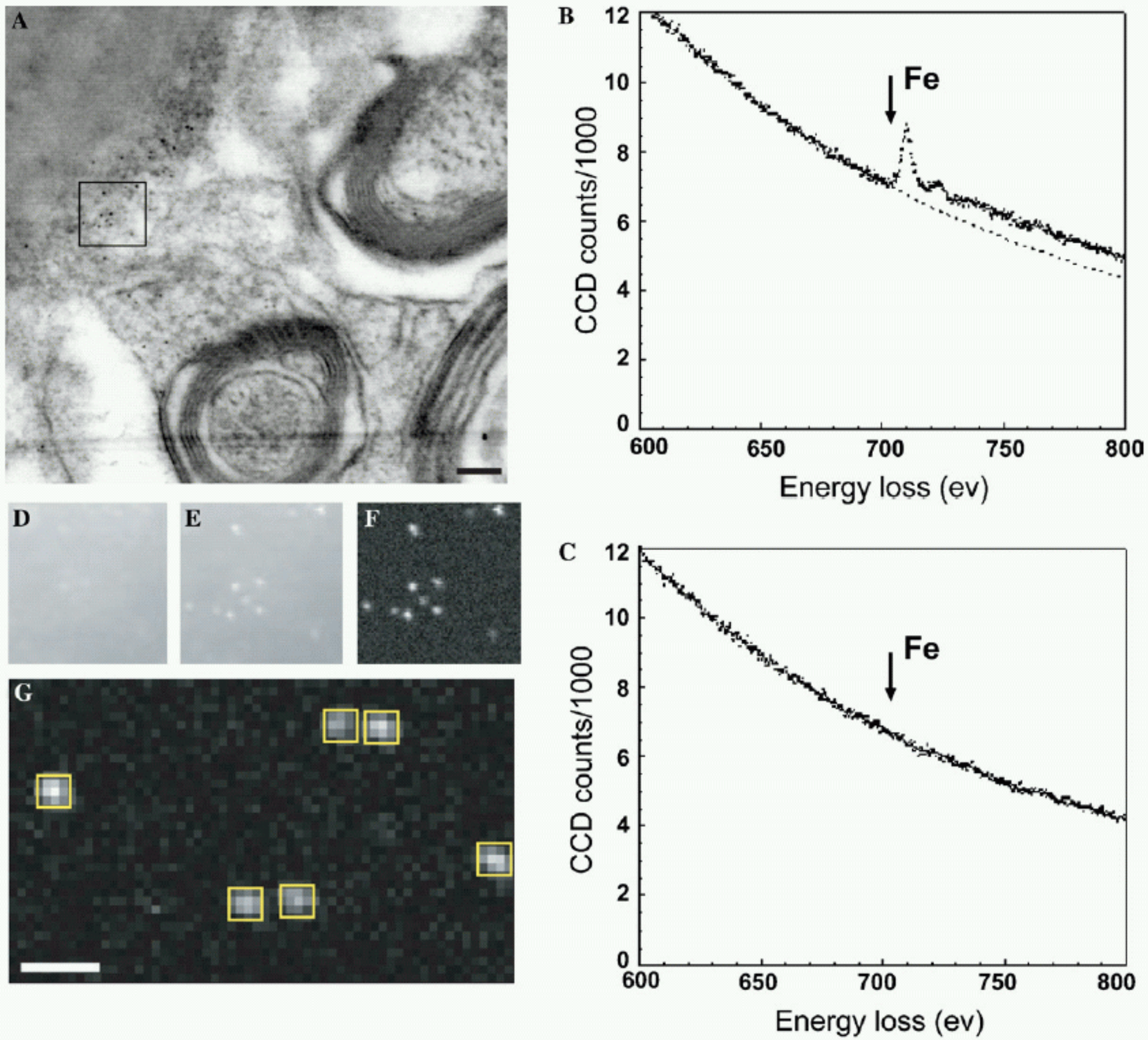

Identification of ferritin molecules. dark field STEM image (contrast reversed) of a thin tissue section from the IRP knockout mouse brain.

Core loss EELS: applications

Accuracy: - 15-20% under normal conditions
- can be lowered to a few % (standards, same thickness, same exp conditions…)

What? (nearly) everything. Good for light elements (H, He difficult).

Det. Limit Normally a few % (1 to 10).
Record: single atom detection

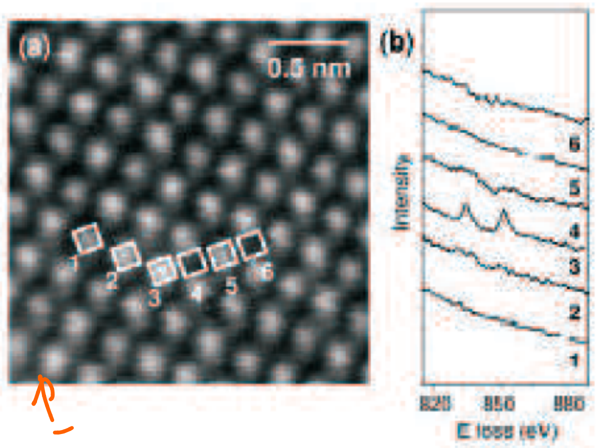

Varela et al PRL 92 (2004) 095502-1

Outline

- Introduction: EELS in the TEM
- Instrumentation
- Core Loss EELS
  - Theory
  - Applications
- Low losses
- Imaging (EFTEM)
- ELNES

Low Loss

Visible light

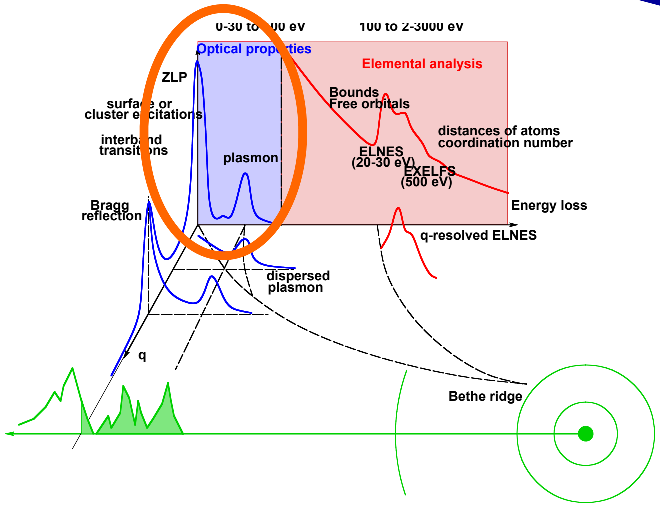

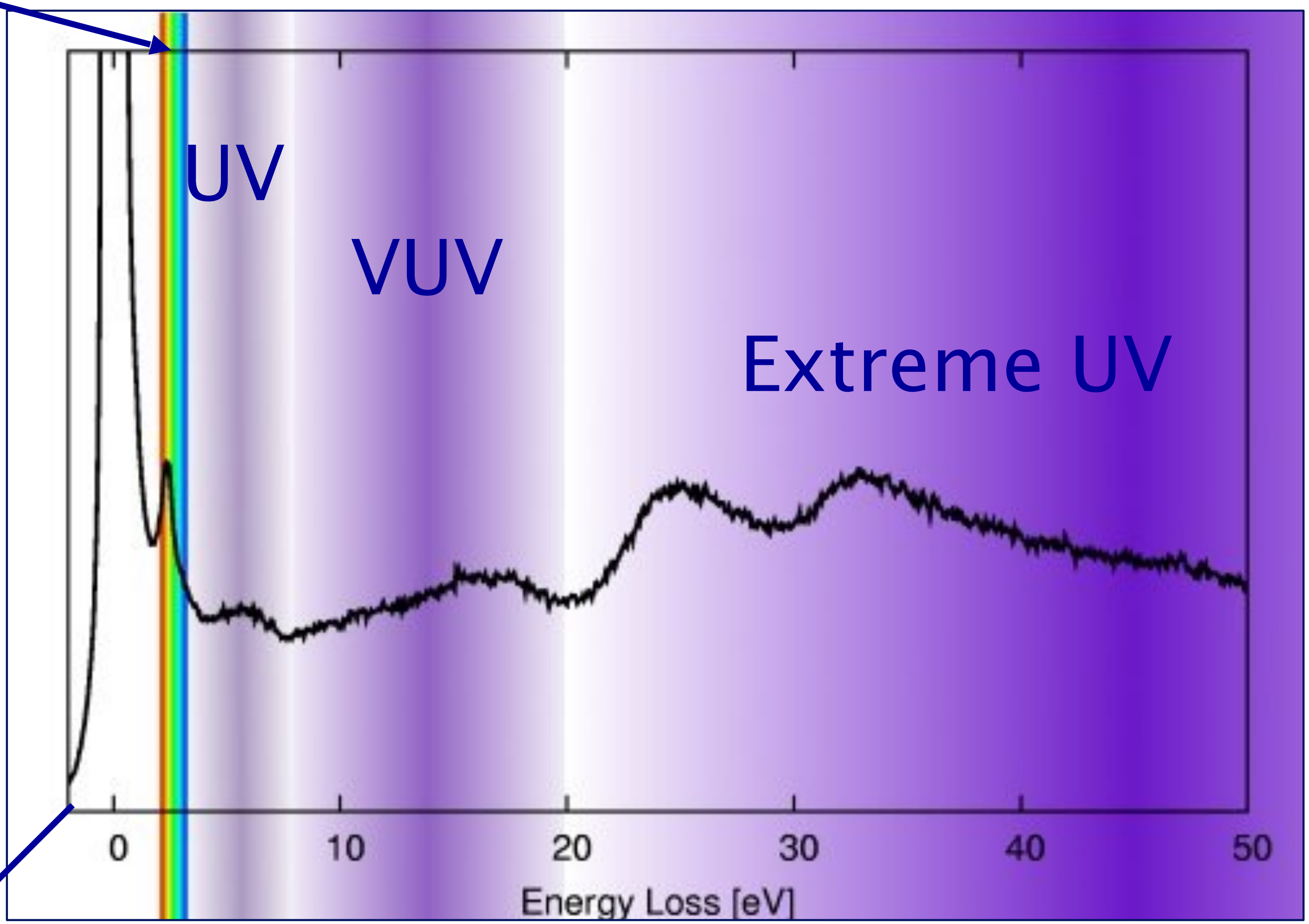

Plasmons (collective oscilations)

Interband transitions

Scattering angle (momentum transfer)

loss function $\mathrm{Im}\left(-\frac{1}{\varepsilon}\right)$ ε = complex dielectric funct. $= \varepsilon_1 + i\,\varepsilon_2$

SSD and loss function

$$S(E) = \left[\frac{e^2}{\pi \hbar v}\right]^2 \cdot D \cdot \Im\left[\frac{-1}{\varepsilon(E)}\right] \cdot \ln\left[1 + \left(\frac{\beta}{\theta_E}\right)^2\right]$$

single scattering distribution

Sample thickness

Loss function

Angular scattering distribution

↳ measure E-loss spectrum

Low Loss: KKA

From the experiment to the loss function: theory

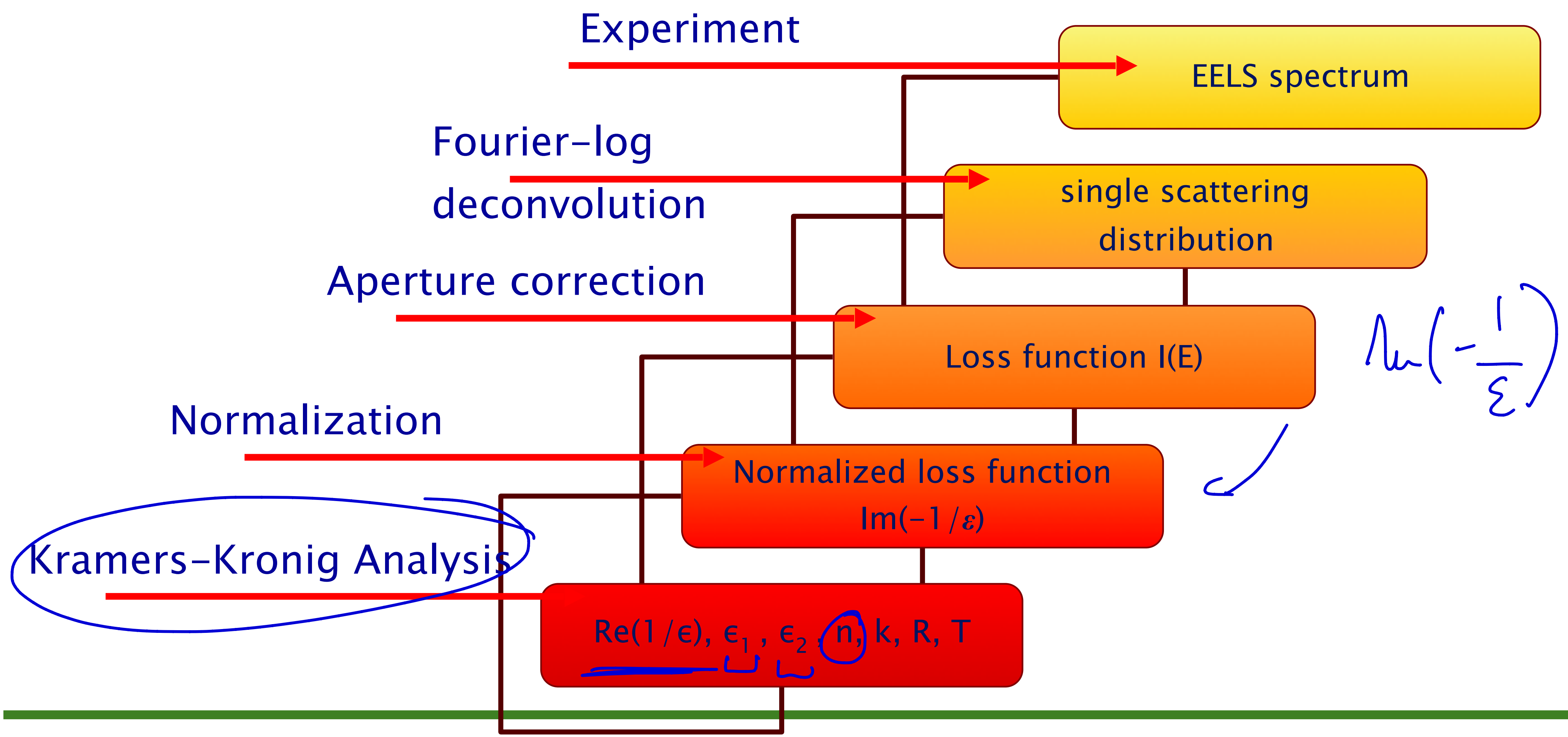

Low Loss: the Kröger equation

The relation between the double differential cross section and the loss function is a „little bit“ more complicated

$$\frac{\partial P(\omega,\mathbf{k}_\perp)}{\partial\omega\partial^2 k_\perp} = \frac{e^2}{\pi^2\hbar v^2}\cdot\Im\Bigg[\frac{\mu^2}{\epsilon\phi^2}\cdot D$$

Volume term + non Cherenkov term

$$- \frac{2k_\perp^2(\epsilon-\epsilon_0)^2}{\phi_0^4\phi^4}\cdot\left\{\frac{\phi_{01}^4}{\epsilon\epsilon_0}\left(\frac{sin^2(\frac{\omega D}{2v})}{L^+}+\frac{cos^2(\frac{\omega D}{2v})}{L^-}\right)\right.$$

$$+\beta^2\cdot\frac{\lambda_0\omega\phi_{01}^2}{\epsilon_0 v}\cdot\left(\frac{1}{L^+}-\frac{1}{L^-}\right)\cdot sin\left(\frac{\omega D}{v}\right)$$

$$\left.-\beta^4\cdot\frac{\omega^2}{v^2}\cdot\lambda_0\lambda\left(\frac{cos^2(\frac{\omega D}{2v})tanh(\lambda D/2)}{L^+}+\frac{sin^2(\frac{\omega D}{2v})coth(\lambda D/2)}{L^-}\right)\right\}\Bigg]$$

Following abbreviations were used:

$$\lambda = \sqrt{k_\perp^2 - \frac{\epsilon\omega^2}{c^2}},\quad \lambda_0 = \sqrt{k_\perp^2 - \frac{\epsilon_0\omega^2}{c^2}}$$

$$L^+ = \lambda_0\epsilon + \lambda\epsilon_0 tanh(\lambda D/2),\quad L^- = \lambda_0\epsilon + \lambda\epsilon_0 coth(\lambda D/2)$$

$$\beta^2 = \frac{v^2}{c^2},\quad \phi_{01}^2 = k_\perp^2 + \frac{\omega^2}{v^2} - (\epsilon+\epsilon_0)\frac{\omega^2}{c^2}$$

$$\phi^2 = \lambda^2 + \frac{\omega^2}{v^2},\quad \phi_0^2 = \lambda_0^2 + \frac{\omega^2}{v^2}$$

$$\mu^2 = 1-\epsilon\beta^2,\quad \mu_0^2 = 1-\epsilon_0\beta^2$$

Z. Phys. 216 (1968), 115-135

Low Loss

Relativistic effects in semiconductors - Bulk

A lower TEM-acceleration voltage allows higher n-materials!

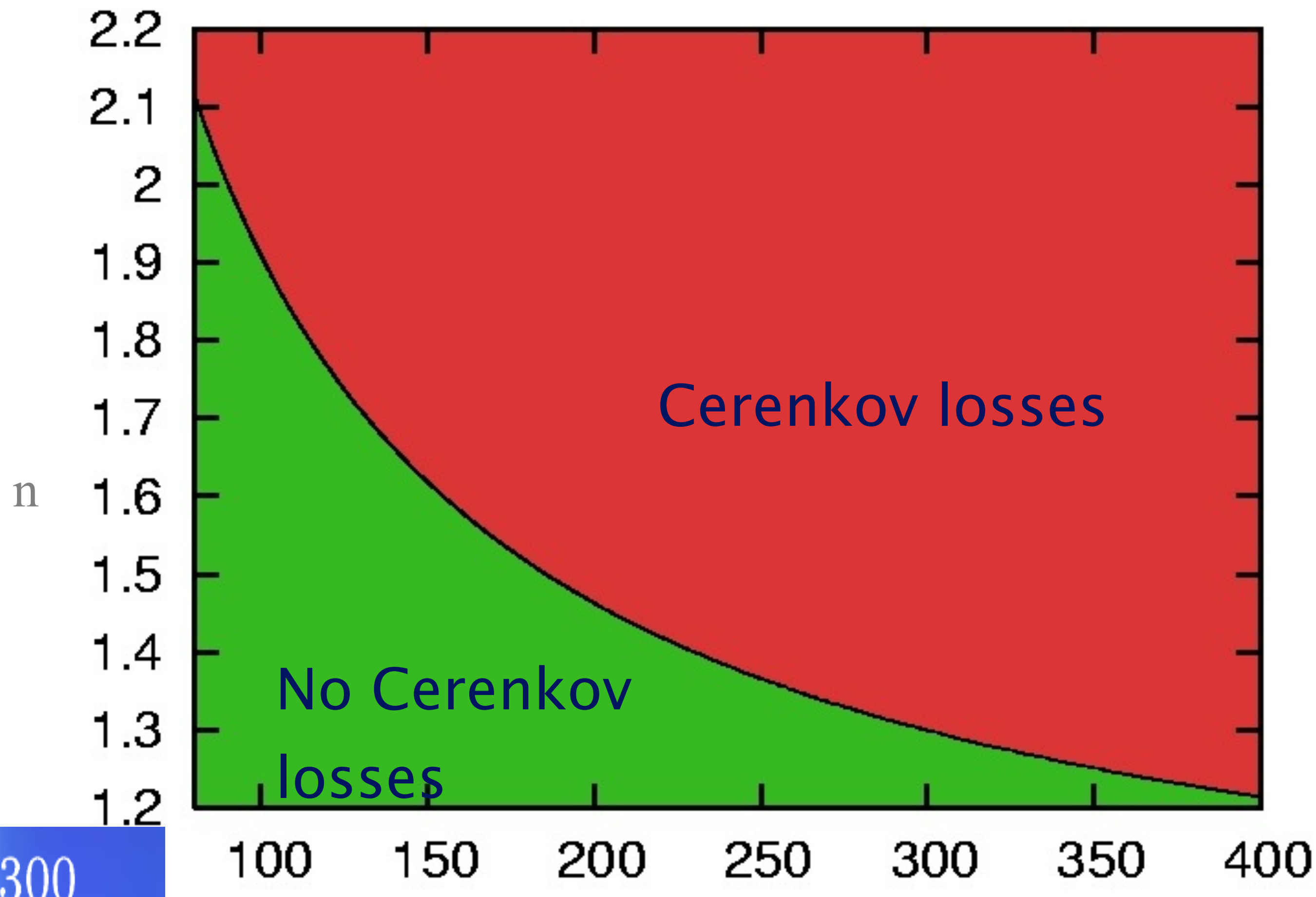

kV	100	200	300
n	1.8242	1.4381	1.2878
ϵ_1	3.3278	2.0683	1.6584

Low Loss: some solutions

Decrease TEM voltage (SiN_x:H)

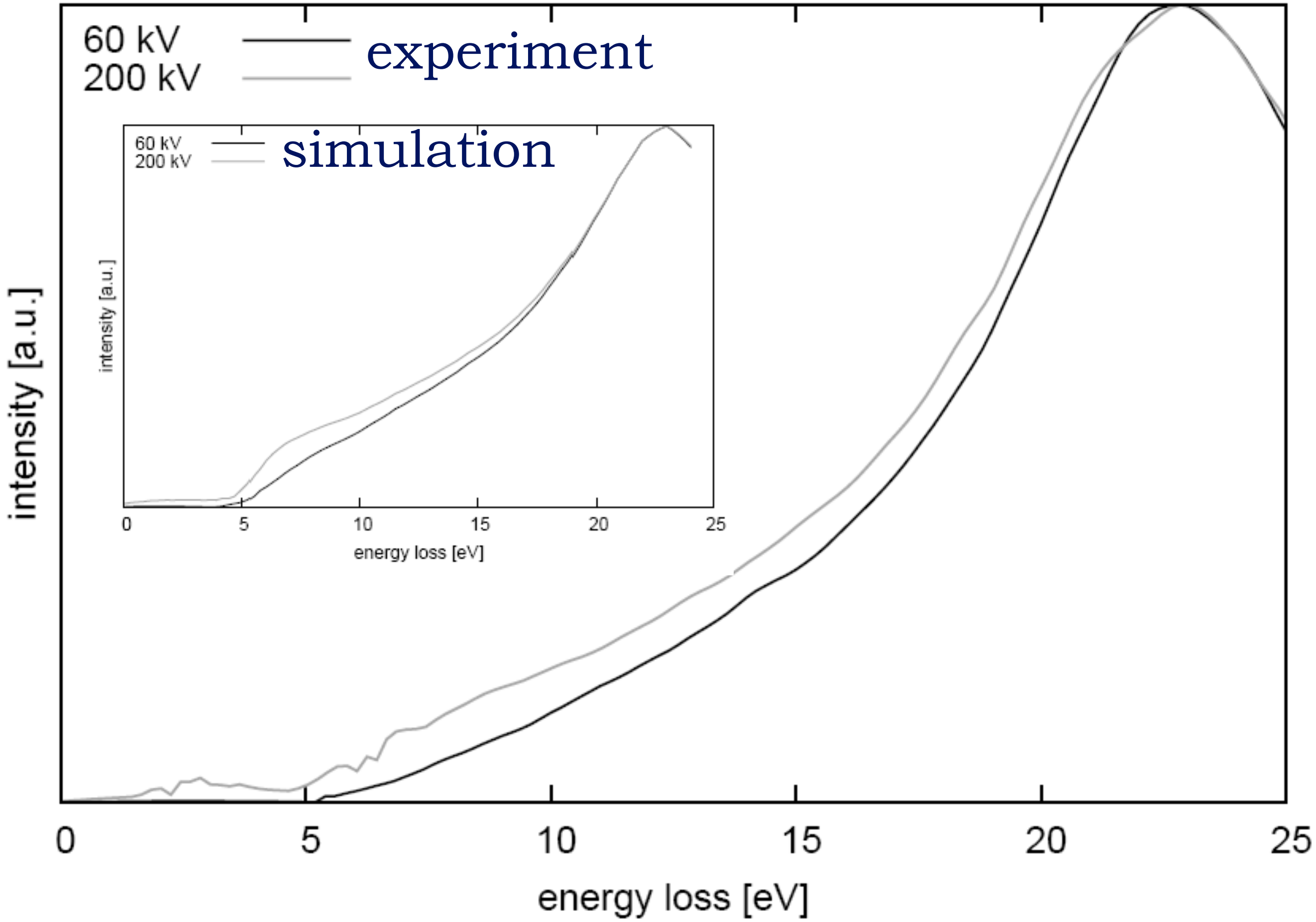

KKA – refractive index

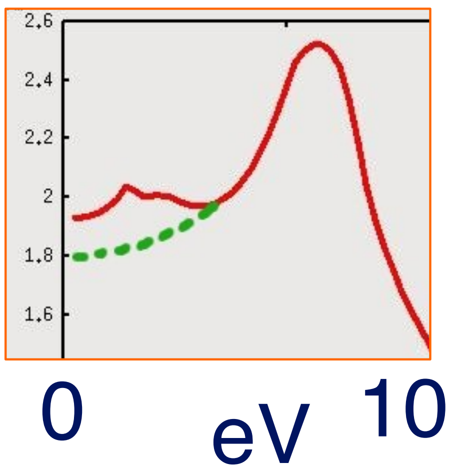

M. Stöger-Pollach, UM 107, (2007) p. 1178-85

Low Loss: some solutions

difference method (Si)

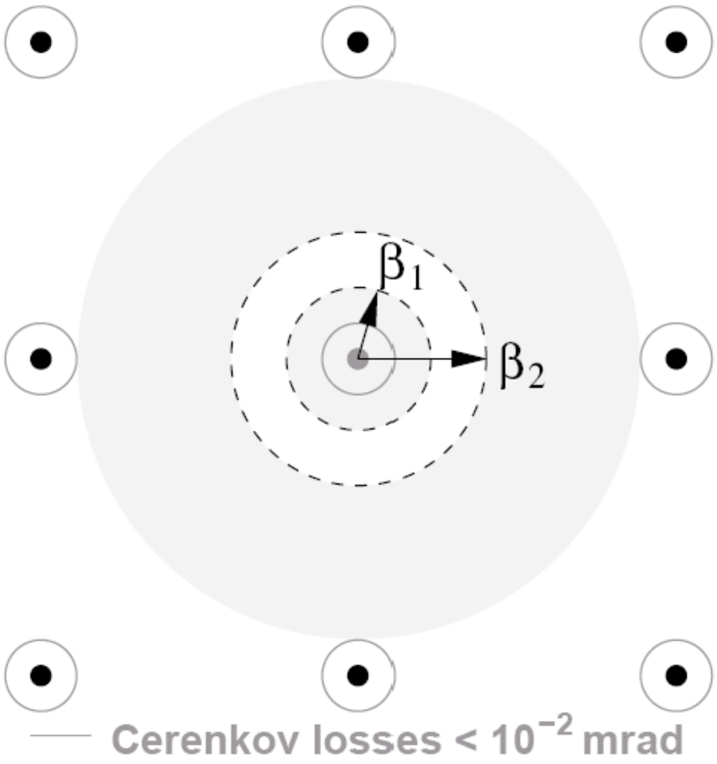

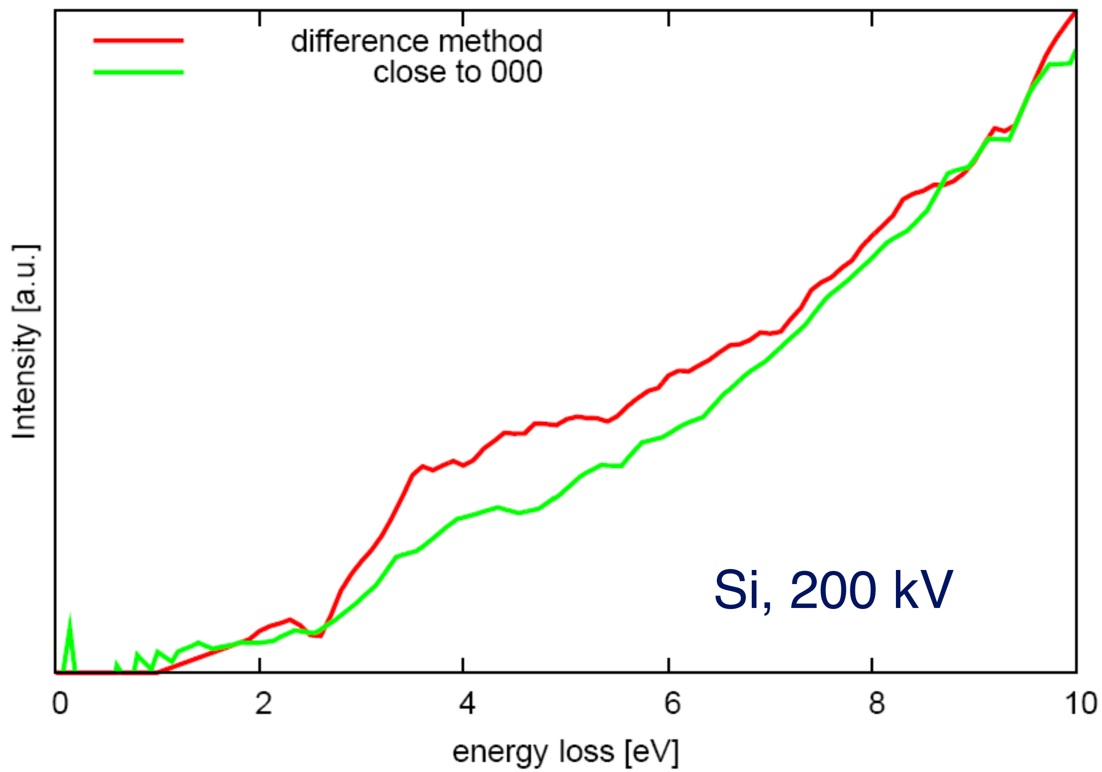

M. Stöger-Pollach, UM 107, (2007) p. 1178-85

Outline

- Introduction: EELS in the TEM
- Instrumentation
- Core Loss EELS
  - Theory
  - Applications
- Low losses
- Imaging (EFTEM)
- ELNES

Imaging (EFTEM)

Operated as energy filter

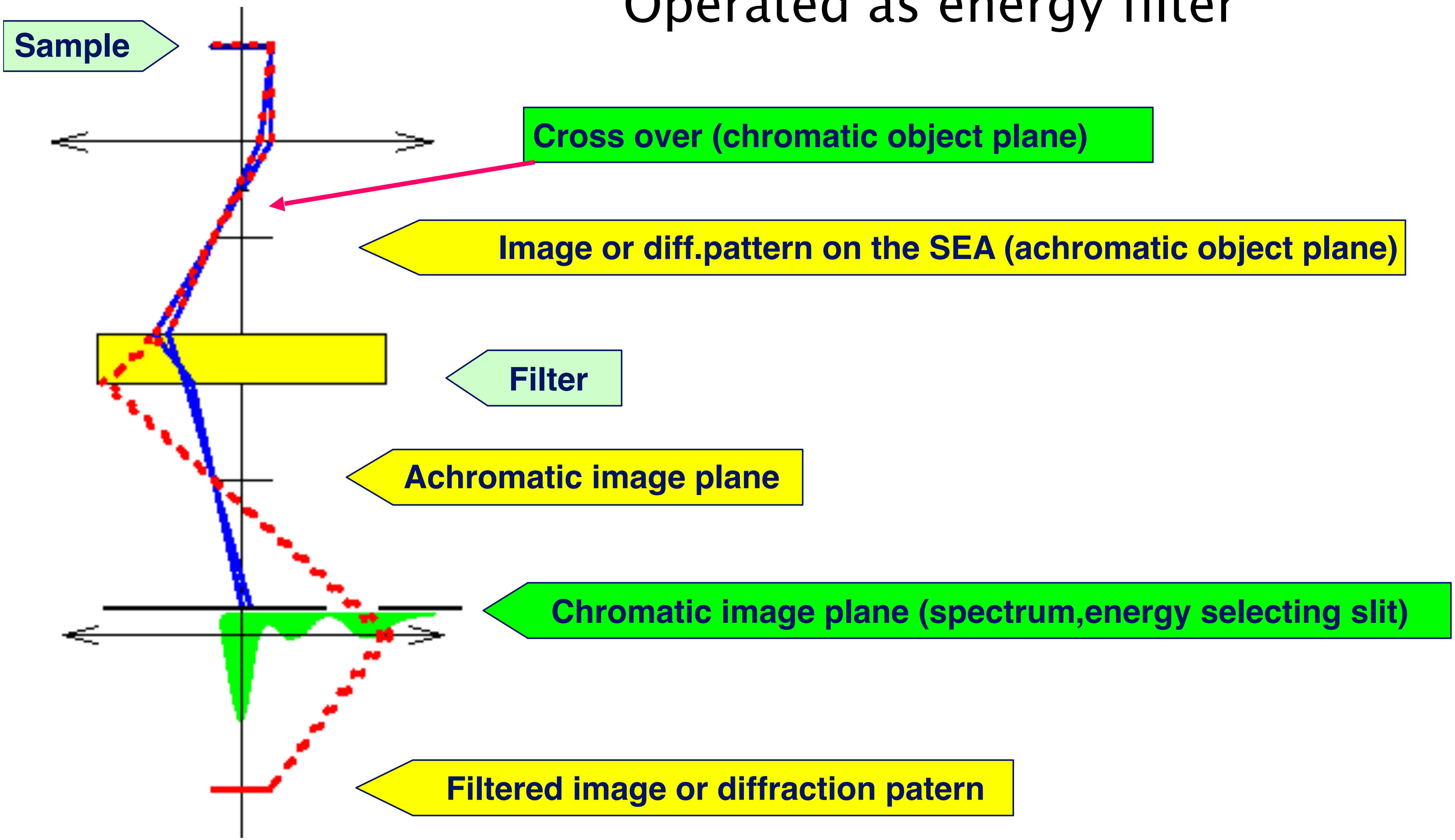

EFTEM: Zero-loss image

300nm thick section of resin embedded brain samples*. 200kV Microscope, 20mrad contrast aperture

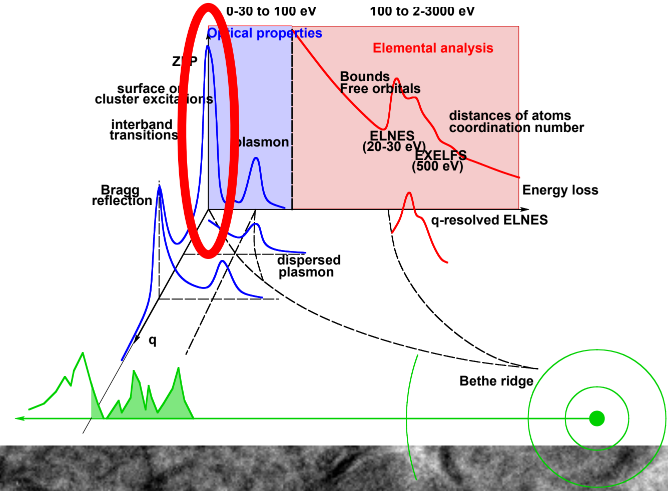

axonal bouton containing vesicles

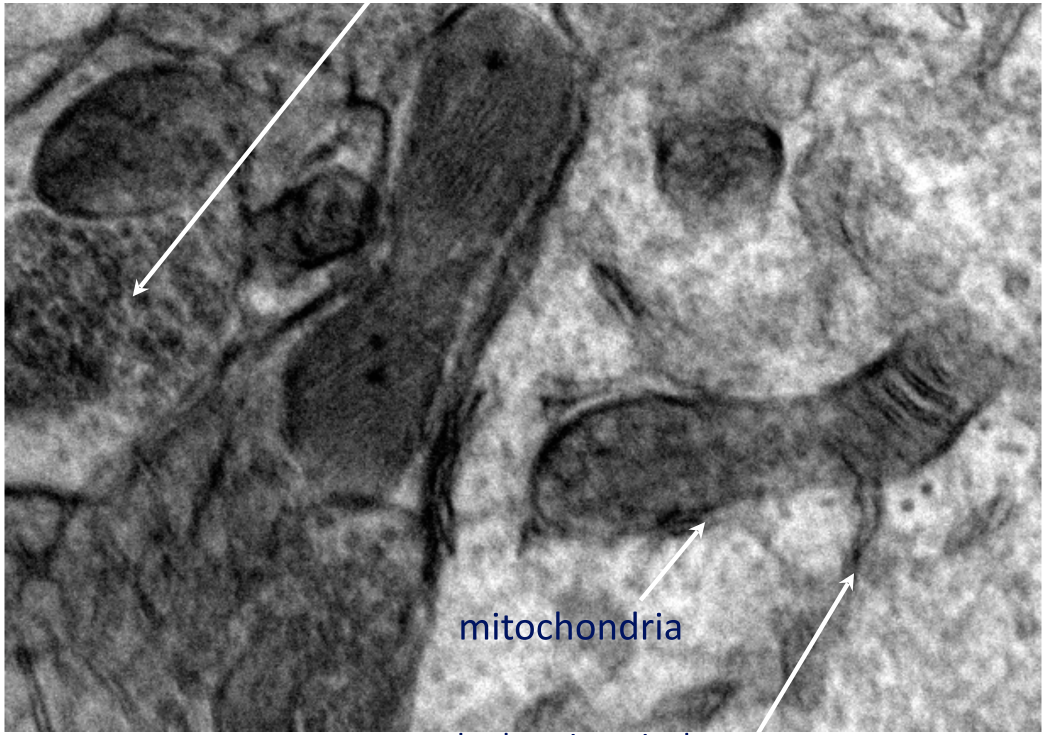

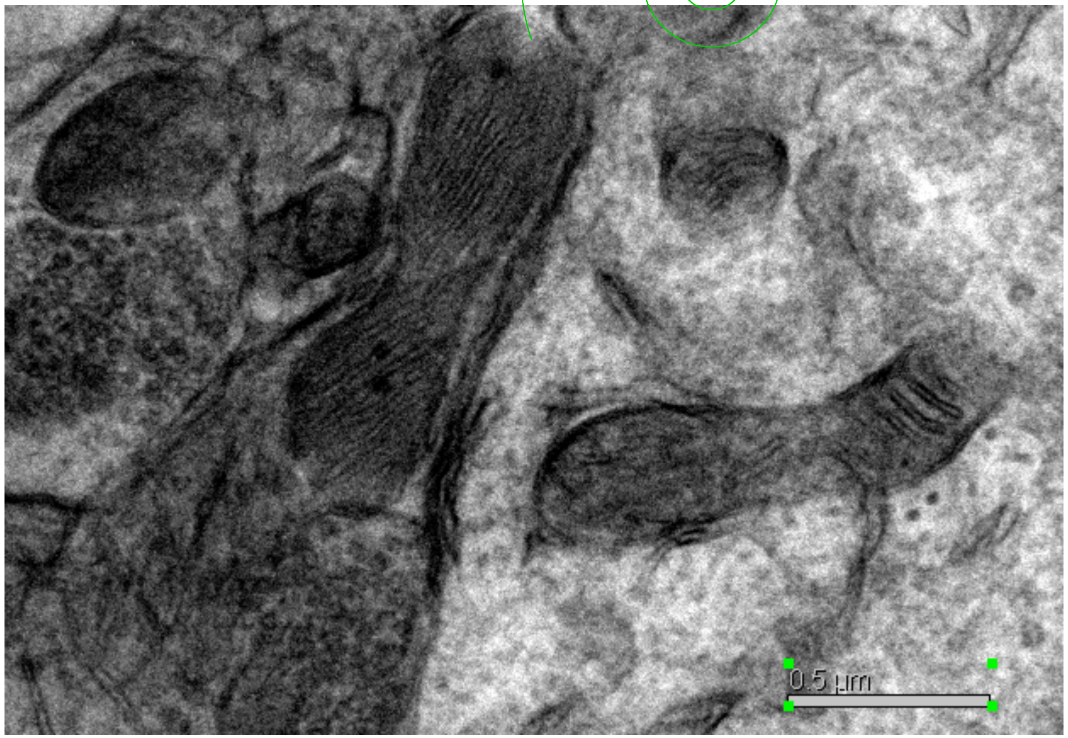

Unfiltered

endoplasmic reticulum

ZLP filtered with 15 eV slit

* adult rat somatosensory cortex, aldehyde fixed, osmium and uranyl acetate stained

EFTEM: Zero-loss image

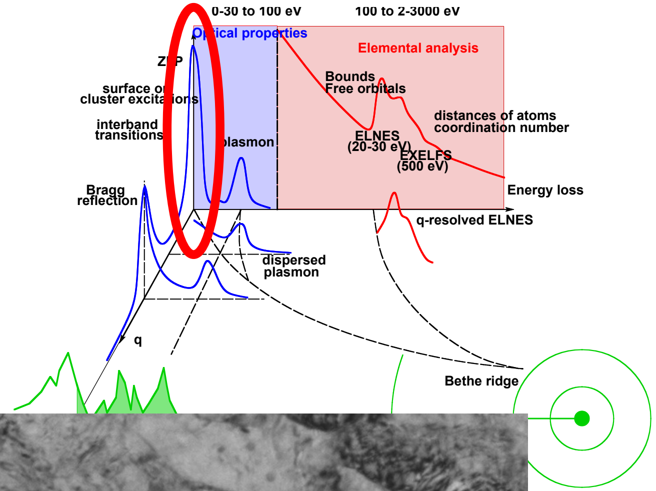

ODS reinforced steel. Left not filtered, right ZLP filtered (7eV slit). 200 kV.
Specimen thicness c.a. 250nm

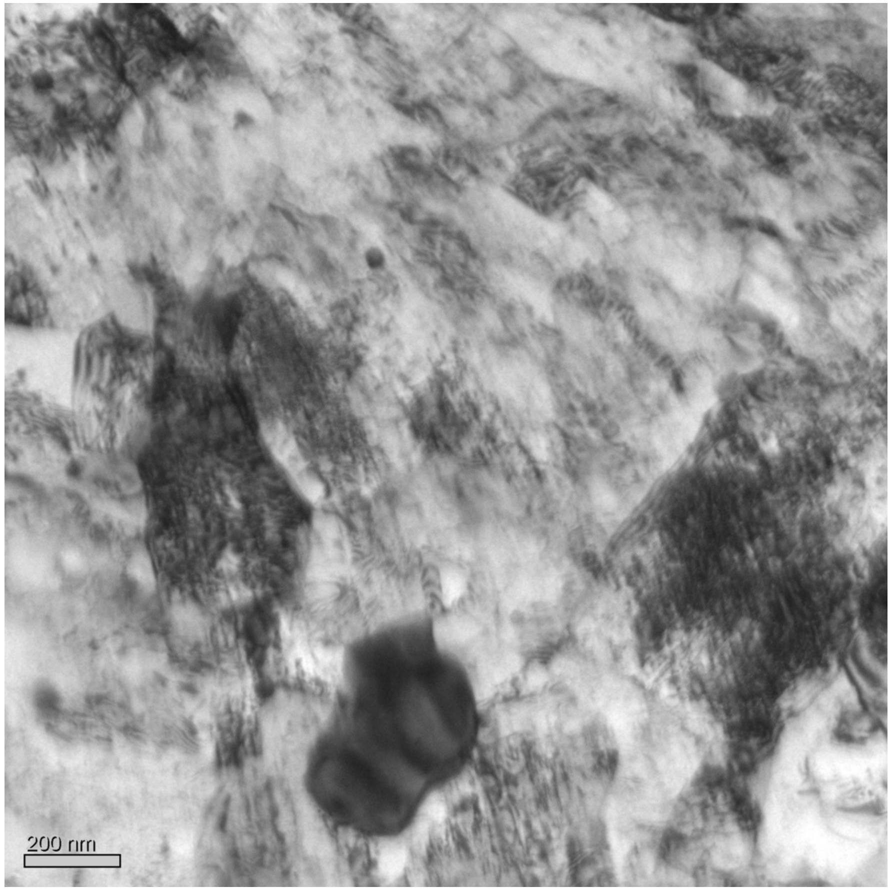

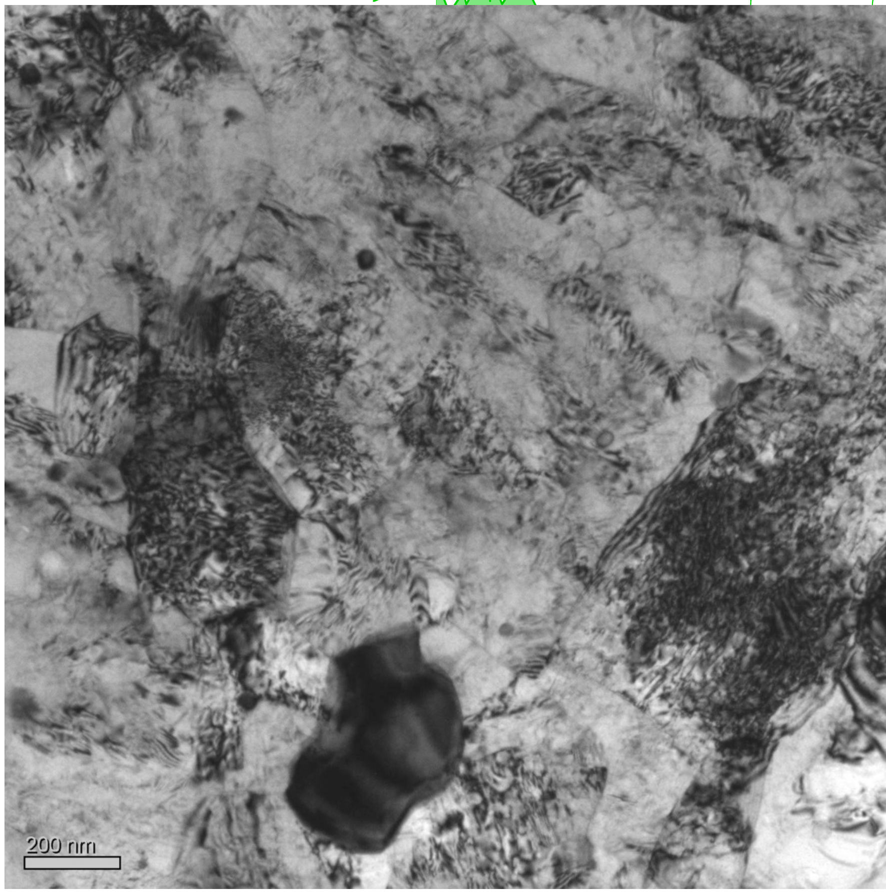

EFTEM: Plasmon images

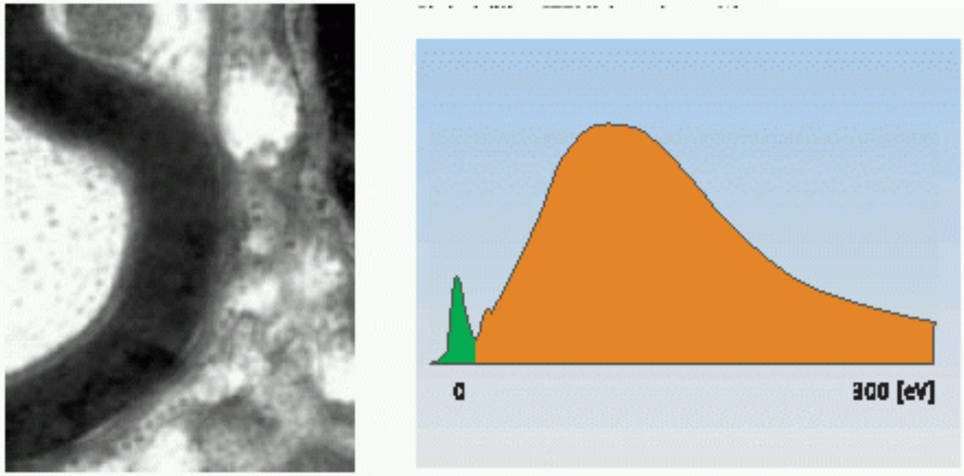

Nerve section of about 500 nm in thickness.

Full electron bandwidth in CTEM imaging.

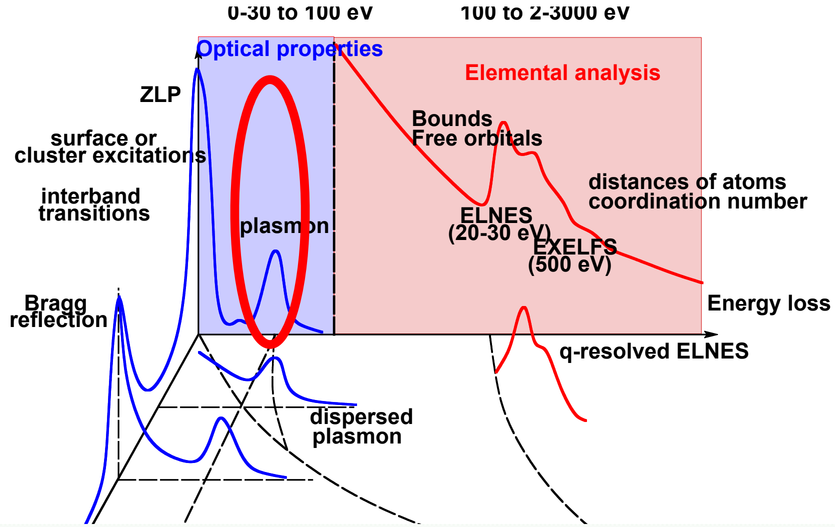

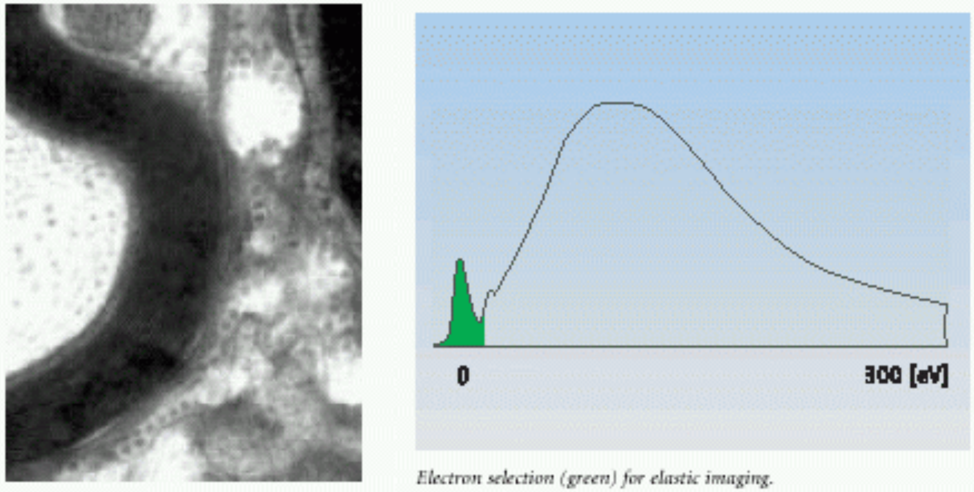

Electron selection (green) for elastic imaging.

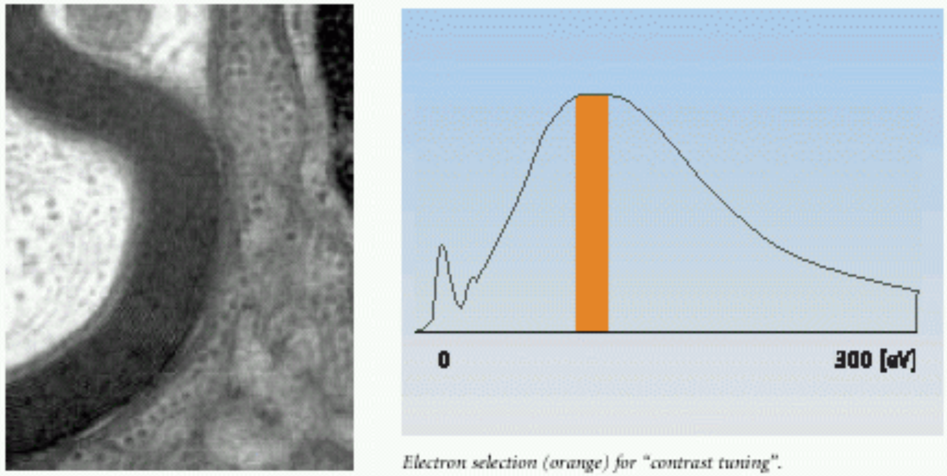

Electron selection (orange) for "contrast tuning".

Nerve section of about 500 nm in thickness.

EFTEM: Plasmon Imaging

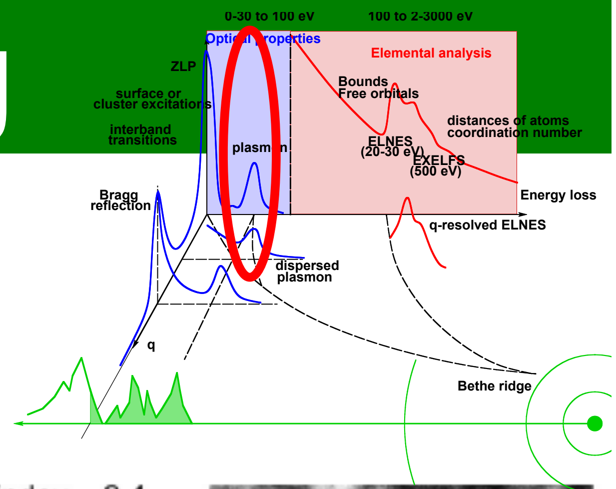

Plasmon EFTEM analysis of SiO_x layers for high-efficiency thin-film solar cells

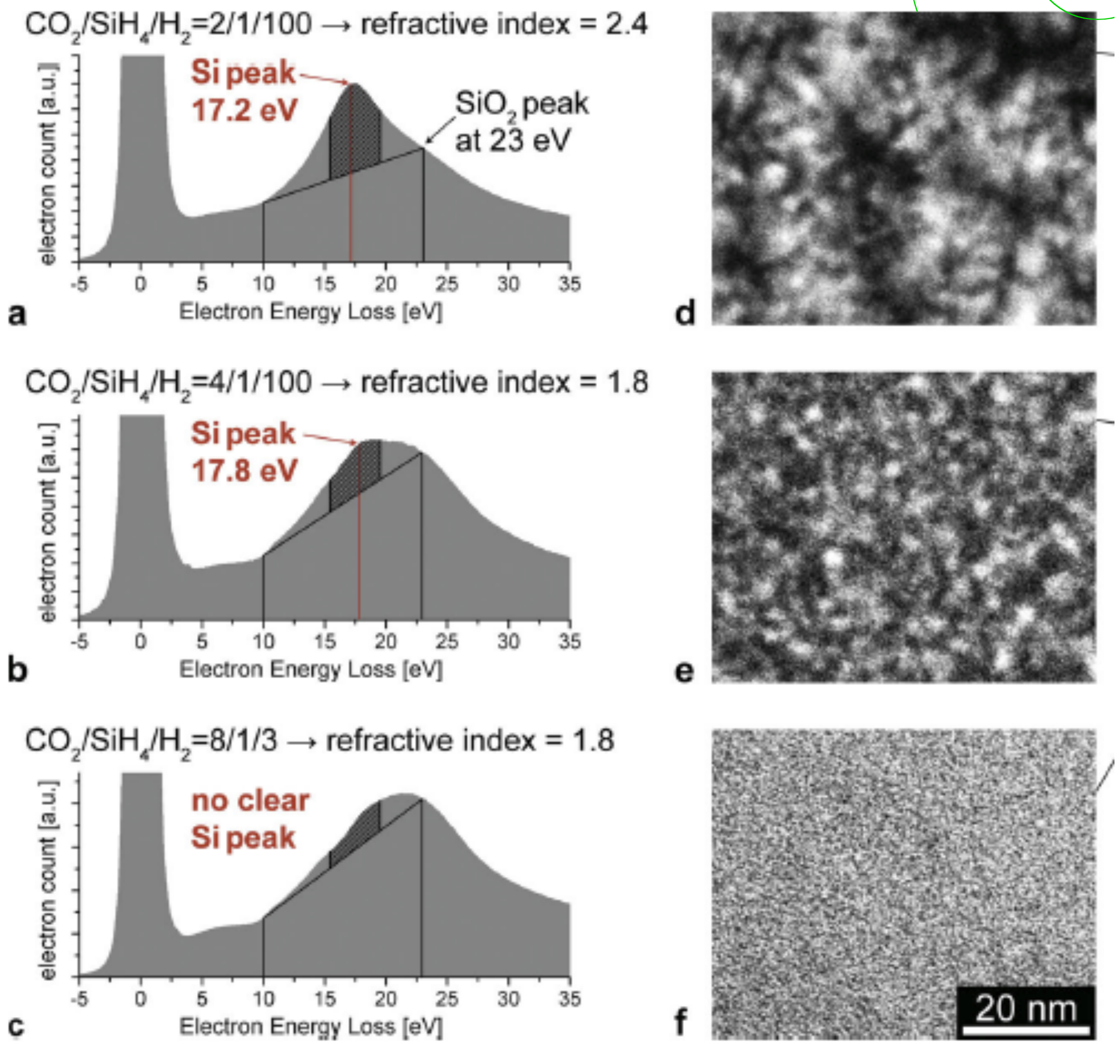

Cuony, P., & al. *Silicon filaments in silicon oxide for next-generation photovoltaics* (2012) Advanced Materials, 24 (9), pp. 1182-1186.

EFTEM: Plasmon Imaging

Comparison of films grown under different CVD conditions:

Plan-view images taken with 4 eV windows

10 eV   18 eV   23 eV

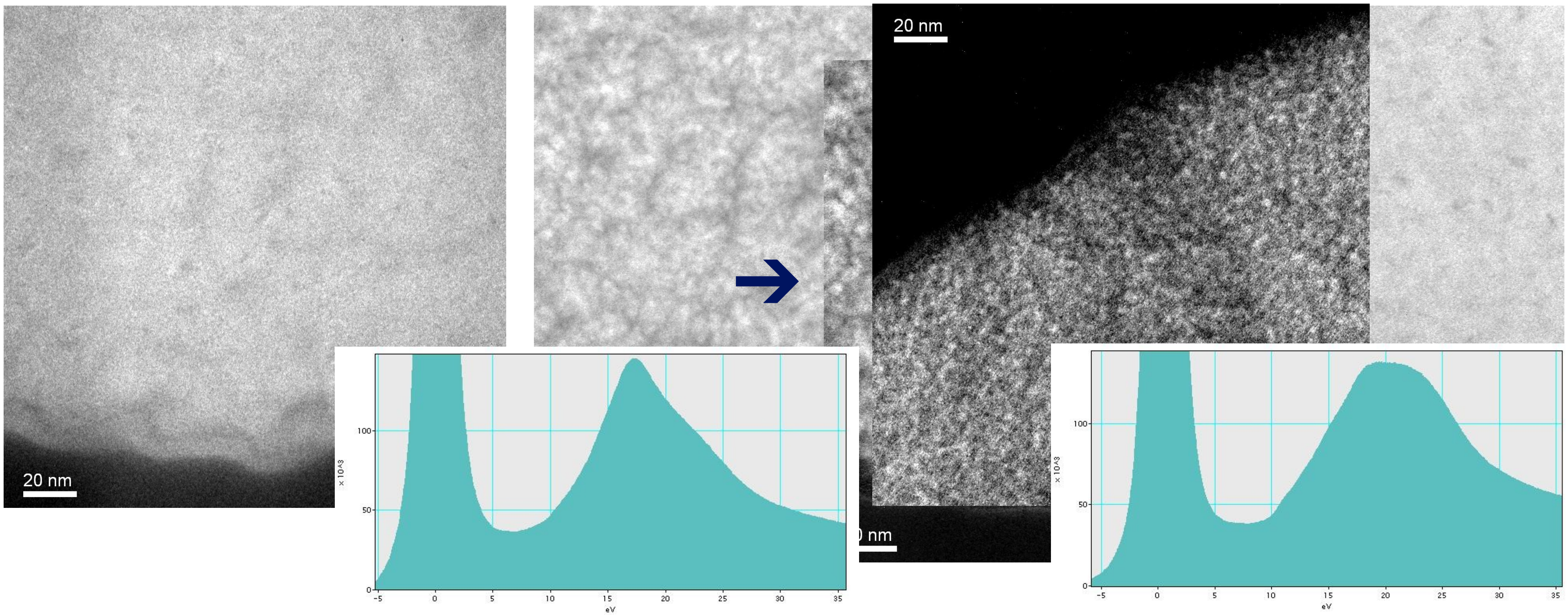

High Si, RI = 2.4   Low Si, RI = 1.8

Drift correction: Schaffer et al. Ultramicroscopy ***102*** *(2004) 27*

EFTEM: Plasmon Imaging

Why do the SiO_x films have poor in-plane but good cross-plane conductivity?

TEM cross-section of test structure:

BF zero-loss image

80 nm nc-Si

400 nm SiO_x

20 nm nc-Si

Si wafer

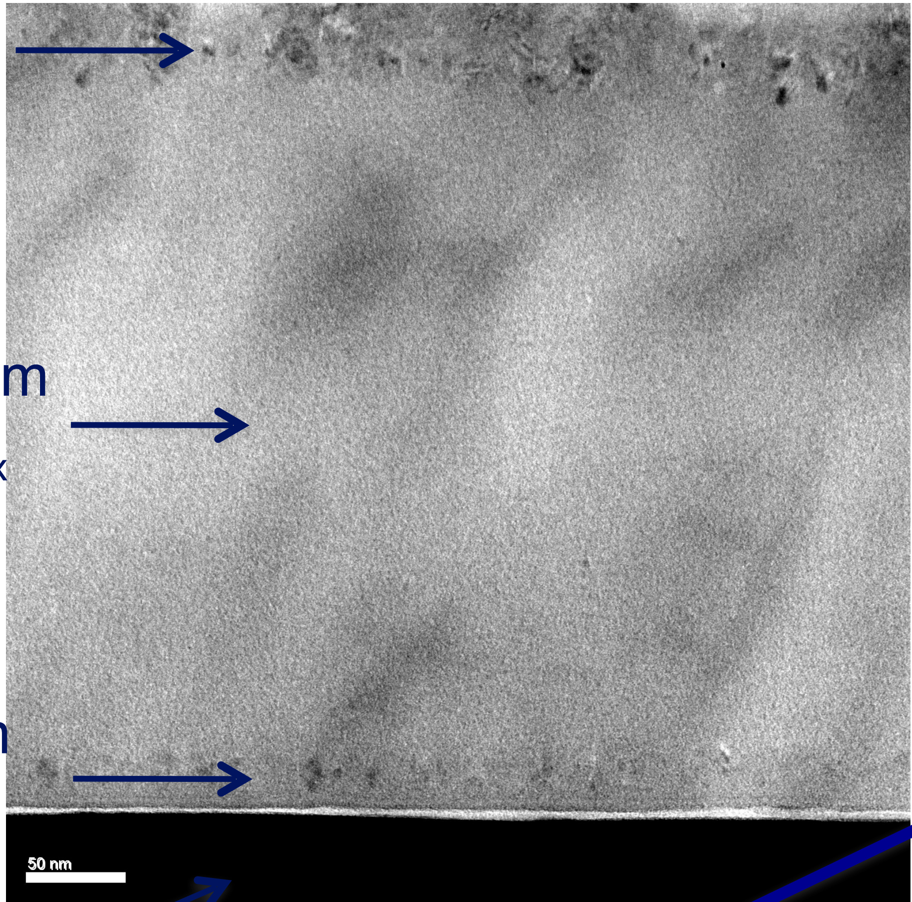

Si plasmon image

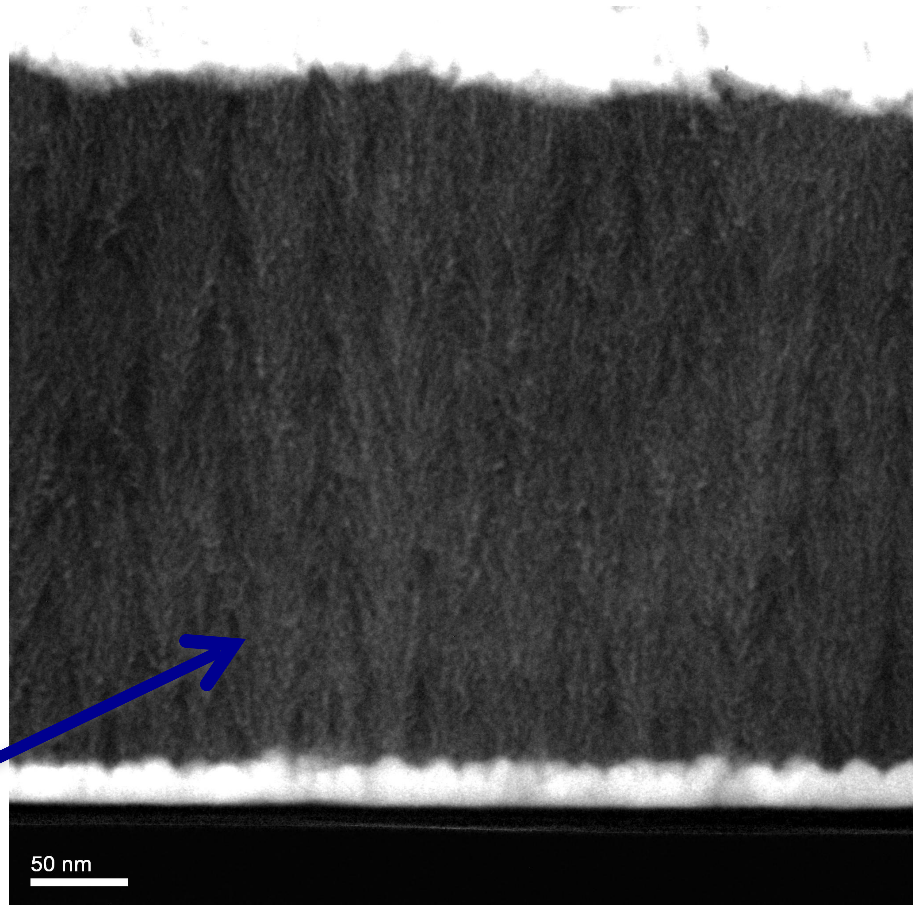

Branched/dendritic Si structures provide conductive paths across the film

EFTEM: Plasmon Imaging

Cross section of a “good” specimen

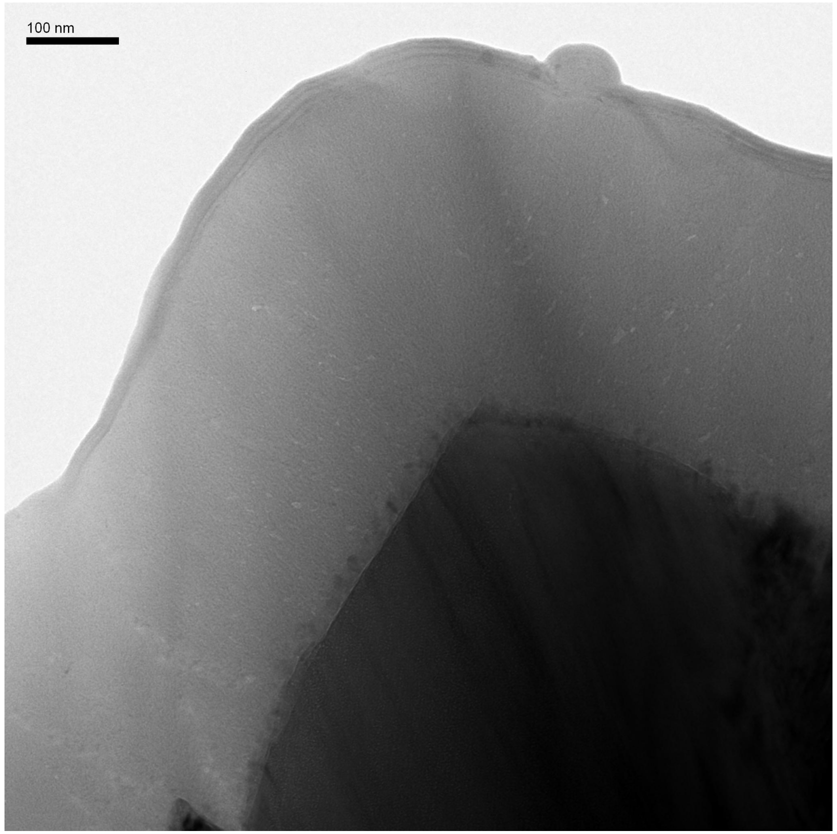

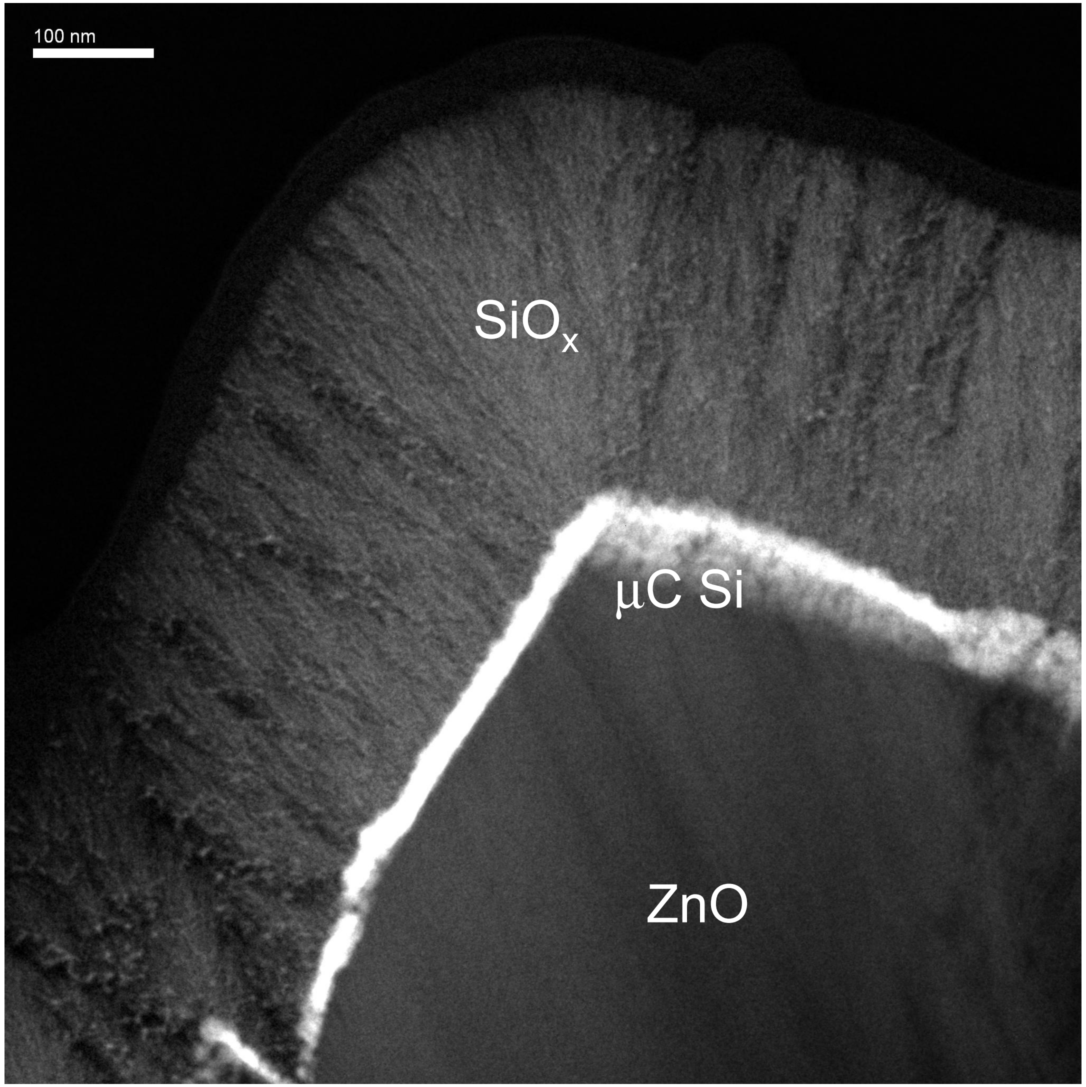

Transplanar conductivity paths retained

EFTEM in core loss: ODS steel

model ODS ferritic alloy Fe-14Cr-2W-0.3Y_2O_3-0.4Ti CRPP EPFL

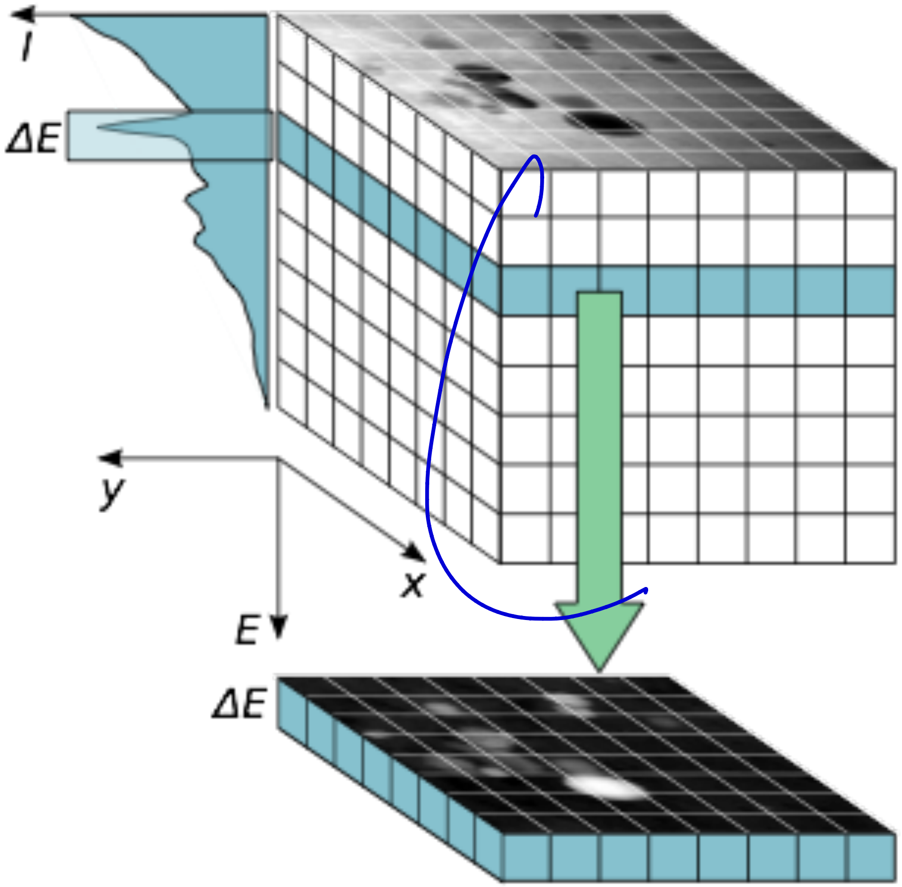

Advantages:
- Large field of view, good lateral statistics
- faster for large images
- Samples drift easier to deal with

But:
- Not good energy resolution

1024 x 1024 pixel; 2.8 Å pixel size c.a. 300 nm field of view.
2 stacks (low loss & core loss, each 300 Mb, total 600Mb data / region)
Covers the most important edges for the expected elements

EFTEM in core loss: ODS steel

Sample preparation: C- extraction

Raw EFTEM datacube.

Energy loss range: 350-760 eV

10 eV slit width, 5 eV step

Microscope: TEM JEOL 2200 FS

200 keV, FEG, in column Omega filter

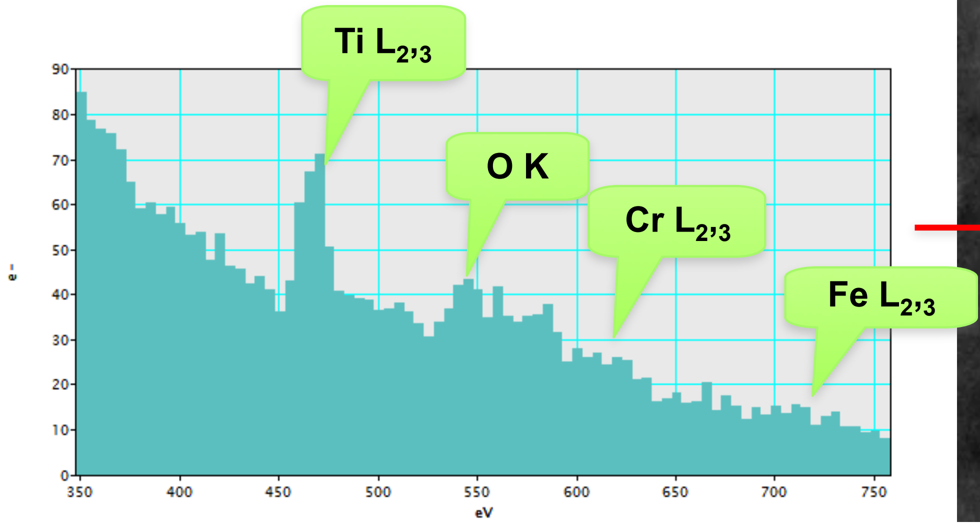

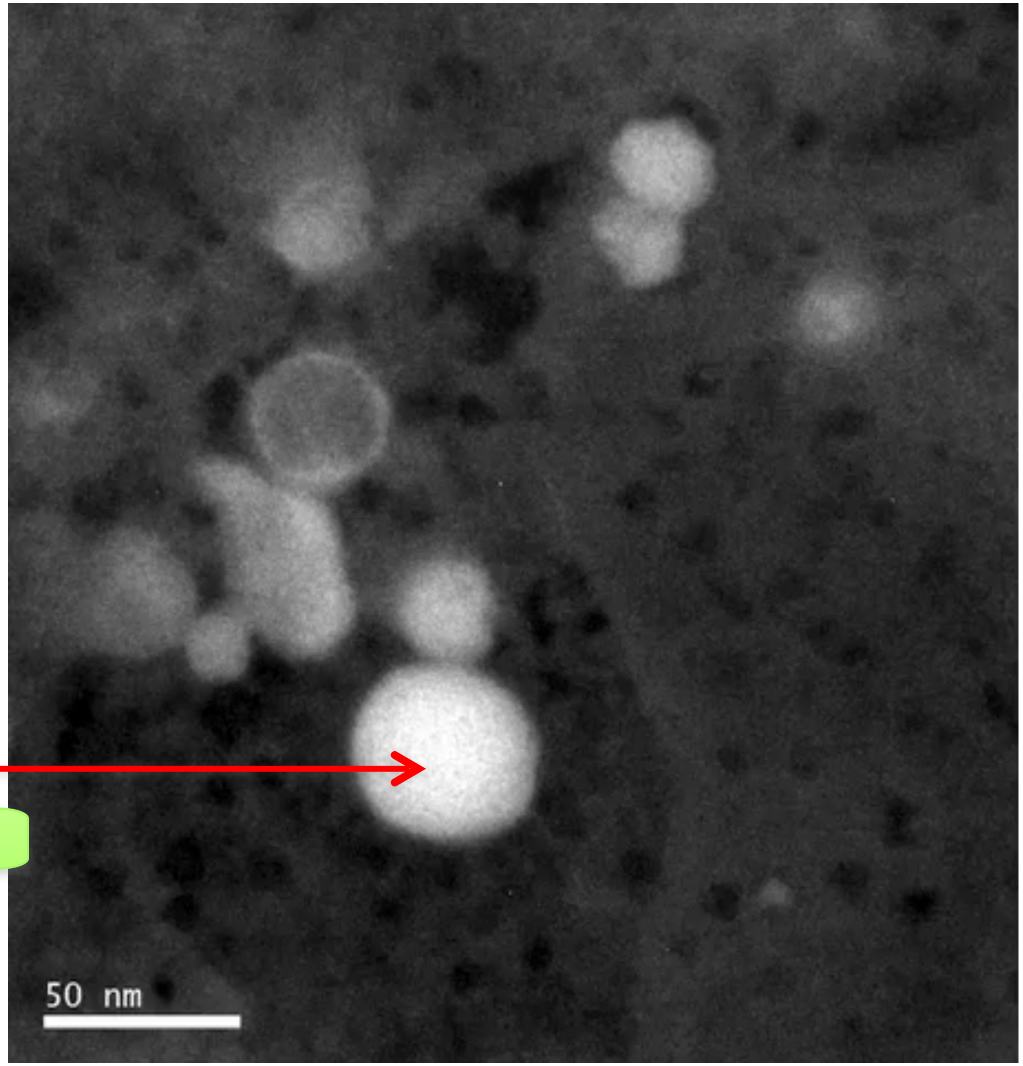

Data cleaning: 1- removal of "X-rays", 2- drift correction, 3- PCA

EFTEM in core loss: ODS steel

Principal Components Analysis applied to EFTEM data cube

Energy loss range: 350-760 eV

Microscope: TEM JEOL 2200 FS
200 keV, FEG, in column Omega filter

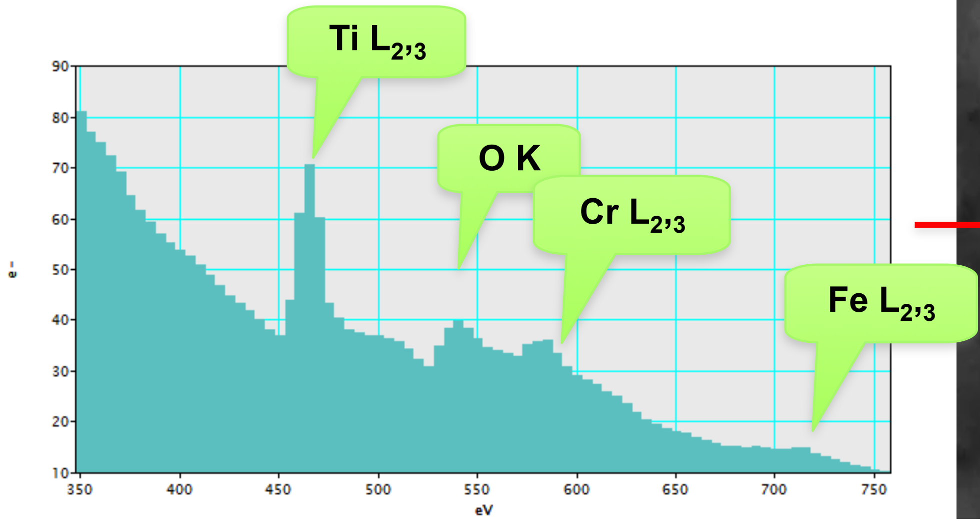

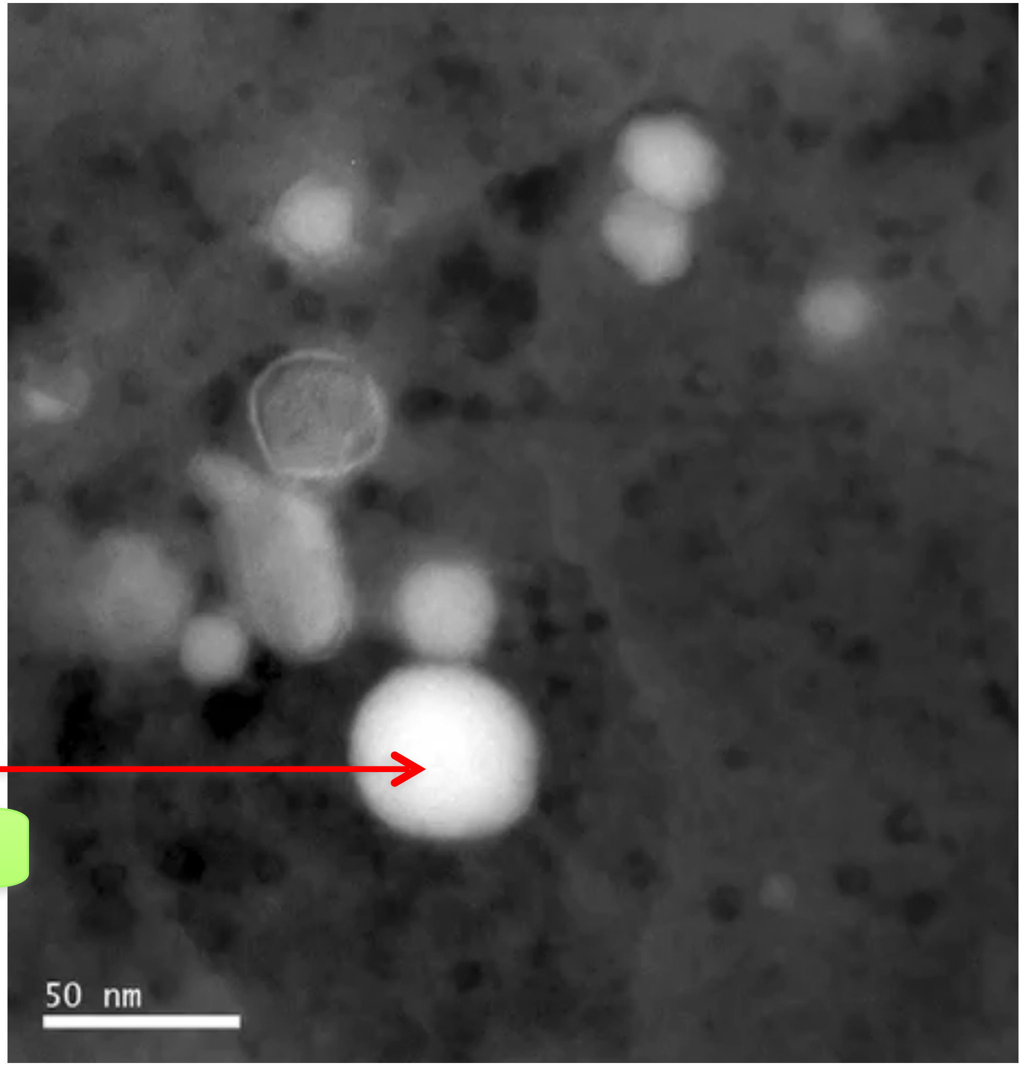

EFTEM in core loss: ODS steel

EFTEM chemical maps

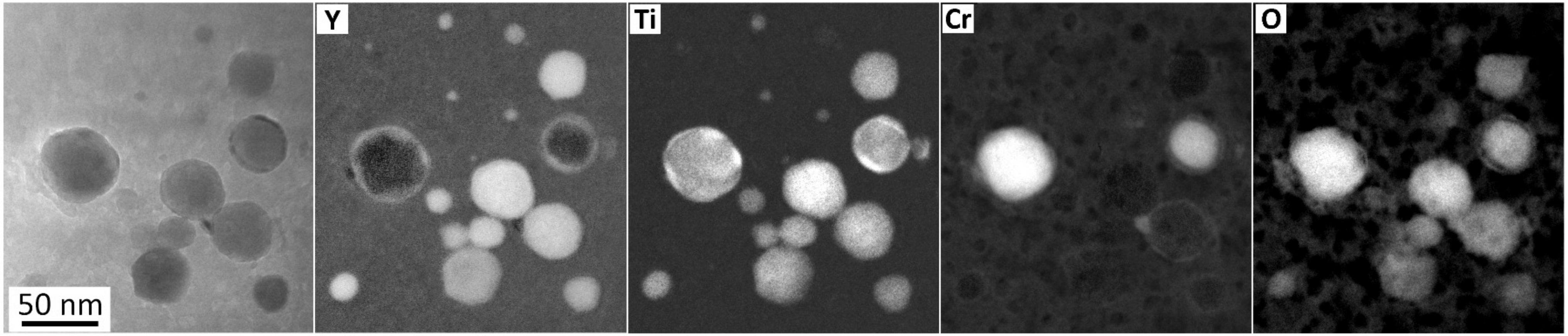

EELS fingerprints:

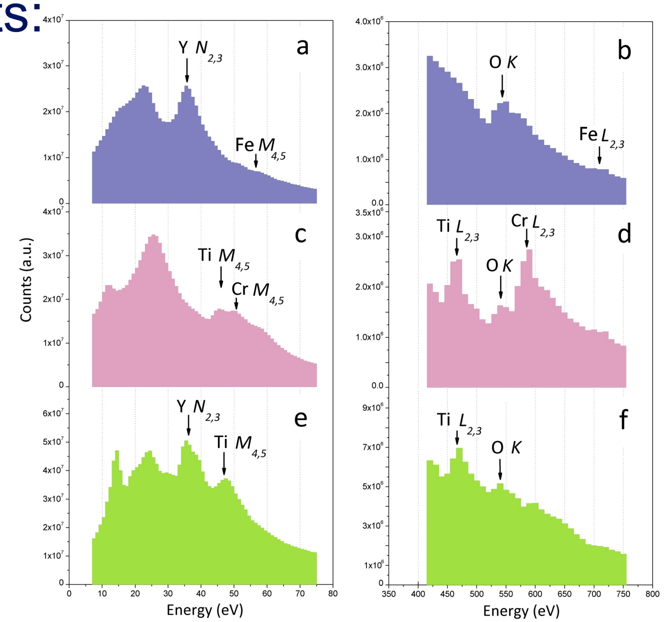

← Y-O particles: 6 %, 16 nm

← Ti-Cr-O particles: 4 %, 33 nm

← Y-Ti-O particles: 90 %, 6 nm

P. Unifantowicz, R. Schäublin, C. Hébert, T. Płociński, G. Lucas, N. Baluc, Journal of Nuclear Materials Volume 422, Issue 1-3, March 2012, Pages 131-136

Outline

- Introduction: EELS in the TEM
- Instrumentation
- Core Loss EELS
  - Theory
  - Applications
  - Imaging (EFTEM)
- Low losses
- ELNES (Energy Loss Near Edge Structures)

Core Loss: fine structure

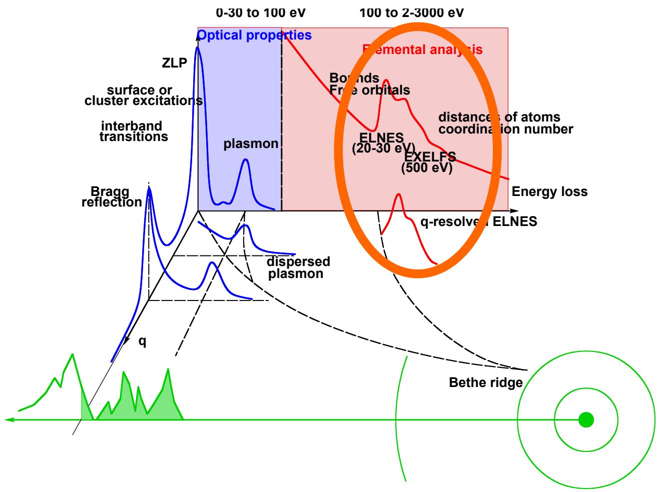

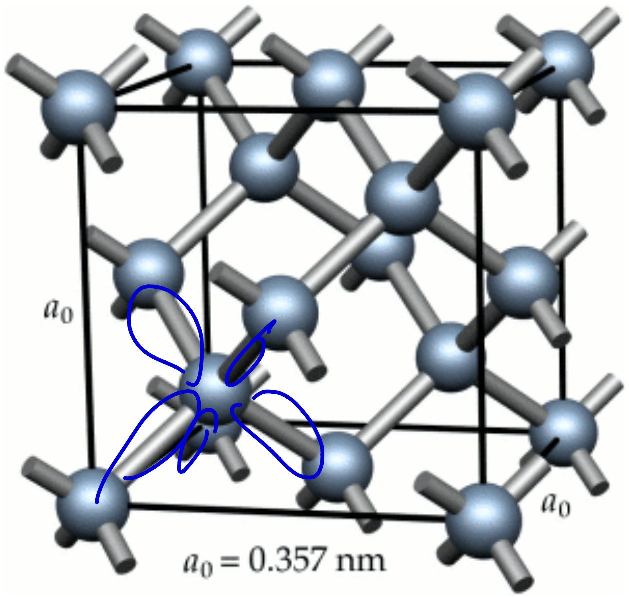

Diamond

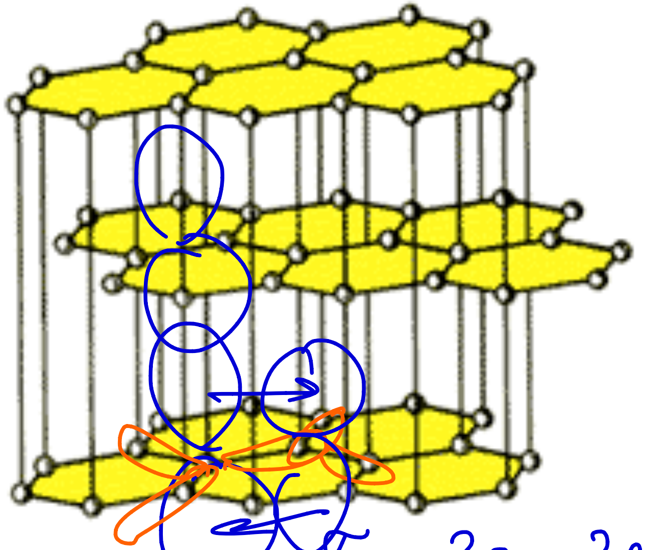

Graphite

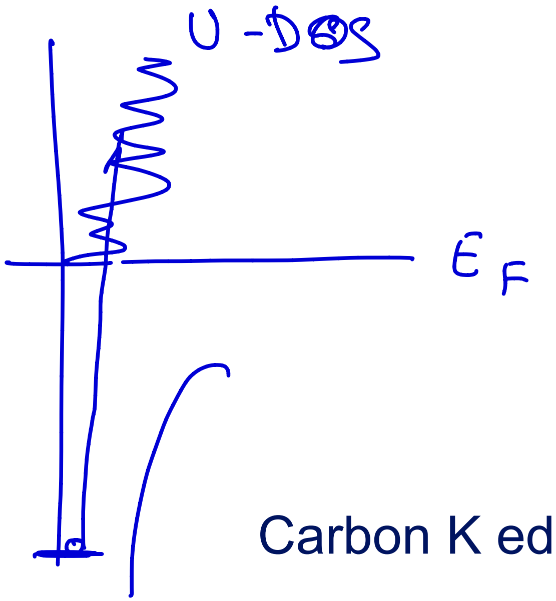

Carbon K edge

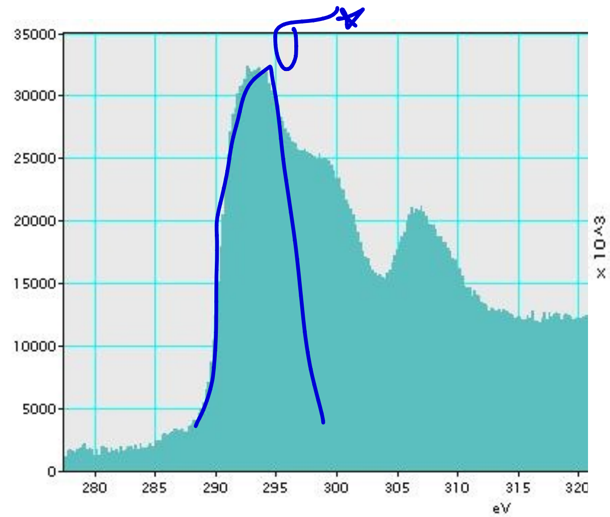

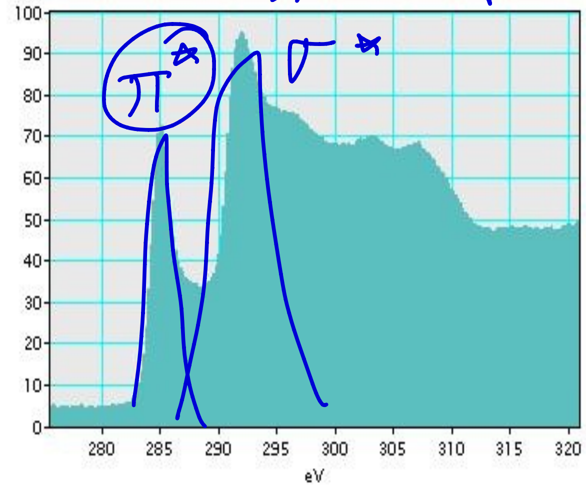

Core Loss: fine structure

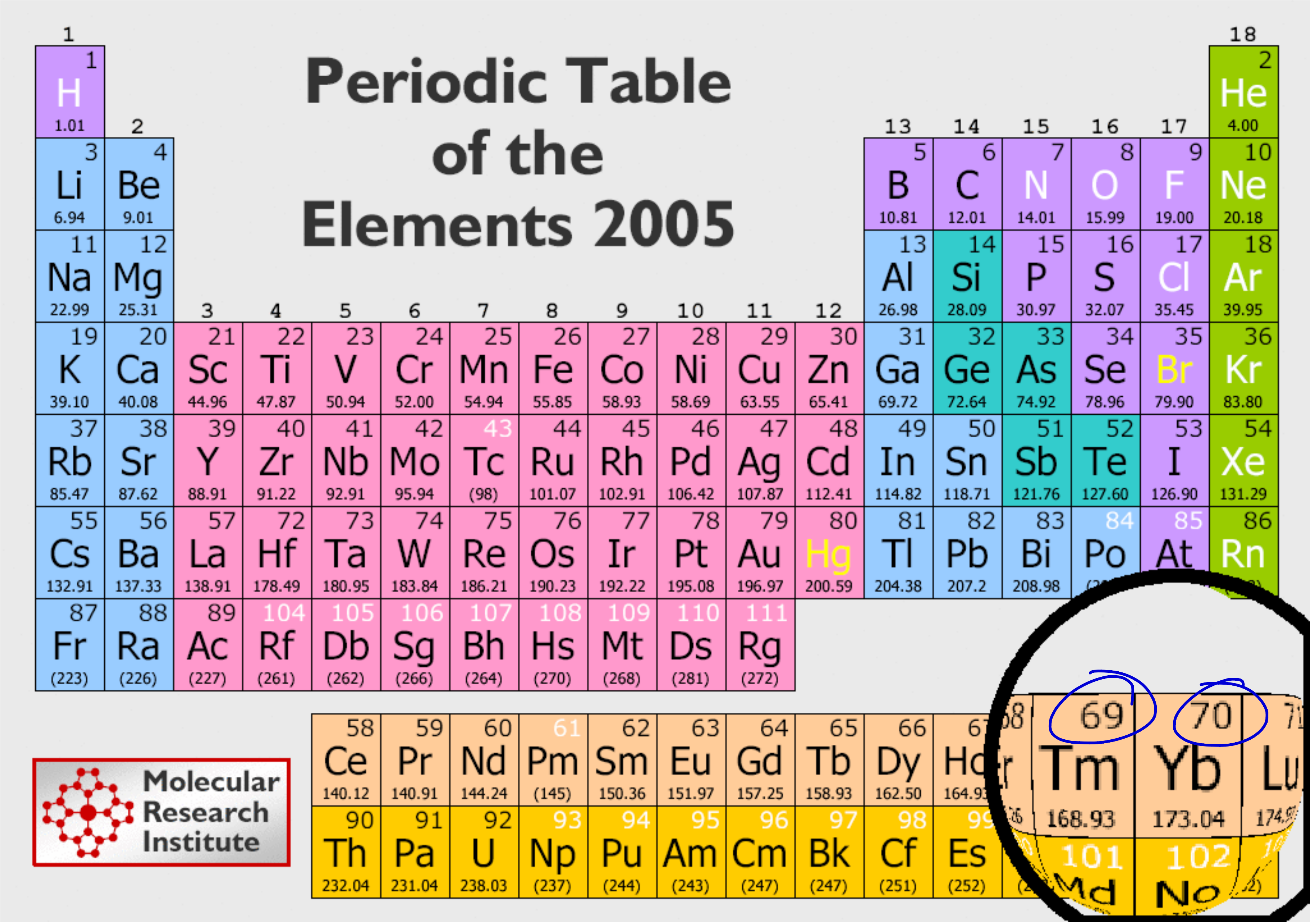

Core Loss: fine structure

Thulium 69

- **Ground state electron configuration:** [Xe].$4f^{13}.6s^2$
- **Shell structure:** 2.8.18.31.8.2
- **Term symbol:** $^2F_{7/2}$

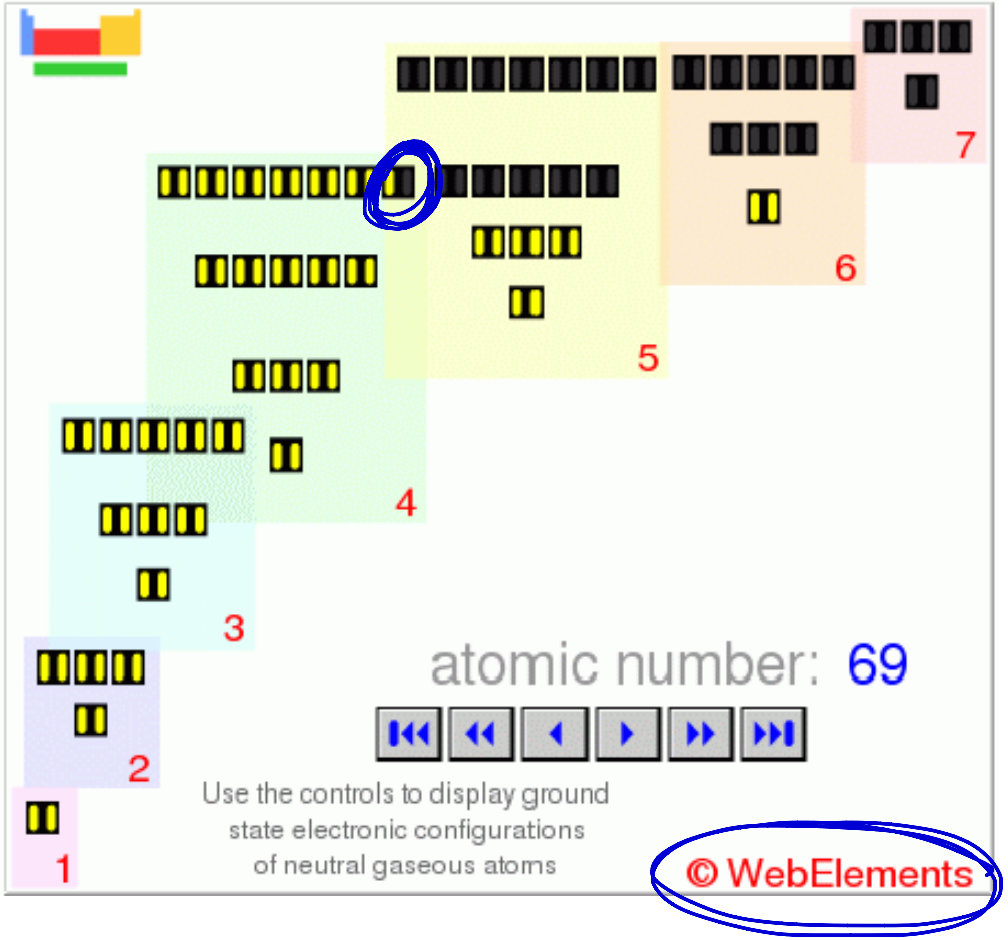

Ytterbium 70

- **Ground state electron configuration:** [Xe].$4f^{14}.6s^2$
- **Shell structure:** 2.8.18.32.8.2
- **Term symbol:** $^1S_0$

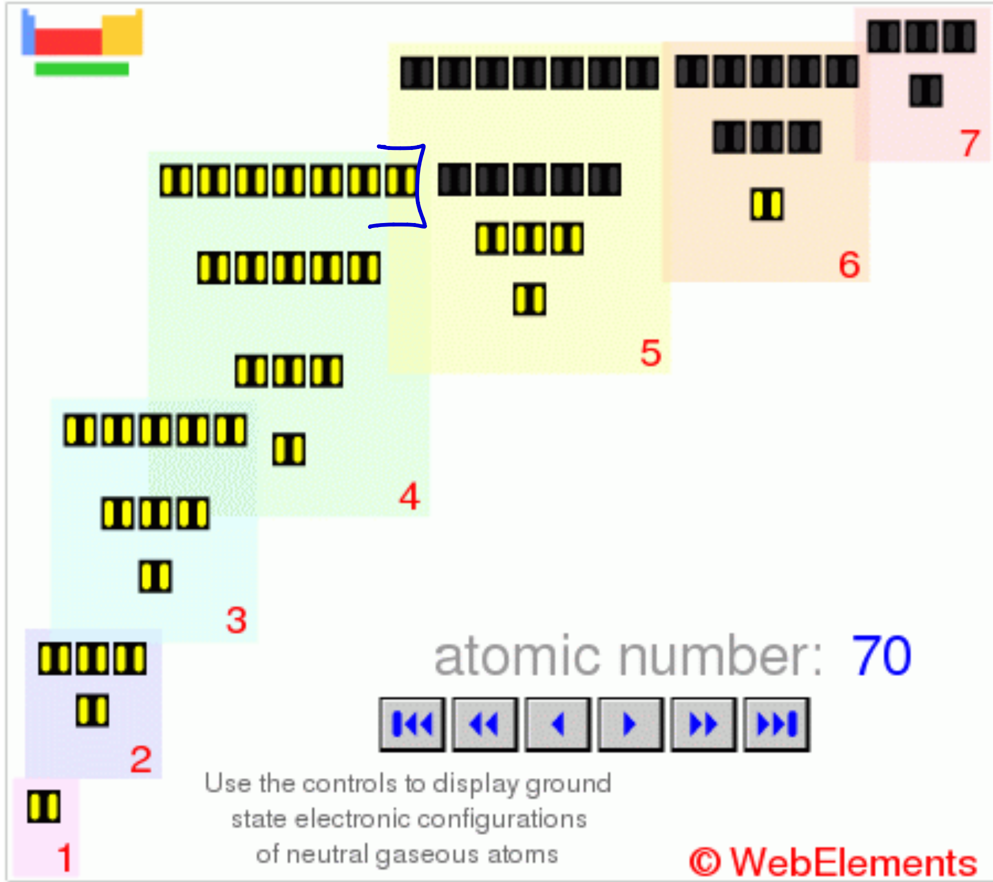

Core Loss: fine structure

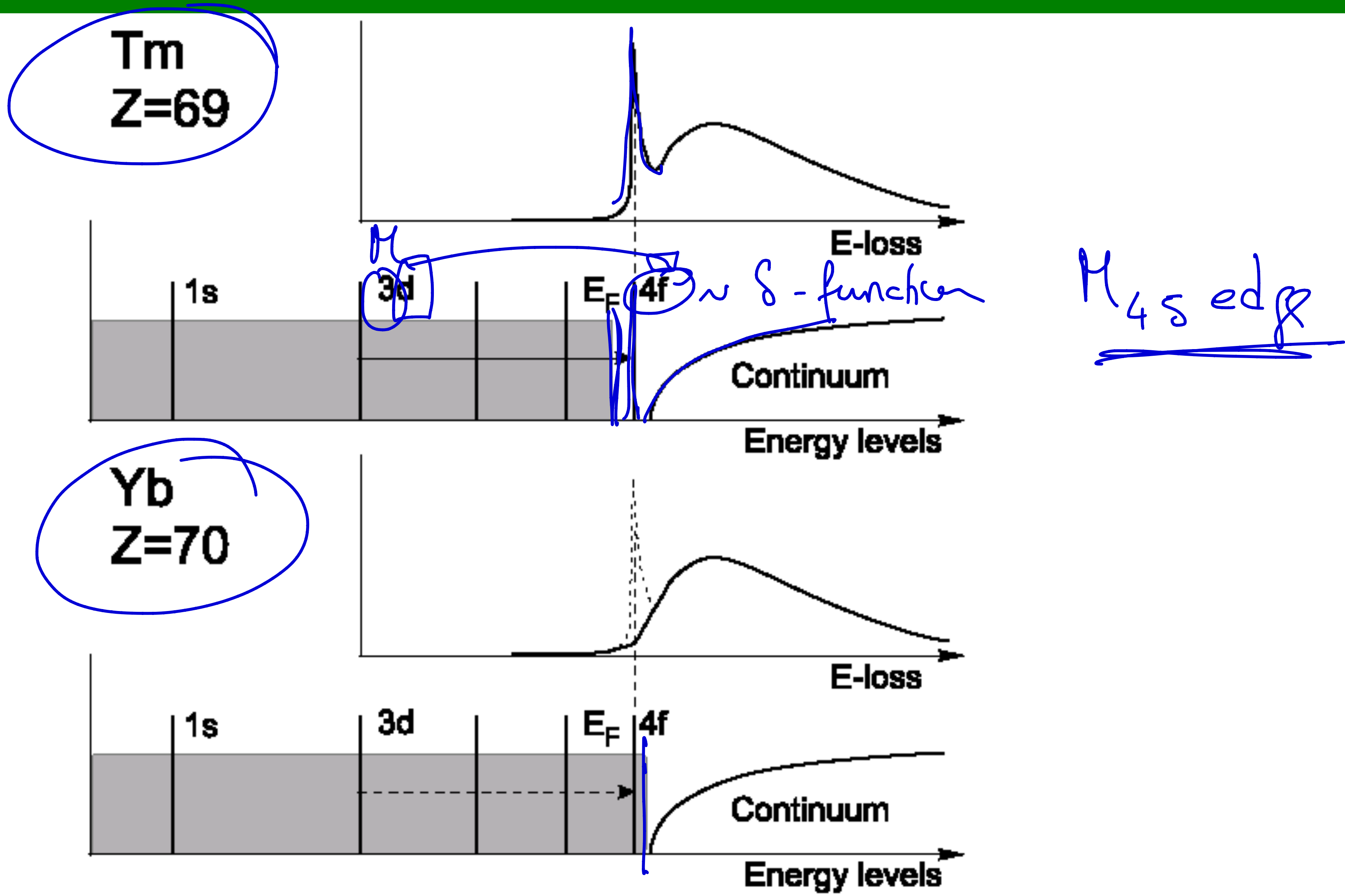

For Yb (Z=70) and higher atomic number, the f-shell is completely filled, and white lines cannot occur.

Core Loss: fine structure

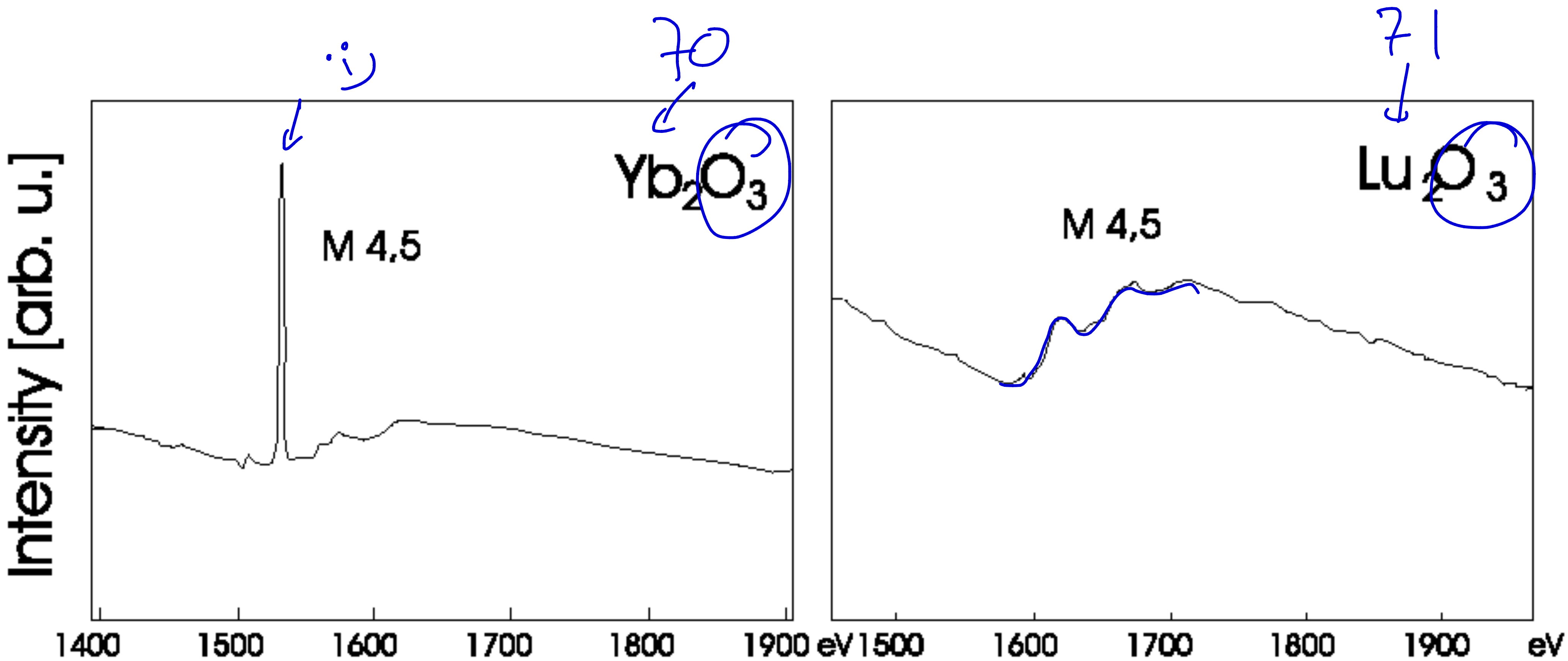

M_{45} edges of Yb and Lu in their oxides, showing the disappearance of white line when the f-subshell is filled.

Using white lines: reduction of NiO

Q. Jeangros, A Hessler-Wyser, Jan van Herle, Cécile Hébert

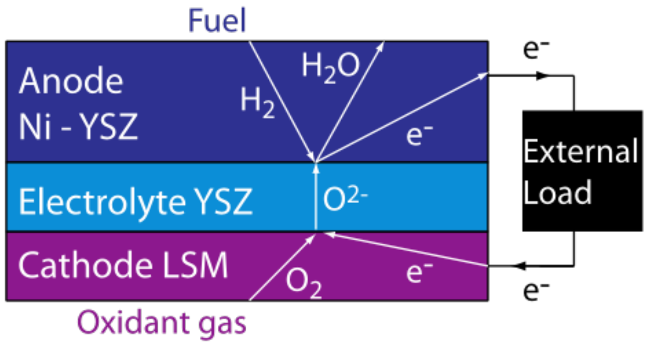

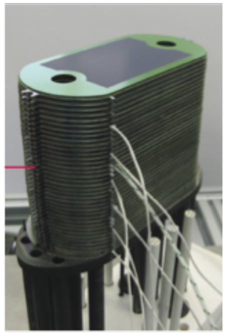

Ni - current conductor & catalyst for H_2 oxidation

YSZ – ionic conductor

Ni structure//chemistry after reduction at 700 °C inside ETEM

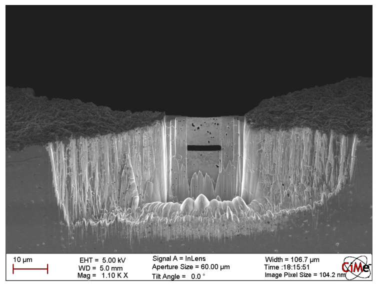

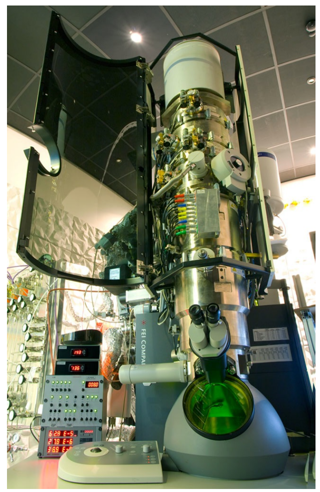

Using white lines: reduction of NiO

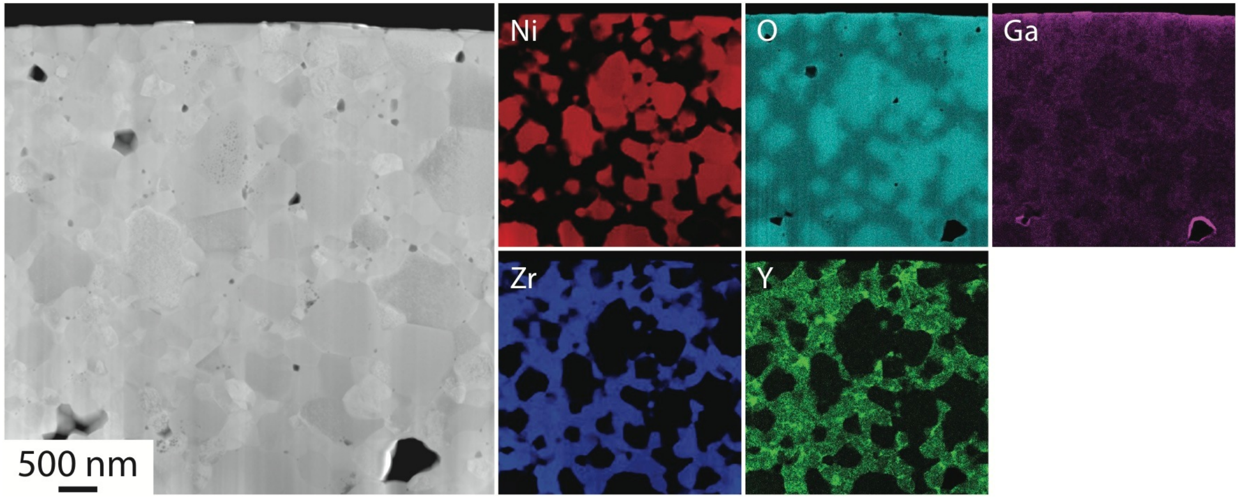

As-sintered NiO-YSZ anode

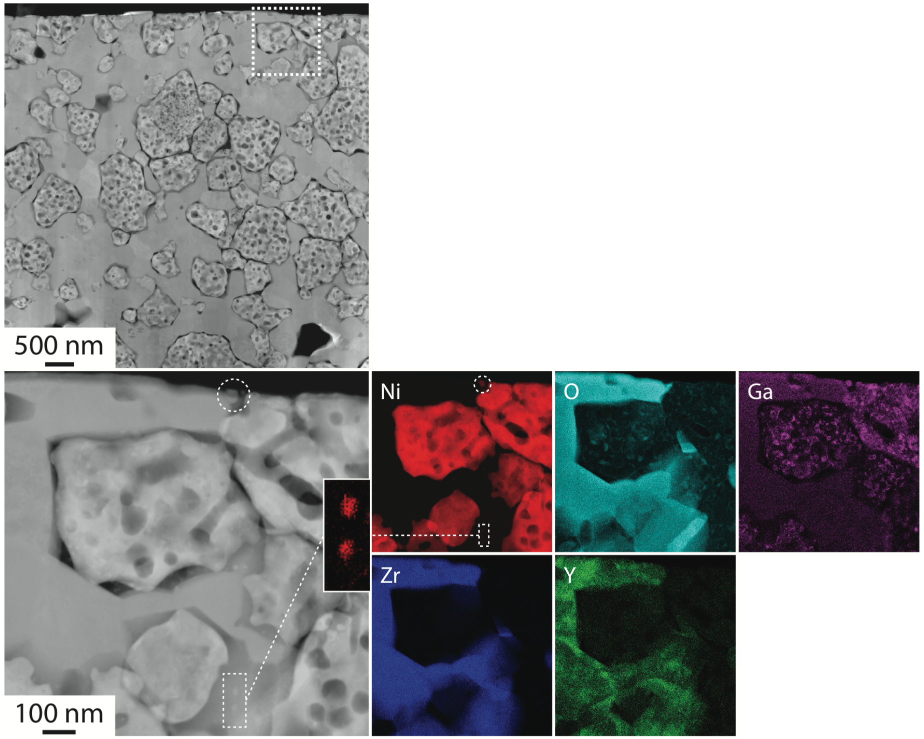

Activated Ni-YSZ anode

Reduction at 700 °C inside ETEM

Porous & inhomogenous Ni structure

Ni nanoparticles

- → Reaction mechanisms
- → $Ni(OH)_2$

Artifact - gallium oxide

Using white lines: reduction of NiO

4 °C/min from 250 to 600 °C

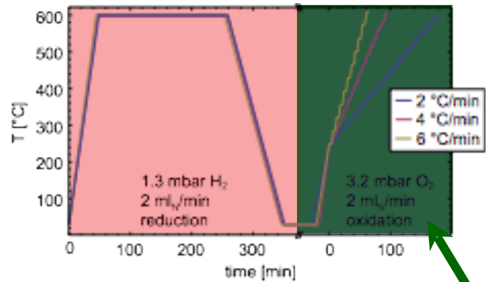

3.2 mbar of O_2

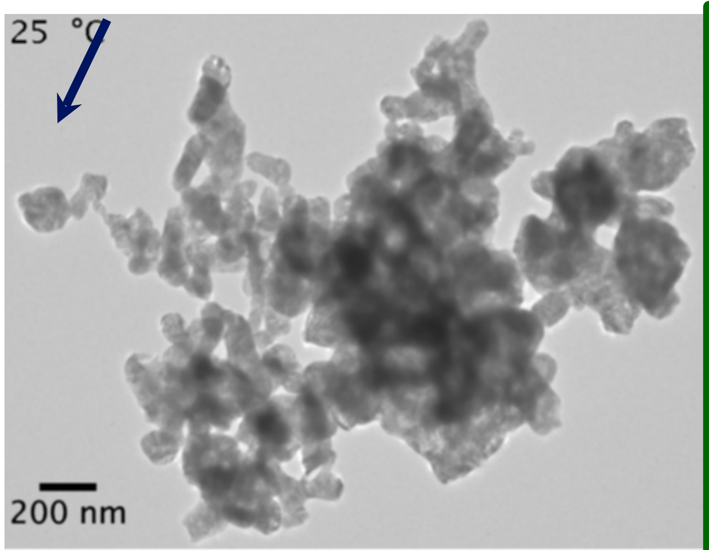

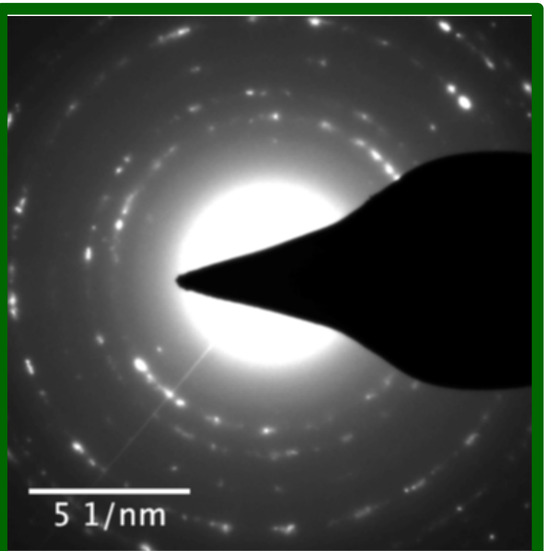

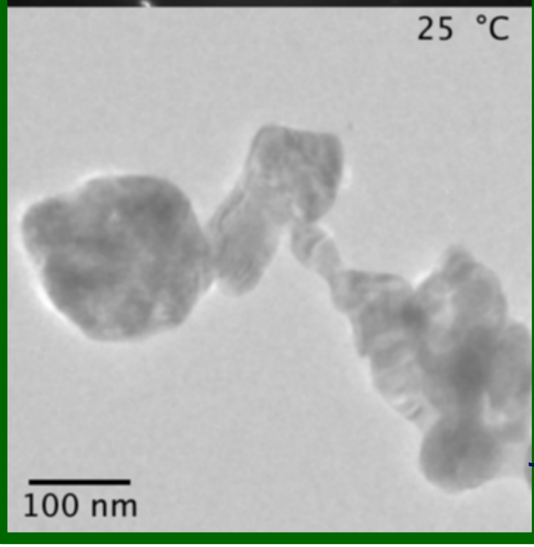

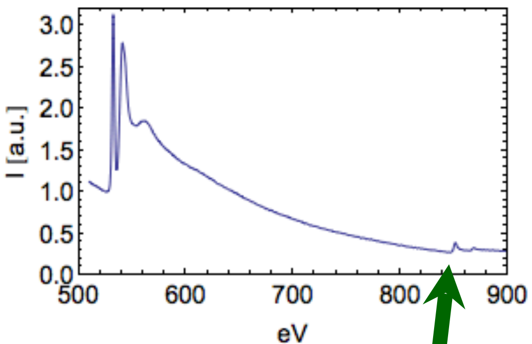

Ni $L_{2,3}$

- Some NiO reflections initially
- Small NiO crystallites with random orientations
- Ni to NiO
- Volume expansion
- Internal interface recession

Q. Jeangros, A Hessler-Wyser, Jan van Herle, Cécile Hébert
Jakob Wagner, Rafal Dunin-Borkowski (DTU)

* 1 image, SADP, EELS every 6 minutes

Using white lines: reduction of NiO

Kinetics by EELS

Changes of shape of Ni $L_{2,3}$

→ experimental Ni & NiO references

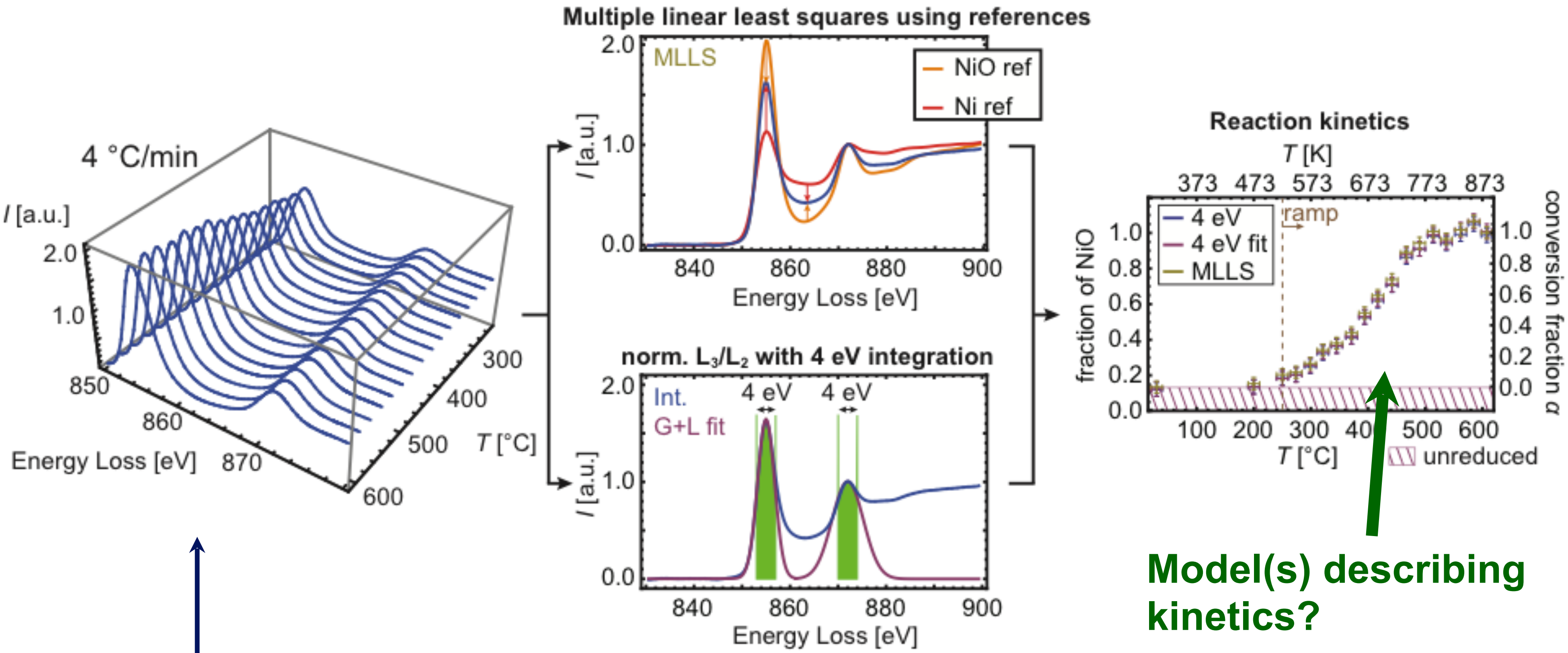

Model(s) describing kinetics?

PCA
Background subtracted
Normalized to 1 at L_2
Energy shift not taken into account (- 0.2 eV)
Convoluted with PSF to get same initial NiO L_3 resolution at 2, 4 & 6 °C/min

$$\beta \cdot \frac{d\alpha}{dT} = A\, e^{-\left(\frac{E_a}{RT}\right)} \cdot f(\alpha)$$

See Jeangros Q *et al.* (2013), JofMS (48).

Using white lines: reduction of NiO

(Linear) diffusion controls the reaction

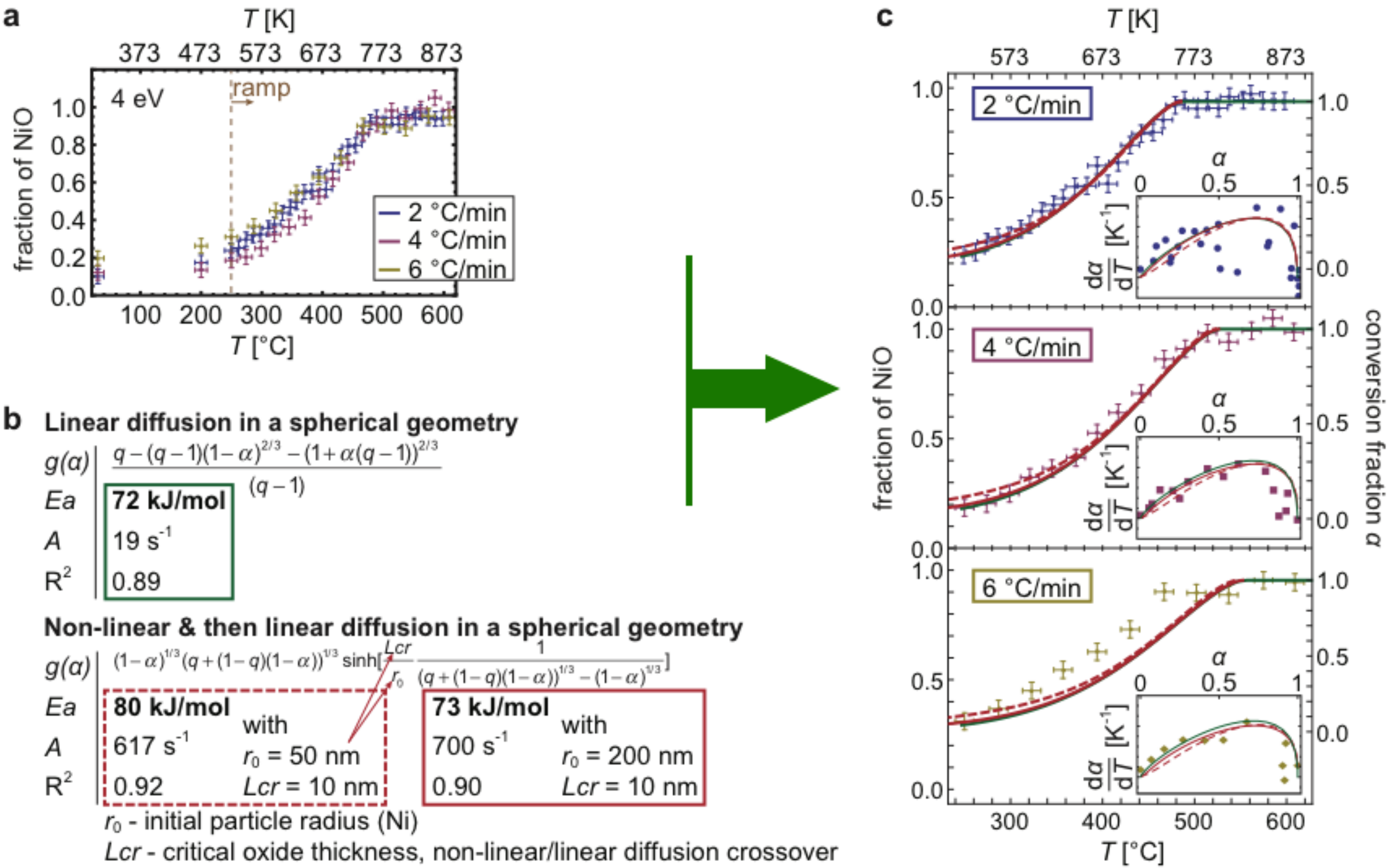

Niklasson *GA, et al.* (2003), Suf. Sci. (532-535) 324.
Fromhold AT, (1988), J. of Phy. & Chem. of Sol. (49) 1159.

Core Loss: ELNES

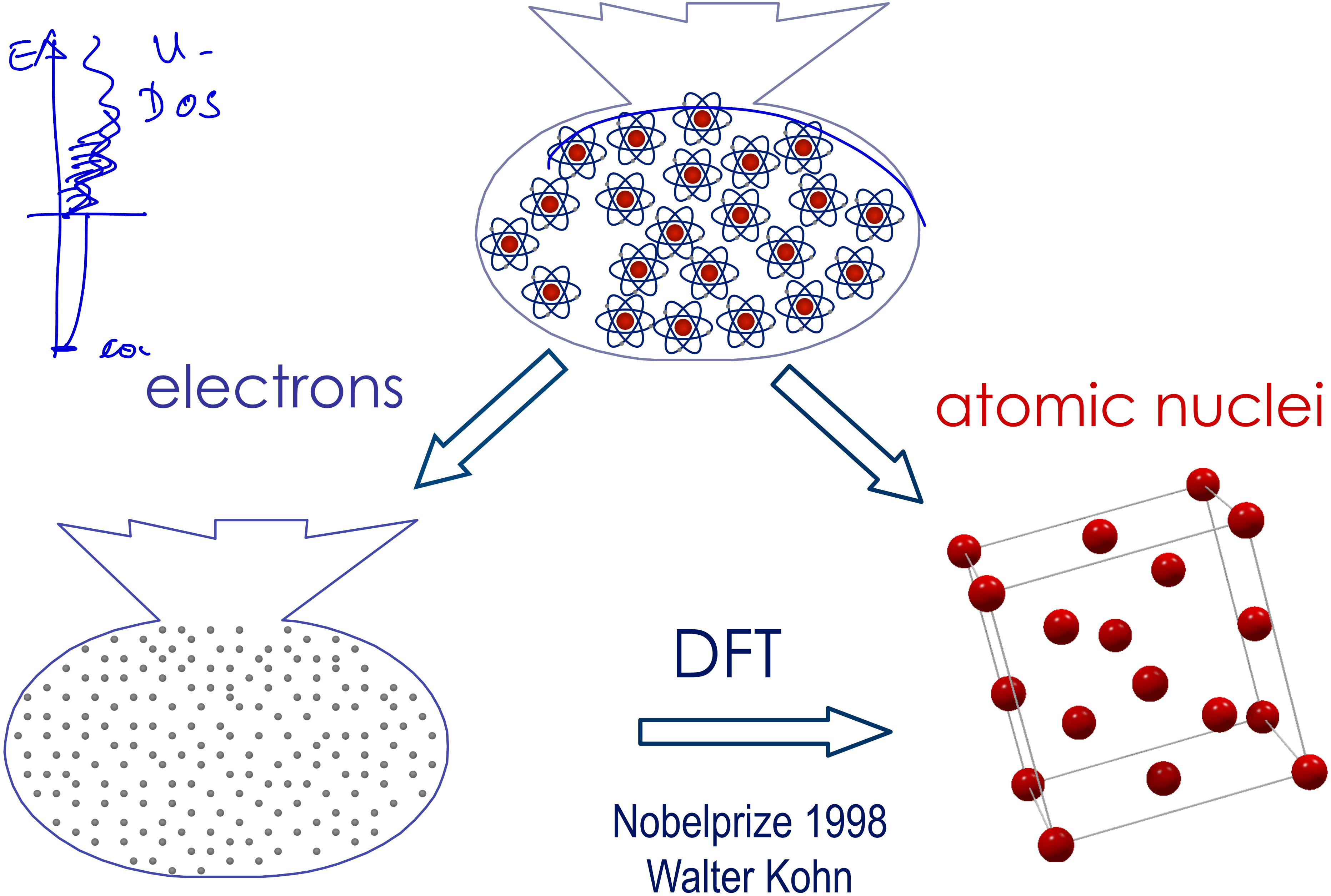

Core Loss: ELNES

Walter Kohn
Nobel prize
laureate 1998
chemistry

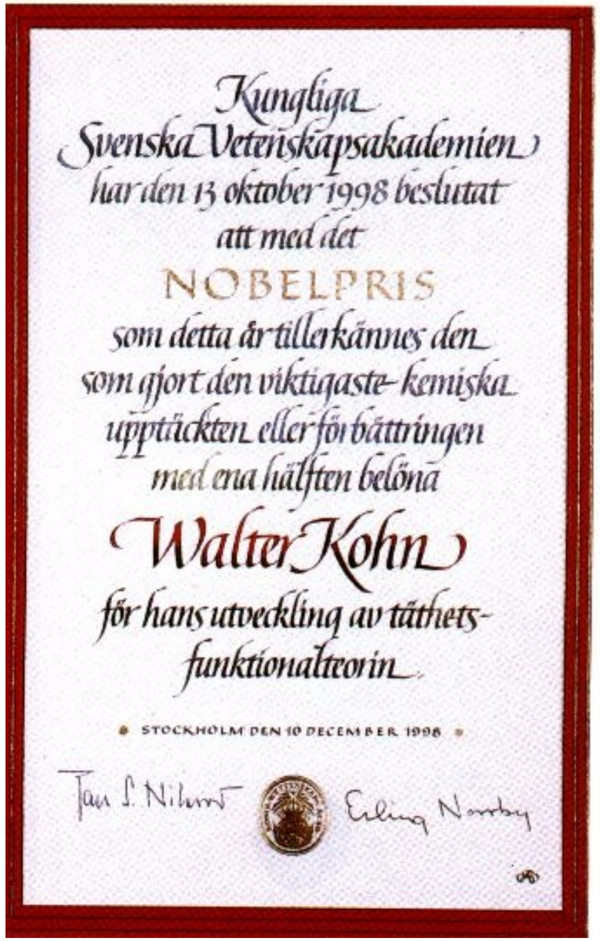

Core Losses: ELNES

WIEN2k

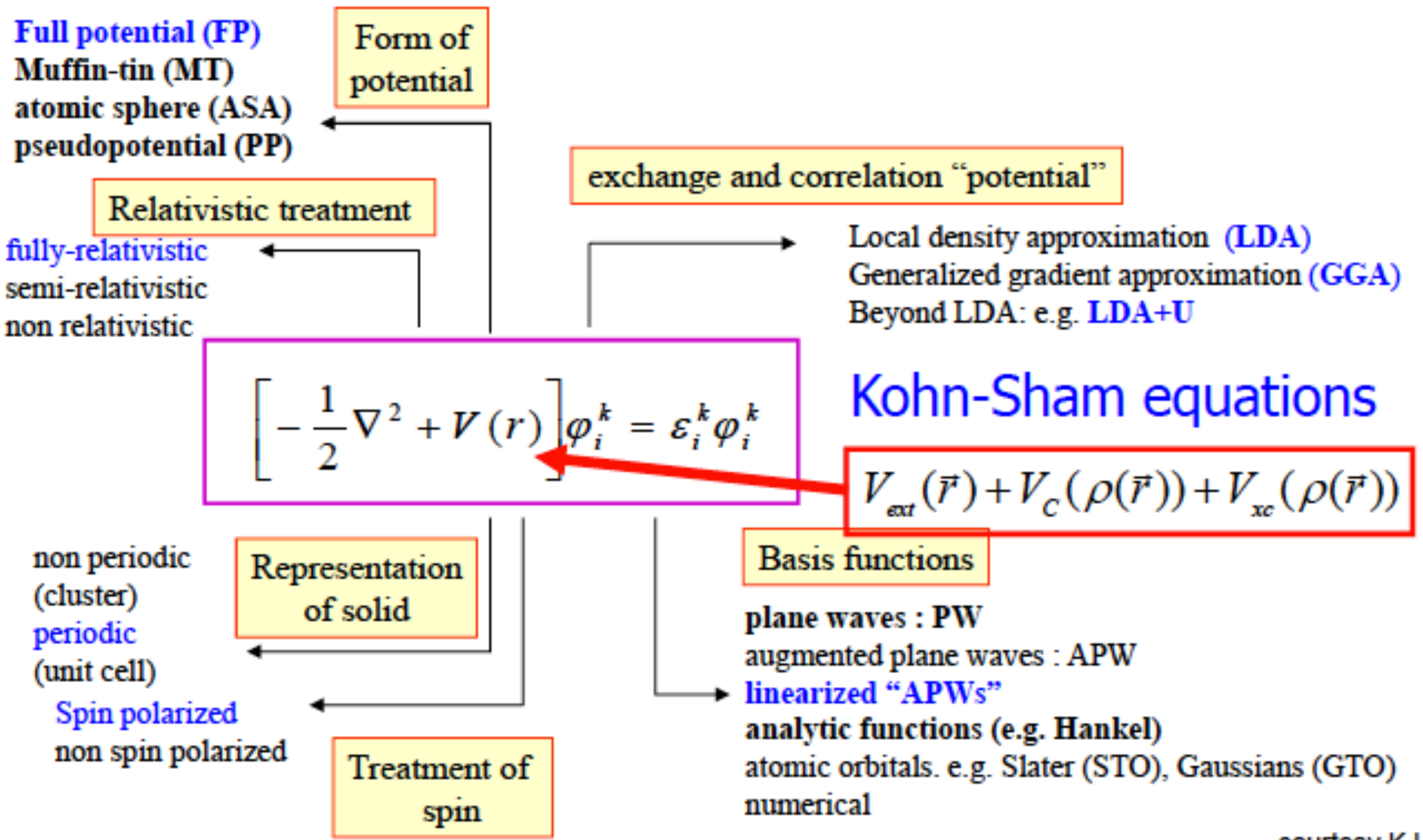

courtesy K.H. Schwarz

Core Loss: ELNES

Electron density
-> Wave functions
-> Density of states
-> unoccupied density of states

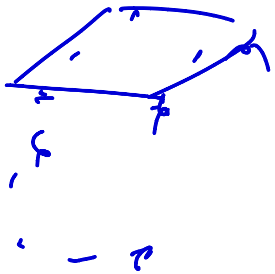

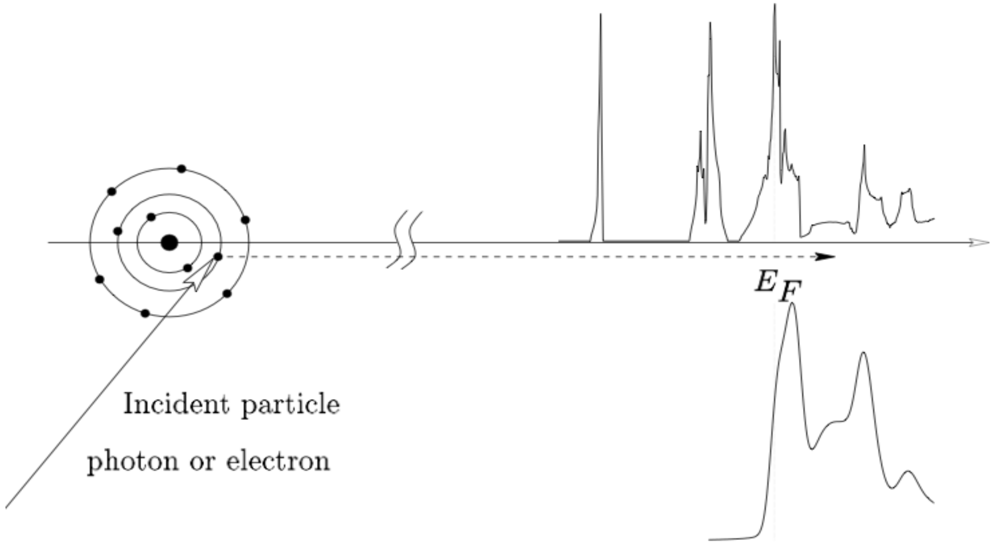

EELS spectrum with fine structures!

Compare with experiment

Core Loss: ELNES

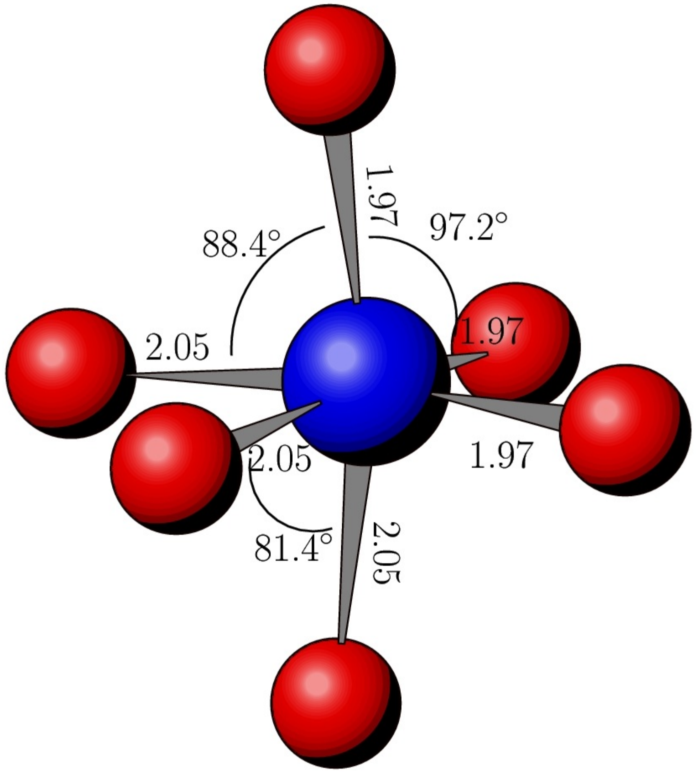

V_2O_5

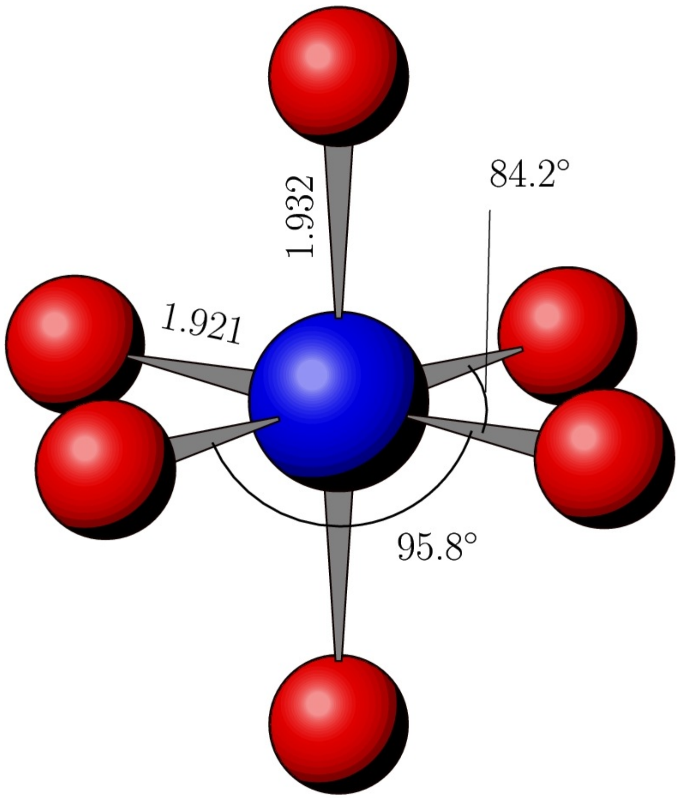

VO_2

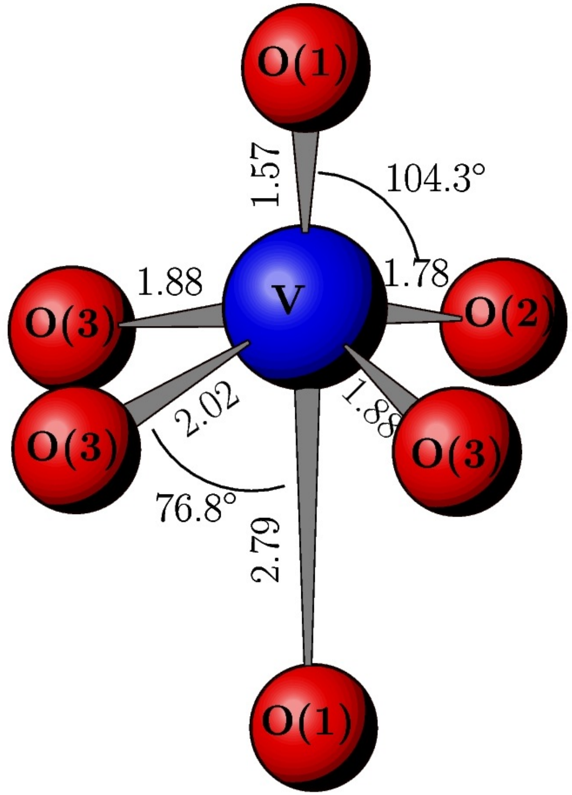

V_2O_3

C. Hébert, et al.
Eur.Phys.J B 28, 407 (2002)

Core Loss: ELNES

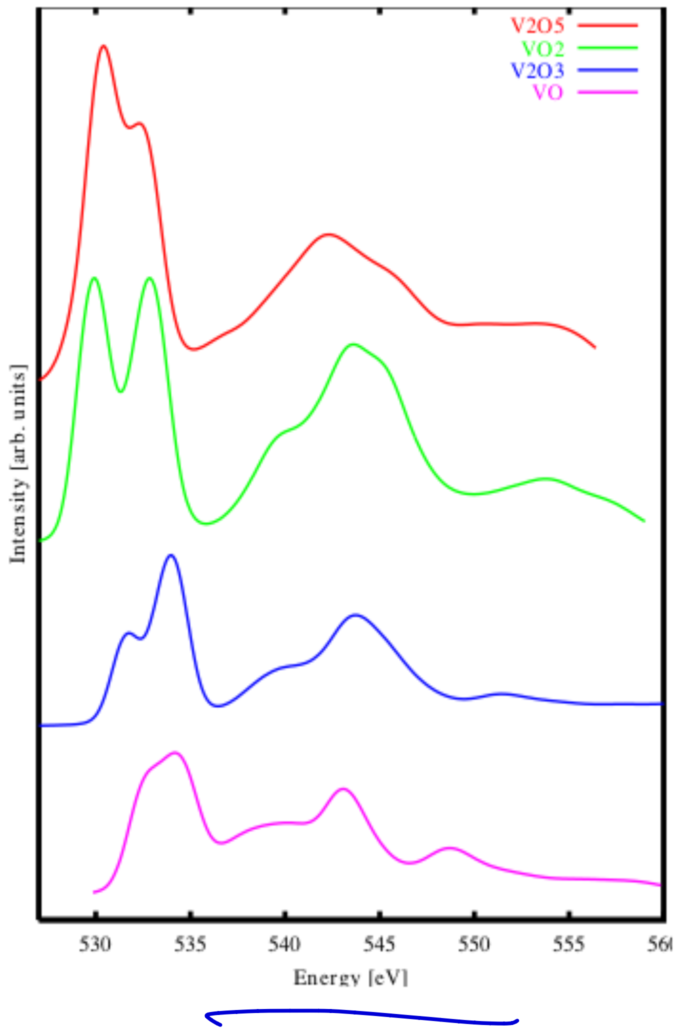

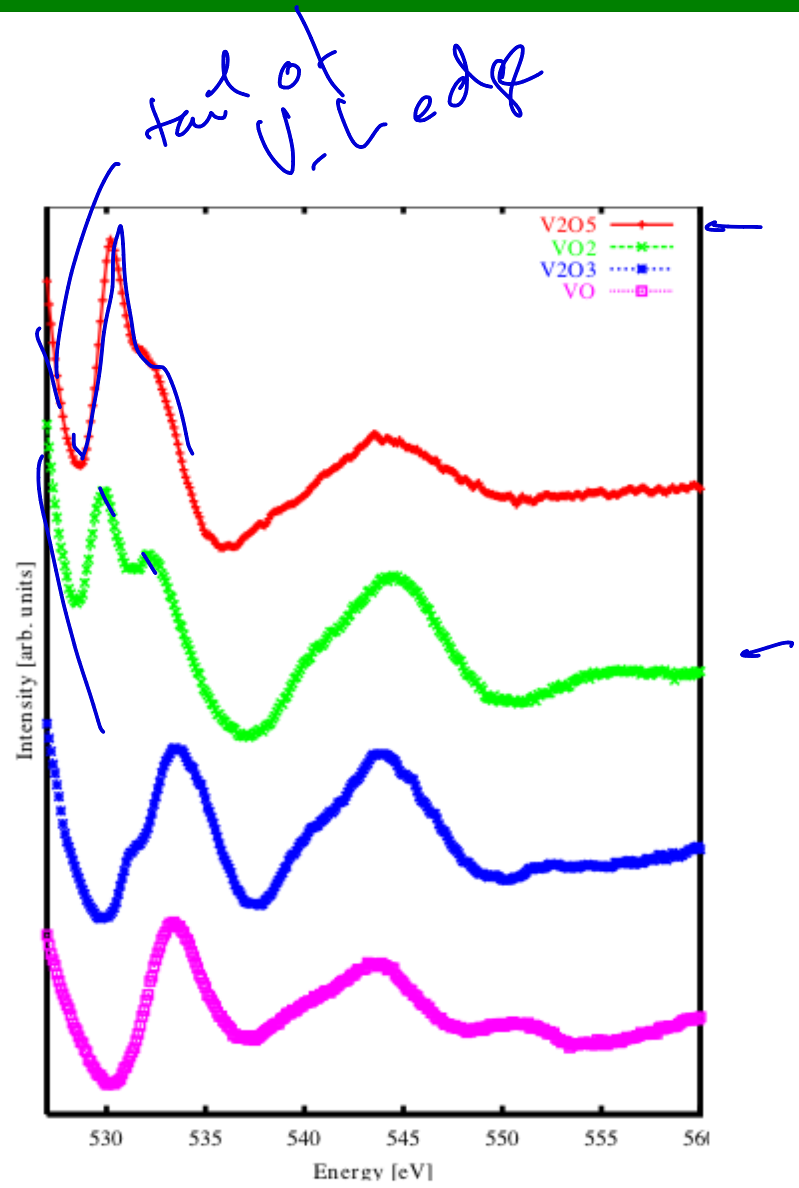

C. Hébert, et al.
Eur.Phys.J B 28, 407 (2002)

Core Loss: ELNES

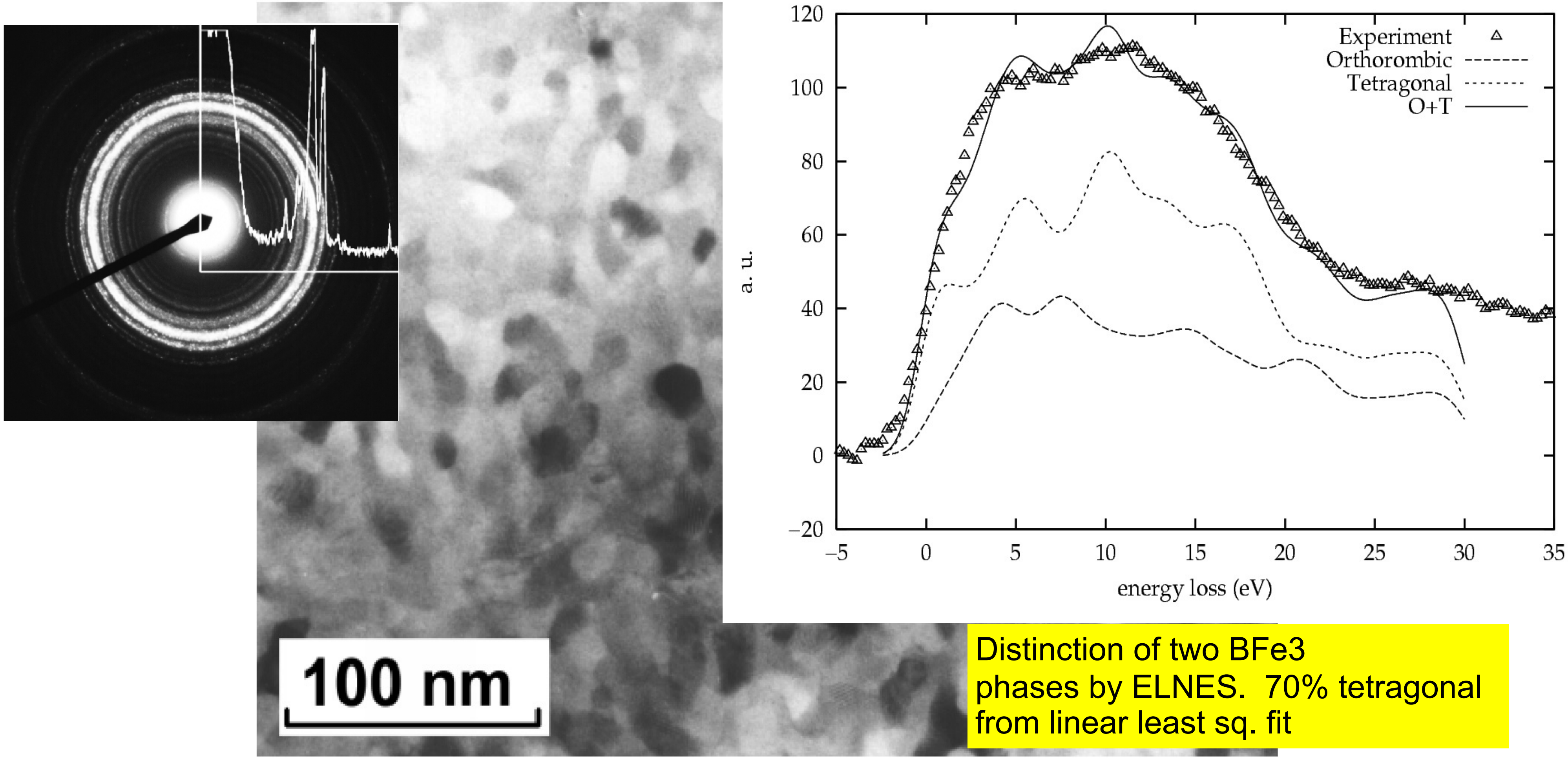

Distinction of two BFe3 phases by ELNES. 70% tetragonal from linear least sq. fit

C. Hébert & al. EPJ– Applied Physics, 9:147 (2000)

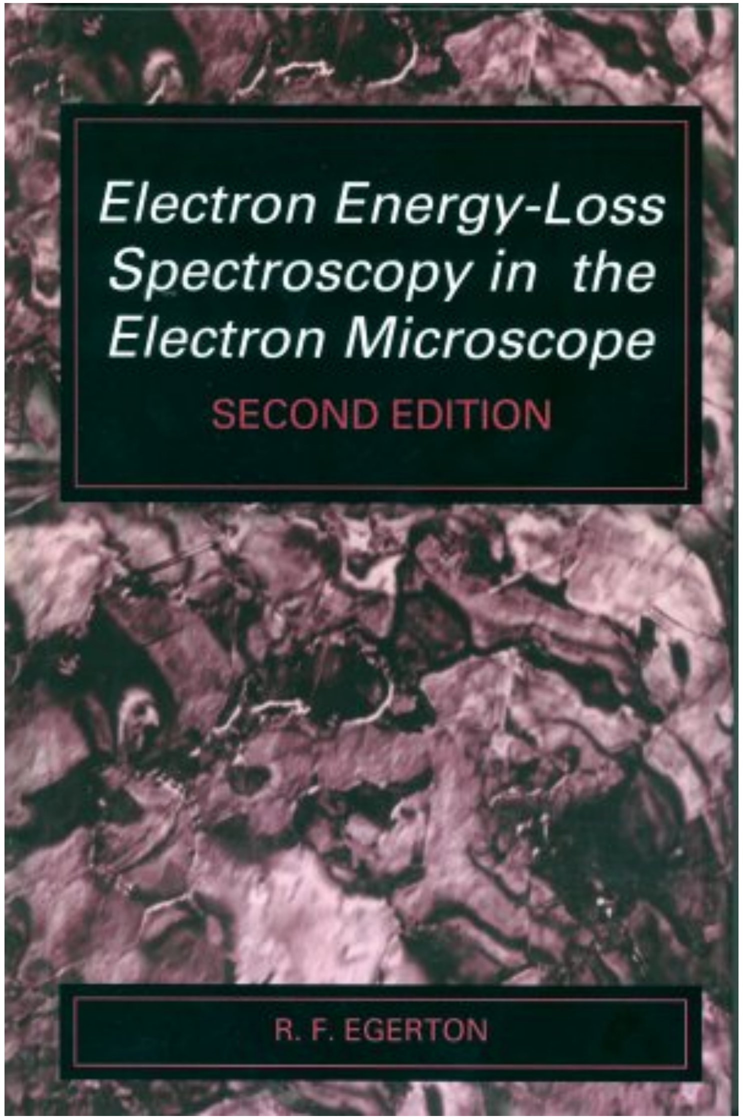

Electron Energy-Loss Spectroscopy In The Electron Microscope
By: R. F. Egerton
Plenum Press © 1989, 1986; 438 pgs., Illustrated Second Edition